Development and Characterisation of Chitosan and Polyhydroxybutyrate Based Polymeric Scaffolds

By Mark Blevins

UNIVERSITY OF BIRMINGHAM

A thesis submitted to the University of Birmingham for the degree of

DOCTOR OF PHILOSOPHY

SCHOOL OF METALLURGY AND MATERIALS
UNIVERSITY OF BIRMINGHAM

May 2014

Abstract

Electrospinning is a versatile method of producing nanofibrous polymeric material with potential applications as tissue engineering scaffolds. The main aim of this project was to produce and characterise electrospun polymeric scaffolds based on chitosan and bacterial polyhydroxybutyrate.

The effect of the parameters used in the electrospinning process were studied and optimised by electrospinning polyvinyl alcohol from 8 wt% and 10 wt% solutions under a variable applied voltage from 10-25 kV. It was shown that applied voltage did not have an effect on the average fibre diameter of the produced fibres but did affect the crystallinity. The electrospinning process had a detrimental effect on the crystallinity showing reductions from 26.6 % in the as received material to 14.1% after electrospinning; however this reduction could be reduced by increasing the applied voltage.

Attempts were made to electrospin chitosan in various solutions including a dilute 2% acetic acid solution and a concentrated 90% acetic acid solution. The operating parameters were also altered throughout their full range; however it was found that it was necessary to create a blend with another polymer in order to produce electrospun chitosan fibres.

PVA-chitosan blends were successfully electrospun at blend ratios of up to 80:20, beyond which fibre formation proved unachievable. The blend ratio was shown to have an effect on both the melting temperature and crystallinity of the produced fibres. The presence of both chitosan and PVA in the produced scaffolds was confirmed by FTIR analysis. Fibre morphology was strongly affected by the solution

concentration, changing from thin ‘bead-on-a-string’ morphologies to uniform fibres as concentration was increased.

A chitosan-hydroxybenzotriazole-PVA aqueous solution was successfully prepared, enabling the production of chitosan/PVA nanofibres without the need for the use of an organic solvent when hydroxybenzotriazole was added to chitosan in a 1:1 ratio. Fibre morphology was unchanged by the alteration in the solvent system.

The suitability of oils to replace the more commonly used sugars as a carbon source for polyhydroxybutyrate (PHB) production was investigated. Polyhydroxybutyrate produced by bacterial synthesis from *R. Eutropha* using three different carbon sources; olive oil, rapeseed oil and glucose were electrospun and characterised. The different carbon sources did not have a significant effect on the morphology or crystallinity of the produced fibres. The average fibre diameter was primarily determined by the concentration of the solution, increasing with increased concentration.

The average fibre diameter of uniform PHB fibres was >1 µm, however with the addition of the conductive salt Benzyl tributylammonium chloride the fibre diameters were successfully reduced by up to 30%

Acknowledgements

I would like to take this opportunity to extend my thanks to my supervisor Dr. Artemis Stamboulis for allowing me the opportunity to conduct this research at the University of Birmingham. She has proved to be an invaluable mentor throughout the course of my work and I thank her for her advice, guidance and wisdom.

I would also like to thank Dr Iza Radecka (University of Wolverhampton), Victor Irorere (University of Wolverhampton) and Dr Soroosh Bagheriasl (University of Birmingham) for their respective roles in providing me with the PHB used in this research project, and Dr Soroosh Bagheriasl for his help in the subsequent characterisation of PHB.

Other notable mentions within the department of Metallurgy and Materials, University of Birmingham go out to Theresa Morris and Paul Stanley for their help in SEM, Frank Biddlestone for his knowledge and expertise in the use of the FTIR and DSC, and Neville Adolphus for letting me know when eagerly awaited new equipment/materials/chemicals had arrived.

I have developed a great number of friendships over the course of this research with people in the Biomaterials group and across the Metallurgy and Materials department; I wish those people all the best in their respective projects and careers and thank them for their support and friendship.

Finally I would like to thank my family for their love and support over the years.

Contents

List of Figures

List of Tables

Abbreviations

ANOVA	Analysis of Variance between Groups
BSM	Basal Salt Medium
BTEAC	Benzyl triethylammonium chloride
BTMAC	Benzyl trimethylammonium chloride
BTBAC	Benzyl tributylammonium chloride
C_6H_{14}	n-Hexane
$CHCL_3$	Chloroform
cP	Centripoise
CS	Chitosan
Da	Dalton
DCM	Dichloromethane
DSC	Differential Scanning Calorimetry
ECM	Extra Cellular Matrix
FTIR	Fourier Transform Infrared Spectroscopy
G-PHB	PHB produced Using Glucose
GPC	Gel Permeation Chromatography
HOBt	Hydroxybenzotriazol

LiCl	Lithium Chloride
Mn	Molecular Mass
Mw	Molecular weight
NaCl	Sodium Chloride
NaOH	Sodium Hydroxide
O-PHB	PHB Produced Using Olive Oil
PHA	Polyhydroxyalkanoates
PHB	Polyhydroxybutyrate
PD	Polydispersity
PET	Polyethylene terephthalate
PLLA	Polylactic Acid
PMSQ	Polymethylsilsequioxane
PVA	Polyvinyl Alcohol
R_4NCl	Tetra-n-heptylammonium Chloride
R-PHB	PHB Produced Using Rapeseed Oil
SEM	Scanning Electron Microscope
T_c	Crystallisation Temperature
TFA	Trifluroacetic acid
T_g	Glass Transition Temperature

T_m	Melting Temperature
TSA	Tryptone Soya Agar
TSB	Tryptone Soya Broth
w/w	Weight by Weight
w/v	Weight by Volume

1. INTRODUCTION AND LITERATURE REVIEW

1.1. Polymer Scaffolds for Tissue Engineering

Tissue engineering has become a highly important field in modern medicine and has developed significantly through multidisciplinary research in fields such as biomedical engineering, biomaterials and cell biology. Tissue engineering can be defined as a field which works to develop biological substitutes that restore, maintain or improve natural tissue function [1]. Despite the ever improving feats of modern medicine which have allowed for surgical techniques such as organ transplants, many patients still die every year due to a shortage of donor organs. The British National Health Service statistics show that over 1000 people die every year whilst waiting for donor organs in the UK alone [2]. Aside from a lack of donor organs and tissues, there are other problems associated with implanting foreign materials into the body, such as the immune response which causes chronic rejection of the donor organ [3]. In the case of burn victims requiring skin grafts, where they provide the donor tissue for themselves, this problem is levitated, however it is a very painful procedure and depending on the degree of burn damage there may be limited supply of healthy skin tissue to be used. Tissue engineering has emerged as a means of solving these problems, using biological substitutes in order to help the body to create new tissue to replace the damage through the use of three-dimensional scaffolds. These scaffolds function to guide cell growth and provide structural support for the formation of a new extra cellular matrix (ECM) [4].

3D scaffolds must conform to a number of requirements in order to be suitable for use in tissue engineering [5], these include being made from a biocompatible material which will not cause a negative immune response. They must have a large surface area-to-volume-ratio in order to maximise cell attachment and organization

that can take place on the scaffold. The scaffold must possess sufficient structural integrity so that it will not fail mechanically under the strain of supporting new tissue growth. The material used should be biodegradable so that the scaffold does not remain in the body once the new tissue has been formed and the scaffold is of no further use. As well as being biodegradable, the degradation rate needs to be controllable for different applications where cell growth may occur at different rates, in order that degradation rate matches cell proliferation rate. Another requirement is that no scar tissue is produced as a result of using the scaffold. In the case of scaffolds used in wound dressings this is a key requirement to be achieved. One further requirement remains that the scaffold be easily and cost effectively produced so as not to limit its application for economic reasons.

These criteria may be obtained through two selections, the process used to make the scaffold and the material it is made from. The processes capable of producing tissue engineering scaffolds will be reviewed first. In order to create scaffolds with a high surface area to weight ratio it is advantageous to work with nanomaterials.

1.2. Applications of Nanomaterials

Nanotechnology is described by NASA as;

> "the creation of functional materials, devices and systems through control of matter on the nanometer length scale (1-100 nanometers), and exploitation of novel phenomena and properties (physical, chemical, biological) at that length scale" [6].

Applications for nanomaterials can be found in a great number of sectors due to their superior properties. Figure 1 presents a spider diagram detailing the different areas in which polymer nanofibres find applications.

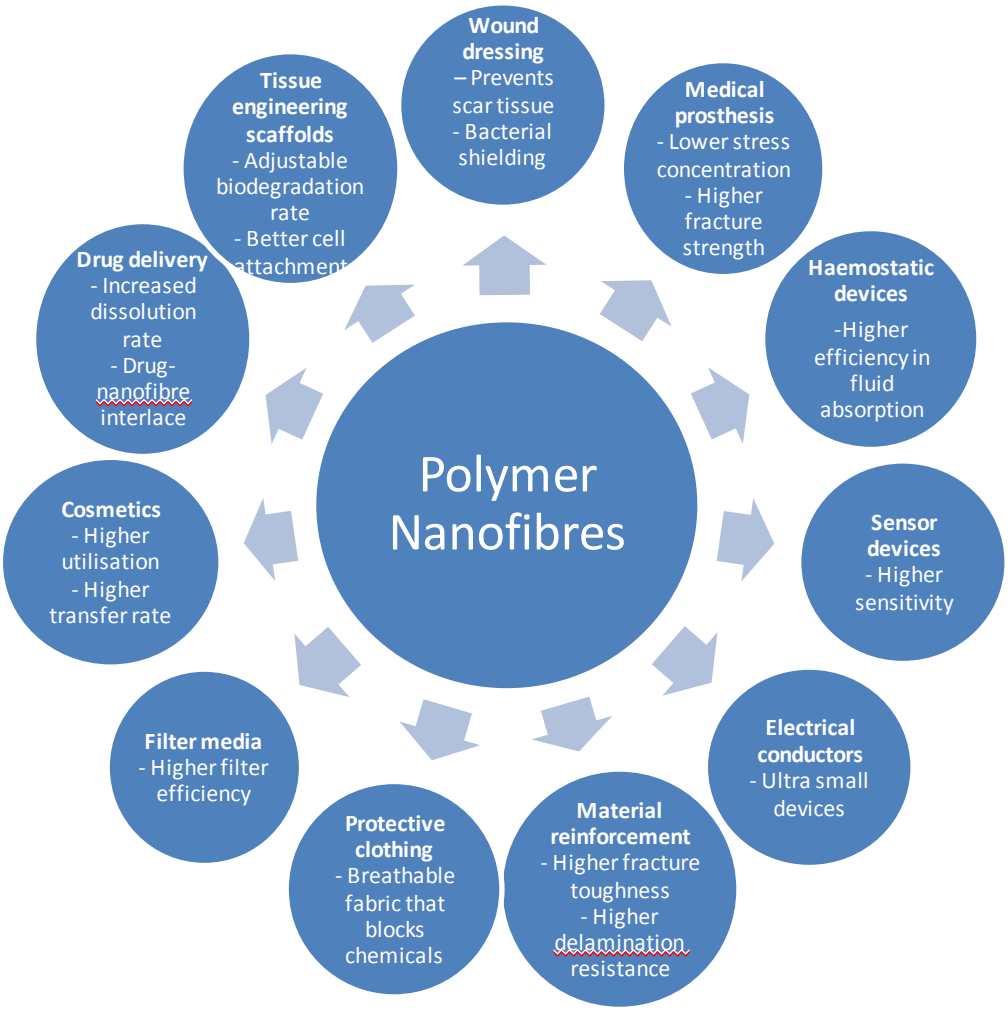

Figure 1 - Spider diagram to show potential applications of polymer nanofibres [7]

There are a number of different techniques that can be used to form polymeric nanofibres. The main techniques are drawing, phase separation, self-assembly, template synthesis and electrospinning [8-10].

1.3. Production methods for nanofibres

1.3.1. **Drawing**

Drawing is a simple process that allows for the formation of a single continuous nanofibre. It is achieved by using a micropipette to pull out a polymer droplet at a specific rate. This process has both advantages and disadvantages. The main advantage is that it is possible to study the properties of individual nanofibres, when scaffolds of nanofibres are produced by electrospinning for example it is very difficult to separate out individual fibres without damaging the sample. Drawing also requires very little equipment. The disadvantages however are that it can only be performed on viscoelastic polymers, which limits the choice of material. It is also a discontinuous process and would take significant time to produce enough nanofibre to form a scaffold suitable for tissue engineering. It is therefore impractical as a technique for application but is suitable for use in a small scale production, for analysis and characterisation [11, 12].

1.3.2. **Phase separation**

Phase separation again requires minimal equipment requirements but is capable of producing a polymeric scaffold with extremely high porosity and fibre diameters in the nanometre scale [13]. This process consists of five key steps.

1. Dissolution of a polymer;

2. Gelation caused by phase separation

3. Addition of water to extract solvent

4. Freezing the gel

5. Freeze-drying in vacuum [13]

This process is long and therefore only suitable in the laboratory environment and not for use in industry. It is also only suitable for a few polymers so as with drawing the choice of material is limited [8].

1.3.3. **Self-assembly**

Self-assembly involves individual components organizing themselves into orders, structures or patterns with pre-programmed non-covalent bonds. Intermolecular forces are generated between the components within the self-assembly such as van de Waals, hydrogen bonds and hydrophobic interactions [14]. This process is suitable for obtaining nanofibres with small diameters however due to the complexity of the process and the low yield it is unsuitable for mass production, it is also only suitable for polymers with certain configurations [13].

1.3.4. **Template synthesis**

In template synthesis a template or mould is used within which a network forms when an electronically conductive polymer is electrochemically or oxidatively polymerized. After polymerisation has taken place, the template can be dissolved to free the nanofibres. The size and morphology of the fibres produced can be controlled by the size and shape of the template used [15]. The disadvantage of this process is that it cannot make continuous nanofibres as it is limited by the template.

1.3.5. **Electrospinning**

Electrospinning produces polymeric nanofibres by passing an electric current through a polymer solution or melt causing an electrostatically charged jet to be ejected. The electrostatic forces cause bending and pulling of the polymer chains resulting in the formation of nanofibres as the solvent evaporates or the polymer solidifies [8].

1.3.6. **Review of the different techniques for producing nanofibres**

As there are so many methods of producing nanofibres as detailed above it is necessary to evaluate which method has the most potential for nanofibre production for application. The ideal process needs to be versatile and flexible, cost effective, simple and scalable. Table 1 shows a comparison of the features of each process.

Table 1: Comparison of attributes of different techniques for producing nanofibres

Process	Suitable for use in lab or industry	Scalable	Repeatable	Convenient	Control of fibre dimensions
Drawing	Lab	-	✓	✓	-
Phase Separation	Lab	-	✓	✓	-
Self-Assembly	Lab	-	✓	-	-
Template Synthesis	Lab	-	✓	✓	✓
Electro-spinning	Lab with potential in industry	✓	✓	✓	✓

From Table 1, it can be seen that electrospinning ticks all of the desired boxes for nanofibre production suitable for application. The control of fibre dimensions is a very important attribute as it allows change of morphology of fibres for different applications. Template synthesis is also a versatile technique also allowing for fibre diameter control, however while it is a fine process for experimental work, it could not been used in industry as the process cannot be scaled up [15].

1.4. Electrospinning

1.4.1. **History**

Electrospinning as a process has been in development for hundreds of years. The effect an electric field could have on liquid droplets was first formally observed by William Gilbert around the year 1600. He devised a series of experiments using charged amber and detailed how it was able to deform the shape of water droplets without physical contact. After this publication there is thought to be no further publications made on the subject until 1882 when Lord Rayleigh devised a theoretical model describing how droplets can be caused to eject liquid by using electrical forces. Attempts to commercialise the phenomenon began in 1902 when the process was patented by J. F Cooley and W.J. Morton and again in 1934 when Anton Formhals registered a patent for using electrospinning for the production of textile yarns. In 1936, the first application for electrospun fibres was developed, using the fibres as a filtration system devised by Petryanov-Sokolov using the theory that thinner fibres make more efficient filter material [16]. Shortly after this, mass production was adopted with 20 million m^2 of electrospun filtration material being produced per annum by the 1960's [17].

While there were already applications of electrospun fibres being produced in the real world in the early 1960's, there had still not been a comprehensive study on the theoretical underpinning of electrospinning. Sir Geoffrey Taylor took up this mantle and undertook a rigorous theoretical study on charged liquid droplets. He observed that under an electric field, the droplets could deform into a new shape resembling a cone [18]. This phenomenon was henceforth known as the Taylor cone.

There was then a lull in electrospinning research until the emergence of nanotechnology towards the end of the 20th century when the true potential of the process was realised. In 1994 Reneker and co-workers coined and popularised the term 'electrospinning' from the previously used term 'electrostatic spinning' [10]. Reneker and his team demonstrated that many organic polymers can be electrospun into nanofibres [19, 20]. Since then, the publications on electrospinning have increased exponentially with many researchers realising the potential of such a versatile process [10].

1.4.2. **Principle**

There are three main components or requirements that need to be fulfilled in order for successful electrospinning to take place [10]

1. High voltage power source
2. A grounded collector
3. A suitable polymer (either as a melt, or more commonly, in a solution) housed in a syringe or suitable container feeding to a pipette or needle of small diameter

Once these are in place, the process can be broken down into four key steps:

1. Charging of the polymer solution
2. Taylor cone formation
3. Thinning of the jet
4. Collection of fibres on the collector

A schematic diagram of a typical electrospinning setup is shown in Figure 2. There are many different configurations of electrospinning setups found throughout the literature. This is partly down to many research groups building their own bespoke electrospinning setups by compiling the three main components, as opposed to buying a commercially produced ‘electrospinning machine’ [21, 22]. Typical variations include the orientation of the setup [8]; Figure 2 shows a vertical setup with the needle and polymer solution located directly above the collecting plate. In this configuration gravity helps the polymer solution flow to the end of the needle tip so a constant supply of solution is present at the needle tip. A horizontal configuration is also common however [23], and in this instance the flow of solution to the needle tip is controlled by a syringe pump. The horizontal configuration has the advantage that any stray droplets that may be ejected from the needle tip in addition to the desired jet will not necessarily fall on the collecting area and be detrimental to the collected fibrous scaffold. A syringe pump may also be used in the vertical configuration in order to quantify the flow rate of the solution to the needle tip.

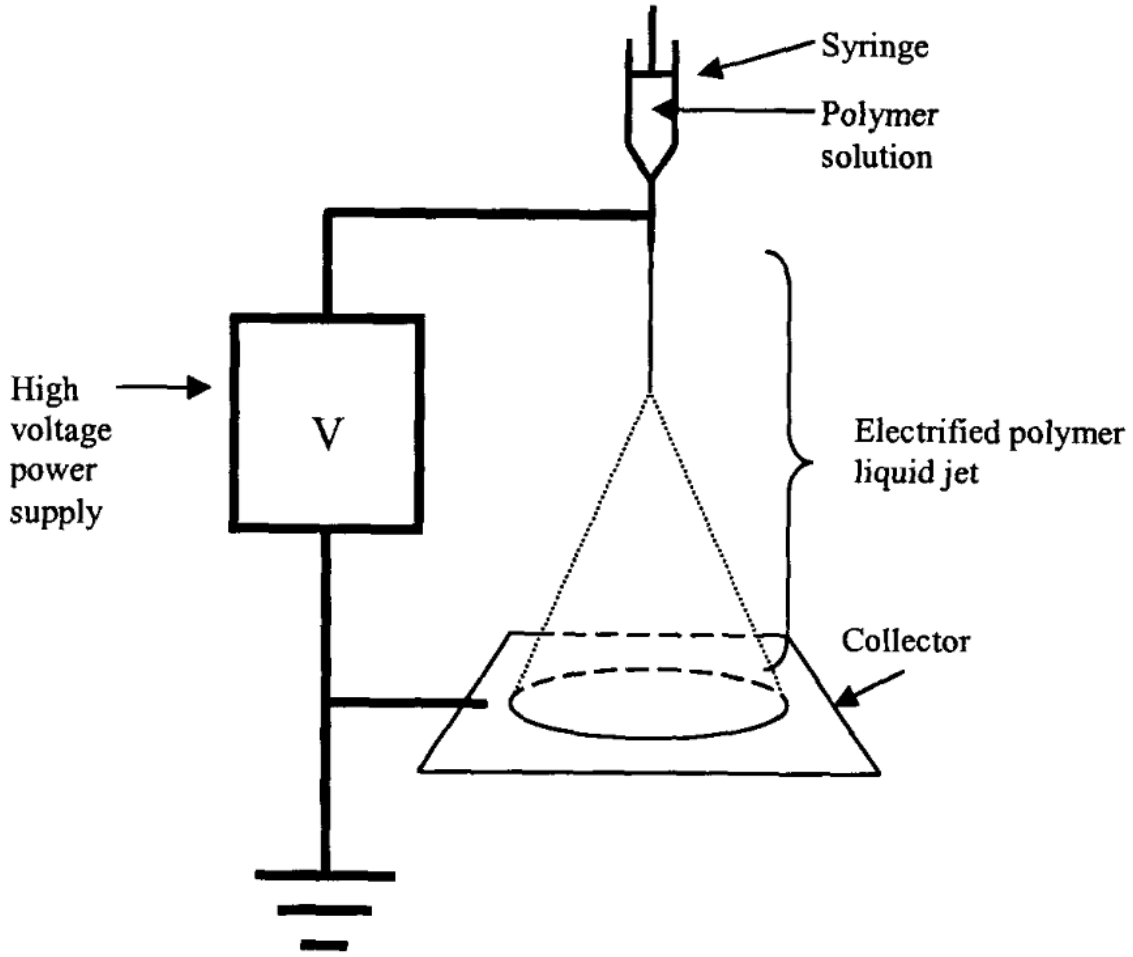

Figure 2: Schematic diagram of a typical electrospinning setup [8]

The equipment is set up and the polymer solution is added to the syringe. The solution is fed to the end of the syringe so that a droplet is held at the end of the needle tip by its surface tension. Once the high voltage is applied, the solution becomes charged. As the voltage is increased, the charge will start to cause deformation of the droplet due to repulsive forces acting within the solution. These repulsive forces begin to exceed that of the surface tension leading to the formation of a conical shape known as the Taylor cone. Once a critical voltage is reached, an electrically charged jet of solution will be released from the Taylor cone and will accelerate towards the grounded collector [8, 10, 24].

Figure 3 shows a depiction of how the jet thins as it travels through the air in the electric field towards the collecting plate. The jet begins by travelling in line with the path from the needle tip to the collector [25] however it soon becomes unstable due to the Coulomb forces. The jet then begins to coil and the increased electrical bending instability causes the coiled jet to form a tighter coil. This continues with the polymer elongating more with every coil [26, 27]. The elongation causes a decrease in the diameter of the jet and in turn increases the surface area per unit mass ratio of the fluid [28]. As this coiling and whipping effect is taking place, the jet is being elongated and the solvent evaporates (or in cases where molten polymers are used the polymer cools) leaving solid polymer fibres. This effect can result in production of fibres with diameters in the sub-micron range [29]. The chain entanglements found within a viscous polymer solution provide enough resistance to prevent the fibres from breaking as they are stretched [30].

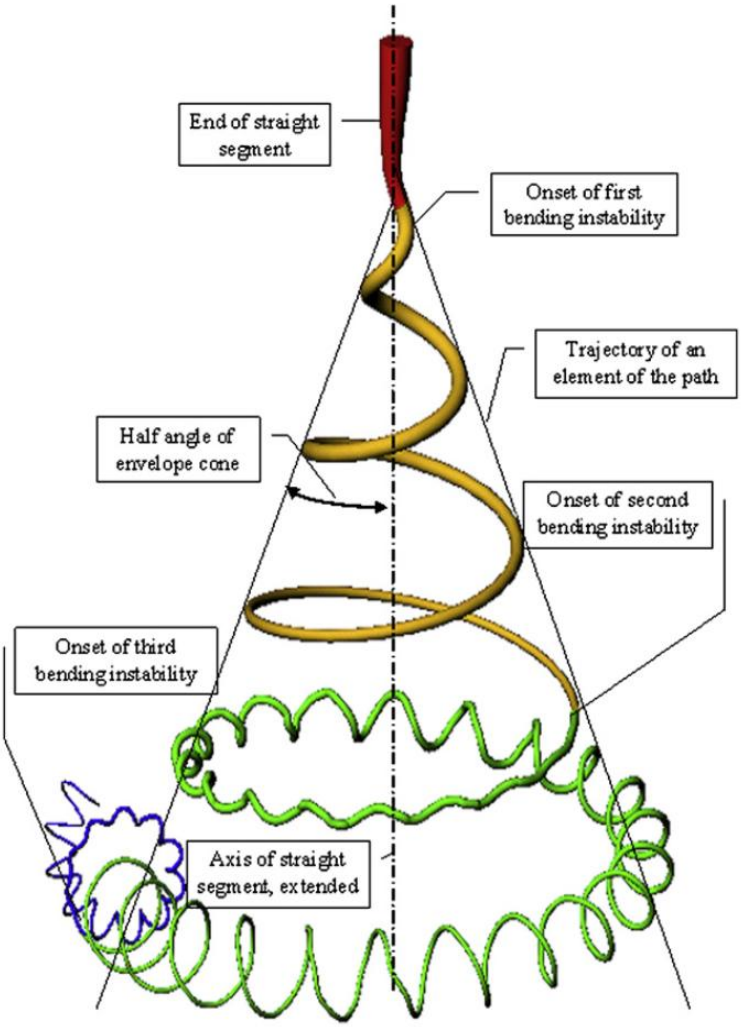

Figure 3: Schematic representation of the coiling and thinning effect exhibited by the jet during typical electrospinning within the electric field [28]

It was originally thought that the bending instability of the jet was caused by the single jet splitting into multiple jets due to the large repulsive forces; the unstable region of the jet takes the shape of an inverted cone which supports this theory. This mechanism was termed “splaying” and it was proposed by Doshi and Reneker that the repulsive forces cause the initial jet to split and then the increased charge density acting on the thinner jet then caused the jet to split again. This process would occur repeatedly until the jet reached the collecting plate and by this time fibres with very small diameters were obtained [19]. Advancements in technology allowed Shin *et al*.

[29] to use high speed photography (1 ms exposure time) to examine the behaviour of the unstable region of the jet and observed, rather than splitting, there was one single continuous jet which formed a non-axisymmetric whipping instability causing the stretching and bending of the jet. This whipping occurs so fast that it may appear that the jet is splitting into smaller jets however this is not the case.

The resultant fibres are deposited as a 3D nonwoven mesh which is commonly referred to as a 'scaffold' on the collector.

1.4.3. **Electrospinning parameters**

The controllable parameters that determine the properties of electrospun nanofibres can be broken down into three main groups [8, 10].

-Solution parameters:

- Viscosity (resultant of concentration of polymer in solution and molecular weight)
- Molecular weight of polymer in solution
- Concentration of polymer in solution
- Surface tension
- Solution conductivity
- Dielectric constant of solvent

-Processing parameters:

- Voltage
- Flow rate
- Distance between the needle tip and the collector

-Ambient parameters (environmental factors):

- Temperature
- Pressure
- Humidity
- Relative airflow
- Electrospinning atmosphere

As there have been so many publications on electrospinning in recent years, the effects that most of these parameters have on the resultant fibres is quite well documented [8]. While differences in the effects are seen with different polymers/blends/composites, the general trends are important to know and understand when trying to optimise an electropinning system to produce desired fibre properties.

1.4.3.1. Solution Parameters

1.4.3.1.1. *Viscosity*

The viscosity is an extremely important parameter in the successful formation of fibres. The electrospinning process is reliant on polymer chain entanglements, found within a viscous polymer solution, to prevent the jet from breaking up when the elongation forces are imposed by the electric field. In cases of very low viscosity polymeric micro (or nano) particles will be obtained instead of fibres [31].

When the viscosity is increased a mixture of beads and fibres may be obtained [32-34]. This mixture of states exists because the parts of the jet which withstand the stretching forces form fibres as desired, but due to the viscosity being too low, some of the chain entanglements are overpowered and break up the jet. The bead

phenomenon is caused by the elasticity of the polymer chains recoiling towards their original shape before solidifying on the collector [35].

When the viscosity is within a suitable range, smooth nanofibres can be obtained [32-34]. Boland *et al.* electrospun polydioxanone and found that fibres could be successfully formed from solutions in the viscosity range of 50 cP - 2856 cP [36].

Once a viscosity that produces smooth uniform fibres is reached, usually raising the viscosity further has been shown to increase the fibre diameter. This trend will continue until the fibres are no longer on the nano-scale. In this instance helix-shaped micro-ribbons may be observed [37].

1.4.3.1.2. Molecular weight

The molecular weight of a polymer determines the length of the polymer chains. The longer the polymer chains, the greater the likelihood of chain entanglements [38]. If the molecular weight of the polymer is increased, but the concentration in solution remains the same, the solution viscosity will increase. As molecular weight is inherently linked with viscosity, the effects of changing this parameter are seen to be the same as changing the viscosity assuming a constant concentration is maintained. Increasing the molecular weight will cause an increase in fibre diameter and eventually micro-ribbons [39]. Decreasing the molecular weight will lead to beading due to insufficient chain entanglements to resist the elongation forces acting on the poymer chains [39].

1.4.3.1.3. Concentration

The concentration of a polymer in a given amount of solution and the molecular weight of the polymer are the two factors which determine the viscosity of the

solution, so concentration, molecular weight and viscosity are related to each other. Concentration may therefore be varied depending on the molecular weight of the polymer in order to achieve a solution with a desired viscosity [40].

1.4.3.1.4. Surface tension

Some degree of surface tension is required in electrospinning solutions in order to hold the solution at the end of the needle tip without it simply flowing out. The surface tension of the solution is mostly determined by the choice of solvent used and is not affected to a great extent by the concentration of the polymer [41]. Yang *et al.* investigated the effect of surface tension on the morphology of electrospun poly(vinyl pyrrolidone) fibres in 2004 and found that beaded fibres could be changed to smooth fibres by reducing the solvent surface tension while maintaining a fixed polymer concentration in solution [37].

1.4.3.1.5. Solution Conductivity

A conductive solution is necessary for electrospinning to take place as the solution needs to carry sufficient charges to provide the repulsive forces required, to first overcome the surface tension of the solution, and subsequently cause elongation and stretching [8]. The solution conductivity is mainly determined by the polymer and solvent used as well as by any salt added to the solution. The addition of an electrically conductive salt, such as NaCl, tetra-n-heptylammonium chloride (R_4NCl) or LiCl, has been shown to decrease beads as a result of increasing conductivity. This is due to increased stretching occurring as a result of greater charges being carried by the solution [33, 42]. While increase in conductivity can improve electrospinning, too high a conductivity is unsuitable as it causes a reduction in the tangential electric field. This results in a significant reduction in the electrostatic

force running along the surface of the solution, which is required for Taylor cone formation [43]

1.4.3.2. Processing parameters

1.4.3.2.1. Voltage

The applied voltage is a very important parameter in electrospinning, without which the whole process would cease to function [8]. Beyond creating a sufficient charge to overcome the surface tension in order to form a Taylor cone and eject the solution, known as the critical voltage, the literature remains unclear as to the effects of increasing or decreasing the voltage beyond this point. The applied voltage can affect properties of the produced fibres, namely the fibre diameter and the crystallinity [8]. There are two sides to the argument over the effect of voltage on fibre diameter. On the one side some researchers [44, 45] have demonstrated that higher voltages facilitate the formation of large fibre diameters. The mechanism they use to explain this phenomenon is that the amount of stretching the jet undergoes is proportional to the flight time of the jet between the needle tip and the collecting plate. When the voltage is increased the electric field is stronger and the potential difference between the charged needle tip and the grounded collector is greater. As a result the solution is ejected with greater force and travels through the air much faster. This reduces the flight time and thus the amount of stretching taking place. In this instance, with this mechanism taking place, it would be beneficial to select a voltage as close as possible to the critical voltage in order to obtain the smallest fibre diameters.

On the other hand, other researchers [46-49] have shown that fibre diameter is decreased when voltage is increased. This is explained by the higher voltage

resulting in greater columbic forces in the jet and a stronger electric field which both act to stretch the fibres further resulting in thinner fibres. It has also been shown by Pawlowshi *et al*. [50] that higher voltages encourage faster solvent evaporation.

It seems likely that both of these mechanisms do take place and that the effect of voltage on fibre morphology will vary depending on the particular polymer solution used.

The crystallinity of a polymer is very important in determining some of the properties of the material. A high crystallinity will result in a larger amount of secondary bonding between polymer chains. This bonding will cause both a reduction in the degradation rate [51] and increase the strength and stiffness [52]. Being able to control the crystallinity is desirable as it allows tailoring of the properties for a particular application.

The applied voltage has an important effect on the crystallinity of the fibres. During the electrospinning process, as the jet travels through the air, molecular orientation is induced as a result of the electric field, and crystallisation of the polymer takes place [45]. It follows, that as the voltage, and therefore the electric field strength, are increased, the degree of molecular orientation imposed on the polymer increases, so the polymer chain alignment is greater and consequently the crystallisation is greater.

Ramakrishna et al. [8] explained that the trend of crystallinity increasing with increased applied voltage was only true up to a certain applied voltage, beyond which the crystallinity would no longer be increased and would actually begin to decrease with further additional voltage. It has been suggested that crystallisation takes place while the jet travels through the air from the needle tip to the collecting

plate. An increase in voltage decreases the flight time due to the greater acceleration of the jet [44]. The crystallinity therefore starts to decrease because there is insufficient time for the polymer to crystallise [45].

It is therefore proposed that there is an 'inverted U' relationship between applied voltage and polymer crystallinity, whereby the crystallinity increases with increased voltage up to an optimum voltage, beyond which it then begins to decrease. It is suggested that this optimum voltage may be unique for each polymer solutions [53].

1.4.3.2.2. Flow rate

The flow rate determines how much polymer solution is distributed to the end of the needle tip per unit of time. An appropriate flow rate needs to be selected to ensure a stabilized Taylor cone can be maintained during electrospinning [8]. Generally speaking, a low flow rate is more conducive to the production of thin uniform fibres as long as it is a sufficient rate to supply solution to the end of the needle tip at the same rate that the solution is carried away by the electrospinning jet. If the flow rate is too low, a continuous jet may not be possible and some solution may solidify at the end of the needle tip, blocking further solution from passing through. As the flow rate is increased there is a greater volume of solution ejected from the needle tip. This leads to a thicker jet with more chain entanglements which are resistant to stretching, resulting in larger fibre diameters [54, 55]. As there is more solution travelling within the jet, it will also take a longer time for the solvent to evaporate. If there is insufficient time for solvents to evaporate, then there may be residual solvent left in the fibres as they are collected which can cause the fibres to fuse together [56].

1.4.3.2.3. Needle tip distance

Shortening or lengthening the distance between the tip of the needle and the collecting plate has a direct impact on the electric field strength; there is an inverse relationship, with a reduced distance increasing the strength and an increased distance decreasing the strength. This means that changes in needle tip distance are similar to changes of voltage [8, 54, 57]. A greater distance also allows more flight time for the jet to stretch and greater time for solvent evaporation, which both favour thinner more uniform fibres, as long as the voltage is also increased in order to counter the reduced electric field strength effect. The needle tip distance needs to be great enough to allow sufficient time for stretching and solvent evaporation, if the distance is not great enough, wide, interconnected or 'webbed' fibres may be produced.

1.4.3.3. Ambient parameters

1.4.3.3.1. Temperature

The temperature of the electrospinning environment can affect fibre diameters and morphologies. A higher temperature has been shown to result in smaller fibre diameters [35, 58]. This is because an increasing temperature has the effect of lowering a polymer solutions viscosity [59], and as discussed is section 1.4.3.1.1 a reduction in the viscosity of a solution favours the formation of thinner fibres.

1.4.3.3.2. Humidity

A low humidity may increase the rate of solvent evaporating while a high humidity can affect the charge on the jet which reduces the stretching forces and results in larger fibre diameters [60].

1.4.4. **Choice of solvent**

As well as the above mentioned parameters, the choice of solvent used is of particular importance as it may have an influence on the parameters discussed above, such as surface tension, conductivity or viscosity. The importance of the choice of solvent is emphasised by Luo et al. [61] with their paper dedicated to the selection of solvents for electrospinning. They devised a spinnabillity-solubility map which was used to methodically develop different solvent systems for the purpose of electrospinning polymethylsilsequioxane (PMSQ). Interestingly, they showed that solvents with a high solubility for PMSQ did not necessarily produce solutions which were suitable for electrospinning and in some cases a solvent with only partial solubility was shown to be more suitable.

Table 2 shows some polymers commonly processed by electrospinning and the respective solvents typically used.

Table 2: Commonly electrospun polymers and their respective solvents

Polymer	**Solvent**
Nylon 6	Formic acid
Polyethylene terephthalate (PET)	Trifluroacetic acid
Polyvinyl Alcohol (PVA)	Water
Polystyrene	Dichloromethane
Polyamides	Sulphuric acid
Polyhydroxybutyrate (PHB)	Chloroform
Chitosan	Acetic acid
Polylactic Acid (PLLA)	Dichloromethane/N,N-Dimethylformamide

It can be seen from the Table 2 that many of the polymers used in electrospinning rely on the use of an organic solvent or acid in order to create an eletrospinnable system. When considering a material for potential application in tissue engineering or other biomedical application the implications of the solvent used has to be considered. Many of these organic solvents are toxic and would be harmful if they were to be applied to human skin or tissue. After electrospinning there will be some residual solvent present in the fibres [62]. This must either be removed by treatment or a non-toxic solvent must be used for electrospinning in order for the scaffolds to be suitable for biomedical application.

1.4.5. **Choice of Polymer**

The selection of the polymer to be used to produce an electrospun scaffold is vital when considering a particular application. Different polymers can have a great range of mechanical and thermal properties as well as some being biocompatible and biodegradable [63]. It is important to select one which exhibits the properties required.

There are two main types of polymer, synthetic polymers and natural polymers. Synthetic polymers are man-made, while natural polymers are produced in nature. There are great concerns over the environmental impact of synthetic polymers both due to pollution in the production and from disposal of the finished product [64]. Natural polymers however can be much more environmentally friendly [65] as well as providing much higher levels of biocompatablility and biodegradability.

1.5. Electrospinning of Chitosan and Polyvinyl alcohol (PVA)

1.5.1. **Structure and properties of chitosan**

Chitosan is a unique polysaccharide derived from chitin. There have been many attempts to use chitosan in the biomedical field for applications such as haemodialysis membranes, artificial skin, substituting or regenerating the blood-tissue interfaces and drug targeting. As chitosan has structural characteristics similar to glycosamino-glycans it seems to be able to mimic their functional behaviour [66].

Chitin is an attractive material as it is a 'natural polymer' and therefore has much greater biocompatibility and biodegradability than most of the synthetic, man-made polymers. Chitin is one of the most abundant polysaccharides in nature, behind cellulose and several billion tonnes of chitin are produced per year by marine copepods alone [67]. It is found in the exoskeletons of crabs, shrimps and other crustaceans, and insects and even found in some fungi.

The chemical structure of chitin is shown in Figure 4. It is a 2-acetamido-2-deoxy-β-D-glucose with the monomers connected through β-1,4-glycosidic bond linkages. This structure is very similar to that of cellulose with the replacement of a hydroxyl group on one of the carbons with an acetamido group [68]. The acetamido groups and hydroxyl groups form hydrogen bonds with neighbouring chains or in the same chain, the acetamido group leads to greater hydrogen bonding compared to cellulose leading to chitin having a higher strength.

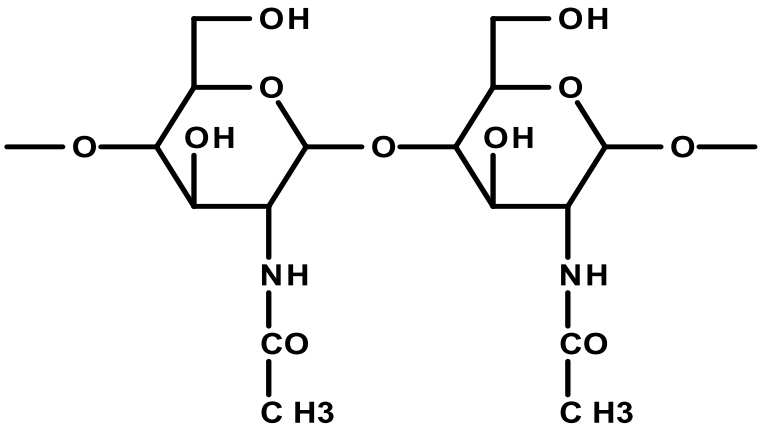

Figure 4: The chemical structure of chitin.

Three different polymorphic forms of chitin have been found, α-chitin, β-chitin, and γ-chitin. In α-chitin the chains are arranged in tight anti-parallel formation resulting in an orthorhombic shape. In β-chitin the chains are parallel in their orientation and have a monoclinic crystal symmetry while γ-chitin contains a mixture of the two previous formations, with some chains arranged in parallel and some anti-parallel [69]. Due to the nature of these formations β-chitin is more susceptible to dissolution compared to α-chitin, due to the chains being less tightly arranged and intermolecular interactions being weaker, however chitin in all its forms is insoluble in most organic solvents due to the strong hydrogen bonding.

Chitin is rarely utilized due to this insolubility, both in water and most commercial organic solvents, however, when N-deacetylated it forms chitosan which is soluble in a number of acidic solvents. The reason chitosan is only soluble in acidic solutions with a pH lower than 6.0 is due to chitosan's amines being protonated when in acidic solutions resulting in the chitosan becoming a water soluble cationic polyelectrolyte [70]. Chitosan is made up of the deacetylated component β-(1-4)-linked D-

glucosamine and the acetylated component N-acetyl-D-glucosamine. The structure of chitosan is depicted in Figure 5.

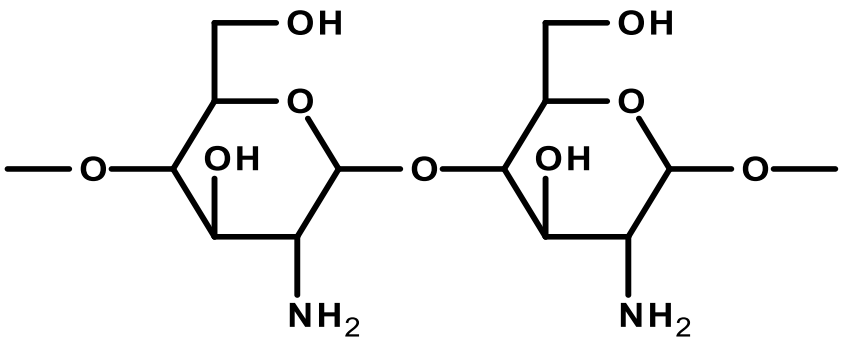

Figure 5: The chemical structure of chitosan.

While chitin has been shown to be predominantly a crystalline material with small amorphous regions, chitosan is more semi-crystalline in structure with the degree of crystallisation dependant on the degree of de-acetylation [71]. Chitosan is insoluble in solvents with a neutral or alkaline pH however is soluble in acidic solvents such as acetic acids, hydrochloric acid, lactic acid and glutamic acid. This solubility greatly improves the prospects for the material in application.

Chitosan has been shown to have antibacterial and antifungal properties making it an ideal material for applications in biomedicine. The mechanisms through which chitosan acts as an antimicrobial material have been summarised as the following;

“(1) The cationic nature of chitosan causes it to bind with sialic acid in phospholipids, consequently restraining the movement of microbiological substances.

(2) Oligomeric chitosan penetrates into the cells of microorganisms and prevents the growth of cells by preventing the transformation of DNA into RNA.” [72]

The cationic amines present in the chitosan structure are positively charged and cause electrostatic interactions with any negatively charged microbial cell membranes [73]. These interactions provide interference to the permeability of the membrane resulting in an osmotic imbalance which will inhibit the growth of microorganisms [74].

Table 3: Strains of bacteria and fungi in which chitosan has been shown to inhibit growth [75, 76]

Bacteria		**Fungus**
Gram-positive bacteria	**Gram-negative bacteria**	
Staphylococcus aureus (S.aureus)	Escherichia coli (E.coli)	Botrytis cinerea
Listeria monocytogenes	Shigella dysenteriae	Rhizopus stolonifer
Bacillus cereus	Pseudomonas Aeruginosa	Aspergillus niger
	Vibrio cholera	Aspergillus parasiticus
	Vibrio parahaemolyticus	
	Aeromonas hydrophila YMI	
	Aeromonas hydrophila CCRC 13881	
	Salmonella tyhimurium	

Chitosan has been shown to inhibit fibroplasia in wound healing and to promote tissue growth and differentiation in tissue culture [77]. It appears chitosan can provide a non-protein matrix for three-dimensional tissue growth, and can play the

role of a biological primer for cell-tissue proliferation and reconstruction. Other properties which make chitosan of high interest for tissue engineering are its ability to cause haemostasis as well as promote normal tissue regeneration [78]. The ability to promote normal tissue regeneration is thought to be due to the presence of the monomeric unit N-acetylglucosamine which is also present in hyaluronic acid, an extracellular macromolecule involved in wound repair. It therefore has characteristics which are favourable to tissue regeneration [79].

1.5.2. **Electrospinning of chitosan**

There are numerous examples in the literature detailing the electrospinning of chitosan [54, 80-82] however very few report on electrospinning of pure chitosan, instead relying on creating blends of chitosan with other polymers such as PEO [82] or PVA [83] to help improve the electrospinnability.

There are two main problems reported with the electrospinning of pure chitosan. One problem addressed by Homayoni et al. [54] is that chitosan is very viscous when in solution, which prevents elongation of the jet and inhibits fibre formation. Another problem arises from the structure of chitosan in solution. Chitosan can be dissolved in most acids and when done so, the chitosan is protonated to form a polyelectrolyte. When a voltage is then applied to the solution during the electrospinning process the ionic groups in the polymer backbone strongly repel each other which prevent the formation of a continuous jet. These repellent forces particularly impact the jet stretching, whipping and bending stage of the process. As a result ultrafine particles rather than ultrafine fibres are produced, even when chitosan solution concentrations are within their optimum range [84].

Numerous researchers have attempted ways to resolve these problems. Ohkawa et al. [80] were successful in producing pure chitosan fibres when using trifluroacetic acid (TFA) as a solvent. TFA was able to produce an electrospinnable solution by breaking down the intermolecular interactions occurring between the chitosan molecules as chitosan forms amine salts with TFA at the C2-amine groups [85]. Ohkawa et al. found that as the chitosan content of the solution was increased; fibres were produced in preference to beads however these fibres were interconnected. With the addition of a second volatile organic solvent, dichloromethane (DCM), they were able to produce homogeneous fibres with fibre diameters ranging from 210 – 650 nm.

Vrieze et al. [86] carried out a feasibility study on the electrospinning of pure chitosan, testing formic acid, lactic acid, hydrochloric acid and acetic acid for their suitability as solvents in electrospinning pure chitosan. Successful fibre production was only achieved with the use of a concentrated acetic acid solution. Vrieze et al. proposed that the optimum parameters from electrospinning chitosan in acetic acid were a chitosan concentration of 3%, an acetic acid concentration of 90%, an applied voltage of 20 kV and a needle tip distance of 10 cm.

Geng et al. [87] had previous success in electrospinning pure chitosan dissolved in concentrated acetic acid and provided some insights into why. Despite chitosan being soluble in both dilute and concentrated acetic acid, only concentrated acetic acid was suitable as a solvent for electrospinning. Geng et al. showed that the surface tension of the solution decreased dramatically with an increase in the acid concentration as well as the charge density of the solution increasing, while the viscosity remained relatively unaffected. These factors improved the electrospinability of the solution and allowed for the formation of uniform fibres. The

result was however limited to chitosan with an M_w of 106,000 g/mol, with higher (398,000 g/mol) and lower (30,000 g/mol) M_w chitosan producing a mixture of beads, droplets and fibres.

Homayoni et al. [54] addressed the issue of the high viscosity by subjecting the chitosan to an alkali treatment using sodium hydroxide (NaOH). This had the effect of hydrolysing the chitosan chains and as a result reduced the molecular weight. Alkali treated chitosan was then successfully electrospun using 70-90% concentrated glacial acetic acid, thus improving on the results of Geng [87] and Vrieze [86] by reducing the concentration of acetic acid required. FTIR analysis showed that the alkali treatment did not have an effect on the chemical structure of the chitosan other than some changes in the secondary hydrogen bonds.

These studies show the extent to which the electrospinning of pure chitosan has been successful. The use of a highly concentrated acidic solvent is not ideal for use in electrospun scaffolds with intended uses in tissue engineering because, due to the nature of the process, there is likely to be residual solvent left on the fibres in the scaffold which may be harmful when applied to human skin or tissue [62]. There is also the economical consideration of the costs involved and environmental factors. If the electrospun scaffolds were adopted for tissue engineering applications on a mass scale the amount of wasted solvent would be huge. A solution to combat both the need for concentrated acetic acid as a solvent and chitosan's poor electrospinnability is to create a blend with another polymer.

1.5.3. **Chitosan Blends**

Polymer blending is a large field in itself and has been used for many years in order to improve the properties a polymer by combining it with another polymer while

retaining, to an extent, the individual properties of the two separate polymers. Products such as car bumpers, disposable coffee cups and biomedical devices are commonly made from such blends [88]. The choice of polymers used is determined by the desired properties dictated by the intended application as well as by the compatibility of the two polymers as to whether they are miscible or immiscible.

Studies have shown that chitosan is miscible with a number of synthetic polymers. These include poly(ethylene oxide) (PEO) [89] and poly(vinyl alcohol) (PVA) [90]. Naveen Kumar *et al*. [90] conducted a compatibility study on the miscibility of chitosan/PVA blends in a 2% acetic acid solution. The results from viscosity, ultrasonic velocity and refractive index measurements led to the conclusion that chitosan/PVA was miscible at blend ratios ranging from 20:80 – 80:20 PVA: chitosan. DSC and FTIR showed strong intermolecular hydrogen bonding between the chitosan and PVA molecules which explains the observed miscibility. Rakkapao et al. [89] showed that PEO was miscible with chitosan through hydrogen bonding. While a number of blend ratios were found to be successfully miscible they concluded that the optimum blend composition which provided the strongest interaction between the chitosan and PEO molecules was the stoichiometric composition whereby the hydroxyl and amino groups of chitosan had a 1:1 ratio with the ether oxygen of PEO. In the blends chitosan was shown to suppress the crystallization of PEO while the thermal degradation of chitosan was suppressed by chitosan.

Blends have also been shown to be made with chitosan and collagen in which each of the materials maintains its individual properties and chitosan did not denature collagen fibres. The addition of chitosan to collagen also showed a decrease in the apparent viscosity of the resultant solutions [91].

1.5.4. **Electrospinning of chitosan blends**

There are many other reports of chitosan electrospinning when it is blended with other materials including synthetic polymers [92-94], proteins [95] and the formation of composites with inorganic nanoparticles [96, 97].

Duan et al. [92] could not produce fibres from electrospinning a pure chitosan solution in aqueous acetic acid however fibres were formed with the addition of PEO in a 2 % acetic acid solution. Fibres were successfully produced with mass ratios of chitosan:PEO at 2:1 and 1:1 with solution concentrations ranging for 4-6% with operating parameters of 15 kV applied voltage, 20 cm needle tip distance and a flow rate of 0.1 ml/h. They found that the conductivity of the chitosan-PEO solution decreased as compared with the same concentration of chitosan solution not containing PEO. A mixture of nanofibres and microfibres were produced during this study, with nanofibre dimensions in the range of 80-180 nm. The morphology of fibres was primarily influenced by the solution concentration as well as the mass ratio of chitosan to PEO. Some phase separation of the chitosan/PEO solutions was observed during the electrospinning processes, which lead to the microfibres predominantly being made up of PEO while the nanofibres were mainly chitosan.

Blends work to improve the spinability of chitosan for a couple of reasons. The first is the effect the blend can have on the overall viscosity of the solution. As discussed chitosan is highly viscous in solution and has even been used as a thickener for electrospinning dilute PVA solutions, allowing the formation of uniform fibres from PVA solutions with a concentration so low that usually a highly beaded scaffold would form [98]. The same principal can be used in the reverse; PVA has a

relatively low viscosity in solution and so by creating a blend with the more viscous chitosan the overall solution viscosity as compared to pure chitosan can be reduced.

The second reason for the improved spinnability is due to the intermolecular forces between polymer chains in chitosan. As mentioned previously the ionic groups in the polymer backbone strongly repel each other which prevent continuous fibre formation. Through the addition of another polymer to form a miscible blend this structure is disrupted and the repellent forces are alleviated. This explains why there is a limit to the blend ratio between chitosan and PVA that can still be successfully electrospun as reported by Jia et al. [99] who found that fibres could only successfully be produced from chitosan/PVA blends when the chitosan content was less than 30%. They also found that the average fibre diameter of the produced fibres decreased with increasing chitosan content from 10-30 %. This is attributed to the increase in conductivity as a result of the addition of more chitosan.

An overview of the previous literature on the subject of electrospinning chitosan is depicted in Table 4. This details the polymer(s) the chitosan was blended with, if any, as well as the solvent system used and the average fibre diameter that was achieved.

Table 4: Overview of the results of electrospinning chitosan and chitosan blends including solvent used, average fibre diameter produced and the proposed application for the produced scaffold

Polymer	Solvent	Degree of Deacylation	Average fibre diameter (nm)	Application	Reference
Chitosan	Acetic acid	54	130	-	[87]
Chitosan	Acetic acid	75-85	70 ± 35	-	[86]
Chitosan	TFA/DCM	95	130 ± 10	-	[100]
Chitosan	TFA/DCM	85	126 ± 20	Tissue engineering	[101]
Chitosan (neutralized with K_2CO_3 solution)	TFA	86.7	235	Filtration	[102]
Chitosan/PVA (removing PVA with 0.5 M NaOH)	Acetic acid	90	80-150	Enzyme immobilization	[103]
Chitosan/ PVA	Acetic acid	90	99 ± 21	Wound Dressings	[104]
Chitosan/ PEO	Acetic acid	80	10-240	-	[105]
Chitosan/ PEO	Acetic acid	67-83	80 ± 35	Filtration	[93, 106]
Chitosan/ UHMWPEO (5%) Chitosan/ UHMWPEO	Acetic acid/DMS	>85	114 ±19 138 ±15	-	[81]

(10%) Chitosan/ UHMWPEO (20%)	O		102 ±14		
Chitosan/ PET	TFA	85	500-800	Wound dressings	[107]
Chitosan/ PCL	HFIP	75-75	450 ±110	Bone tissue engineering	[108]
Chitosan/ nylon-6	HFIP/FA	85	80-310	Filtration	[109]
Chitosan/PVA-PLGA (by multi-jet electrospinning method)	Acetic acid/ THF/DMF	90	275 ±175	Tissue engineering	[110]
Chitosan/ collagen (crosslinked by GA vapour)	HFIP/TFA	85	434-691	Tissue engineering	[95]
Chitosan/ collagen/ PEO (crosslinked by GA vapor)	Acetic acid	95	398 ±76	Wound dressings	[111]
Chitosan/ SF	Formic acid	86	180-790	-	[22]
N-CECS/PVA	Water	82.5	131-456	Wound dressings	[112]
H-CS	Chloroform	88	640-3930	Skin tissue engineering	[113]
G-CS	Formic acid	85	160	Liver tissue engineering	[114]
Q-CS/PVA (crosslinked by UV	Acetic acid	80	60-200	Wound dressings	[115]

irradiation)					
PCL-g-CS/PCL	F/chloroform	91	-	Tissue engineering	[116]
CS-HOBt/PVA	Water	85	190-282	Drug delivery	[117]
Chitosan/HAp/UHMWPEO	Acetic acid/DMSO	>85	214 ±25	Bone tissue engineering	[96]
Chitosan/HAp/PVA	Acetic acid	91	49 ±10	Bone tissue engineering	[118]
Chitosan/HAp/PVA	Acetic acid/DMSO	88	100-700	Bone tissue engineering	[119]
Chitosan/PEO/AgNPs	Acetic acid	80	~100	Wound dressings	[120]
Chitosan/gelatin/AgNPs	Acetic acid	87	220–400	Wound dressings	[121]

1.5.5. **Polyvinyl alcohol (PVA)**

As discussed in section 1.5.4 Poly(vinyl alcohol) (PVA) can be successfully blended with chitosan in order to facilitate electrospinning

PVA is a synthetic water-soluble polymer. It is produced by the hydrolysis of poly(vinyl acetate). The chemical structure of PVA is shown in Figure 6.

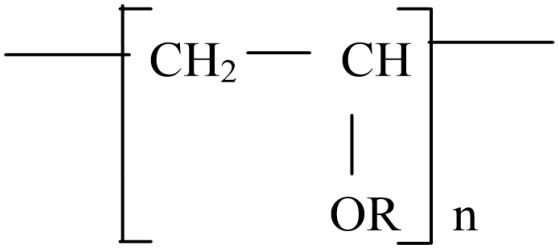

where R = H or $COCH_3$

Figure 6: Chemical structure of poly(vinyl alcohol) [122]

PVA has a simple structure containing a pendant hydroxyl group. PVA is available in a number of different grades based on the degree of hydrolysis. These are grouped into fully hydrolysed and partially hydrolysed. The degree of hydrolysis is determined by the amount of acetate groups remaining in the polymer backbone. This degree of hydrolysis has an effect on the chemical properties, crystallisability and solubility of the material [123].

It has been shown that the higher the degree of hydrolysis the harder it is to dissolve PVA in water. The residual acetate groups in partially hydrolysed PVA are hydrophobic and weaken the intermolecular hydrogen bonds between the hydroxyl groups resulting in easier dissolution. For PVA with a high degree of hydrolysis to dissolve typically a temperature above $70^{o}C$ is required [124].

PVA has been shown to be highly biocompatible as well as non-toxic and as such it finds applications in a wide range of fields including medical, food, cosmetic, pharmaceutical and packaging [125].

1.6. Electrospinning of Polyhydroxybutyrate (PHB)

1.6.1. **Background of PHB**

Polyhydroxybutyrate (PHB) is a polymer which is a part of the polyhydroxyalkanoate (PHA) family of polyesters which can be naturally synthesised from sugars and lipids by bacterial fermentation [126].

PHAs are naturally produced as a way for bacteria to store carbon as an energy source. This occurs when nutrient supplies are imbalanced and there is a shortage of phosphorous, nitrogen and oxygen while maintaining an excess supply of a carbon source [126, 127]. The discovery of bacteria's ability to produce PHA's was made by Lemoigne in 1926 with PHB being identified as the material of the inclusion bodies [128].

The bacterially produced PHA's were shown to have similar properties to synthetically produced polypropylene and was shown to be a viable replacement [129]. Synthetic polymers have been hugely popular, thanks primarily to their low costs of production compared to the much greater cost of PHA production. This has meant that PHAs have been somewhat ignored in favour of the much cheaper synthetic polymers [130]. There are three main factors contributing the high cost of PHB production; the cost of the carbon source, fermentation process, polymer extraction and purification. Many advances have been made towards refining the production process over the years to make it more economically viable [131].

Even now the production costs of PHAs are far greater than synthetic polymers; however, thanks to an ever growing theme of the masses turning to environmentally friendly products, research into PHA production has become more popular. In recent

years the damaging environmental effects of synthetic polymer production has become more apparent and more of a concern due to the use of potentially harmful chemicals [132]. As a result there has been a boom in the amount of research carried out to find non-polluting polymers to be used as a replacement.

The primary focus of research into PHA production is to make the process more economically viable. One method of bringing down the cost of production is the use of alternative carbon sources which are less expensive and have higher yields of PHA production [133]. Table 5 gives a list of some carbon sources commonly used in PHB production and the respective costs and PHB yields from each carbon source.

Table 5: Carbon sources used in PHB production along with corresponding cost and theoretical yield of PHB [134]

Carbon Source	Yield of PHB/substrate (g)	Approximate cost (¥ /kg)	Approximate cost (£/kg)
Methanol	0.54	55	0.31
Ethanol	0.62	110	0.63
Acetic acid	0.48	200	1.14
Glucose	0.48	120	0.68
Sucrose	0.50	28	0.16

PHB can be produced by using plant oils as a carbon source as opposed to the other substrates commonly used. Plant oils contain a much greater amount of carbon atoms per gram compared to these other substrates and bacteria are able to achieve a higher theoretical yield [135]. A theoretical yield of 0.98 g/g has been shown to be possible from bacteria utilising plant oils [136]. It can be seen from Table 5 that less than half this yield, 0.48 g/g, can be achieved when using glucose [134].

1.6.2. **Structure and Properties of PHB**

PHB is a homopolymer made of chains of the same monomer unit which has the same basic structure of (R)-3-hydroxyalkanoic acid, the same as all the PHAs, as shown in Figure 7, with CH_3 as the functional R group.

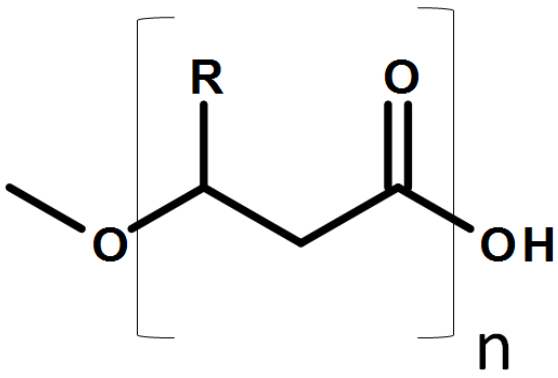

Figure 7: Chemical structure of PHAs whereby the R group is replaced with a functional group, CH_3 in the case of PHB

PHB is a semi-crystalline polymer, made up of both an amorphous region and a crystalline region [137]. The amorphous region of a polymer is made up of polymer chains in a random orientation with no degree of order. The crystalline region however is very ordered, with chains lined up in a linear fashion. The degree of crystallinity within a polymer determines many of its properties. Highly amorphous polymers are typically transparent while highly crystalline polymers have a greater refractive index and are typically opaque [138]. PHB is known to have a high crystallinity which can be greater than 50 % crystalline [139].

The degree crystallinity contributes to determining the stiffness of a polymer. As expected for a polymer with a high crystallinity, PHB has been shown to be both stiff and brittle [140]. This property is generally not desirable in a material and makes PHB unsuitable for many commercial applications. Electrospinning has been shown to be capable of reducing polymers crystallinity if the right parameters are used during the process [141]. If PHB were to be electrospun under the right conditions these stiff and brittle properties could potentially be greatly improved to a ductile material.

As mentioned in section 1.6.1 PHB has been suggested as a replacement for polypropylene because it shows similar thermal and mechanical properties without the negative environmental concerns from production. Table 6 shows a comparison of the main properties of PHB compared with polypropylene.

Table 6: Physical and mechanical properties of polypropylene and PHB [142]

Property	**Polypropylene**	**PHB**
Melting temperature (^{o}C)	176	175
Glass transition temperature (^{o}C)	-10	4
Tensile strength (MPa)	38	40
Extension to break (%)	400	6
Crystallinity (%)	70	80
Density (g/cm^{3})	0.905	1.250

PHB is particularly suitable for tissue engineering applications because of its high biocompatibility. *In vivo* PHB has been shown to degrade by a hydrolysis reaction. The ester bonds are broken down to produce carbon dioxide and water as waste

materials [143]. *In vivo* it has been shown that tissue reaction to PHB film implants is relatively low and was the same as the tissue reaction to the glass plate used as a control. This indicates high biocompatibility and is thought to be due to the presence of natural PHB oligomers and 3-hydroxybutyrate, which are the intermediate degradation products of PHB, in animal tissues under normal conditions [144].

There are many different bacteria capable of producing PHAs when subjected to unbalanced growth conditions with a number of these specifically producing PHB.

Table 7 has been modified from the review paper by Verlinden et al. [126] and shows an overview of the bacterial strains that can be used to produce PHB.

Table 7: Overview of the bacterial strains used to produce PHB including the initial carbon source used

Bacterial strain	Initial carbon source	Reference
Alcaligenes latus	Malt, soy waste, milk waste, vinegar waste, sesame oil	[145]
Bacillus cereus	Glucose, e-caprolactone, sugarbeet molasses	[146]
Bacillus spp.	Nutrient broth, glucose, alkanoates, e-caprolactone, soy molasses	[147]
Burkholderia sacchari sp. nov	Adonitol, arabinose, arabitol, cellobiose, fructose, fucose, lactose, maltose, melibiose, raffinose, rhamnose, sorbitol, sucrose, trehalose, xylitol	[148]
Burkholderia cepacia	Palm olein, palm stearin, crude palm oil, palm kernel oil, oleic acid, xylose, levulinic acid, sugarbeet molasses	[149]

Caulobacter crescentus	Caulobacter medium, glucose	[150]
Escherichia coli mutants	Glucose, glycerol, palm oil, ethanol, sucrose, molasses	[151]
Halomonas boliviensis	Starch hydolysate, maltose, maltotetraose and maltohexaose	[152]
Legionella pneumophila	Nutrient broth	[153]
Methylocystis sp.	Methane	[154]
Microlunatus phosphovorus	Glucose, acetate	[155]
Ralstonia Eutropha	Glucose, sucrose, fructose, valerate, octanoate, lactic acid, soybean oil	[126, 156]
Rhizobium meliloti, R. viciae, Bradyrhizobium japonicum	Glucose, sucrose, galactose, mannitol, trehalose, xylose, raffinose, maltose, dextrose, lactose, pyruvate, sugar beet molasses, whey	[157]
Rhodopseudomonas palustris	Acetate, malate, fumarate, succinate, propionate, malonate, gluconate, butyrate, glycerol, citrate	[158]
Spirulina platensis (cyanobacterium	Carbon dioxide	[159]
Staphylococcus epidermidis	Malt, soy waste, milk waste, vinegar waste, sesame oil	[160]

Ralstonia eutropha (also known as *Cupriavidus nectar* or *Alcaligene eutrophus)* is one of the most extensively studied strains of bacteria for PHB production as it is the most cost-effective process and is capable of producing high yields of PHB ~90 %w/w [126]. *R. eutropha* are a versatile strain of bacteria to use for studying PHB synthesis because they are able to utilize a number of different carbon sources, including vegetable and plant oils, to accumulate PHB [161].

1.6.3. **Applications of PHB**

PHB is an attractive material to study because it is suitable for a number of different applications across a range of fields. As mentioned previously it shares similar properties with polypropylene and other synthetic polymers which are currently used for packaging materials, and by making blends and composites the properties of PHB can be further enhanced to make them more suitable for packaging. PHB's characteristic of being completely nontoxic make it particularly attractive for food packaging [162].

PHB can be used as an implant material in medicine due to its biodegradable and biocompatible properties which mean that PHB does not cause any immune response and therefore the body will not reject the implantation [163]. The biodegradable nature of PHB means it does not have to be removed from the body after serving its function. The body can reabsorb PHB as it degrades as the monomer of PHB is a metabolic in the blood so PHB can be used as a seam thread for healing wounds and blood vessels [144]. Other medical devices have also been made from PHB such as screws and plates for bone fixation, bio-absorbable surgical structures, surgical meshes [164] and wound covers [165]. PHB has also attracted some interest recently for use in tissue engineering applications.

In an attempt to improve the mechanical properties of PHB copolymers of PHB have been produced. By using mixed substrates in the production of PHB using bacteria, such as using valerate in addition to glucose, the micro-organisms may convert the substrates into poly(3-hydroxybutyrate-co-3-hydroxyvalerate) (PHBV) or poly(3-hydroxybutyrate-co-4-hydroxybutyrate) (PHB4B) [166]. Figure 8 shows the two monomers, PH3B and poly-hydroxyvalerate (PHV) and how they combine to form

PHBV. When a mixture of substrates are used, the copolymer formed typically consists of a random composition of monomer units however the composition of the copolymer can be manipulated through altering the concentrations of the different substrates to achieve the desired ratio of the two monomers [167].

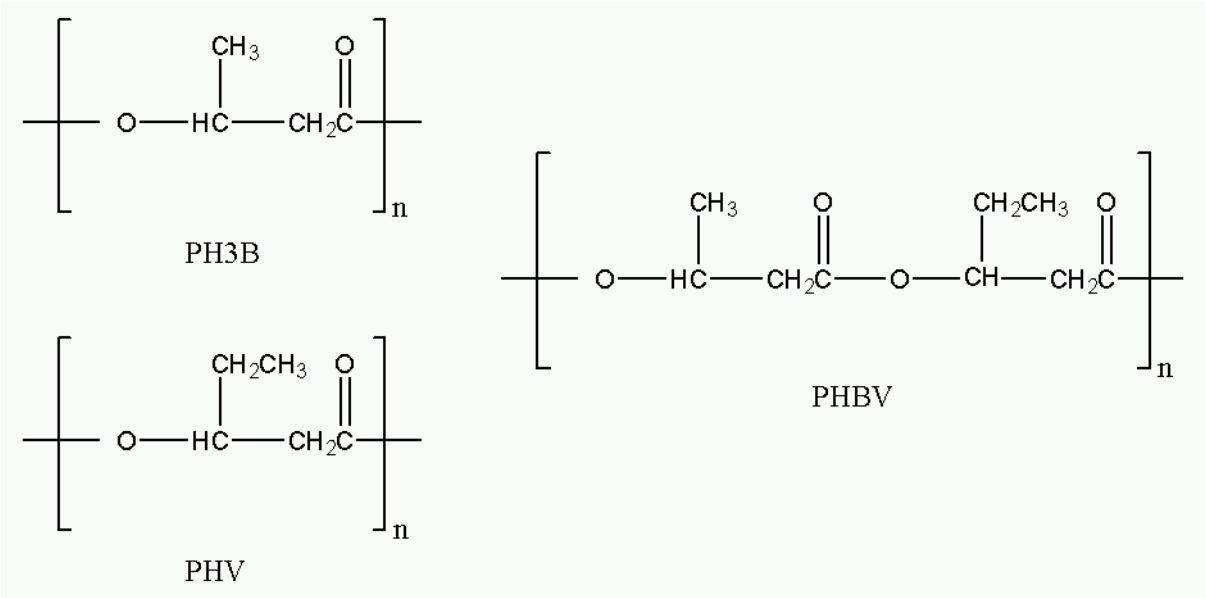

Figure 8: Chemical structure of PHBV copolymer [168]

Copolymers such as PHBV have been shown to be less brittle and less stiff than the homopolymer PHB but still retain most of the other positive mechanical properties of PHB [126].

1.6.4. **Electrospinning PHB**

Despite the popularity of electrospinning in recent years and the potential of PHB as a biomaterial there are relatively few papers detailing the electrospinning of PHB. Sombatmankhong et al. [169] reported the electrospinning of PHB and the

copolymer PHBV. They used commercially purchased PHB and PHB with M_w of 300,000 g/mol and 680,000 g/mol, respectively. They were able to successfully produce fibres from solutions ranging from 10-16 % using chloroform as the solvent. The average fibre diameter obtained from PHB fibres ranged from 1.6 – 8.8 µm and 1.6 – 4.7 µm for PHBV. These are very large fibre diameters by electrospinning standards, a process which has been shown to produce fibres smaller than 100 nm [20]. The natural extracellular matrix has been shown to be made up of collagen fibres with diameters ranging from 50-500 nm [170], it would therefore be desirable to replicate these dimensions as closely as possible so as to produce a scaffold suitable for cell attachment and proliferation.

The reports of the production of large fibre diameters when electrospinning PHB are not exclusive to the work of Sombatmankhong et al. Suwantong et al. [171] produced even larger diameters at 2.7 ±1.7 µm also using commercially purchased PHB with a molecular weight of 300,000 g/mol dissolved in a 14% chloroform solution and electrospun at 12 kV with a needle tip distance to the ground collector of 20 cm. The use of the co-polymer PHBV, molecular weight 680,000 g/mol, once again resulted in smaller fibre diameters of 2.3 ± 2.1 µm.

The large fibre diameter of electrospun PHB had previously been acknowledged by Choi et al. [172]. They had produced PHBV fibres with diameters ranging from 1 µm-4 µm but recognised that these were too large for the scaffolds to be a viable replacement for the natural extracellular matrix, which is made up of randomly oriented collagen fibres with nanometre-scale dimensions. As an attempt to reduce the fibre diameter they utilised the addition of salt in order to improve the surface tension and conductivity of the solution. As previously discussed increased solution conductivity can lead to greater elongation forces and thinner fibres. Three salts

were studied in the work by Choi et al. [172] and were chosen due to their solubility in chloroform, the solvent used for PHB electrospinning, and the ease of removing the salt from the produced scaffolds by a methanol treatment. These salts were benzyl trimethylammonium chloride (BTMAC), benzyl triethylammonium chloride (BTEAC) and benzyl tributylammonium chloride (BTBAC). The salts were added up to a concentration of 3 wt%. A small addition of salt was shown to result in a decrease in average fibre diameter, a reduction from ~ 2.6 µm with no salt present to ~ 1.0 µm with the addition of 1 wt% BTEAC. Further addition of salt beyond 1 wt% did not yield any further diameter reduction. The addition of the three salts did not have a significant impact on the viscosity of the solution nor the surface tension, but did significantly increase the solution conductivity. The degradation rate of the scaffolds were seen to be higher in the scaffolds electrospun with the salts however this was attributed to the reduction in fibre diameter and therefore increase in surface area as opposed to a change in the chemical properties.

1.7. Aims and objectives

The main aim of this work is the production and characterisation of electrospun polymeric scaffolds based on chitosan and bacterial polyhydroxybutyrate produced using three different carbon sources; glucose, olive oil and rapeseed oil.

1.7.1. **Specific objectives**

1. Electrospin PVA under different solution and operating parameters in order to determine the optimum parameters for PVA scaffold production in terms of creating uniform fibre morphologies and a high crystallinity.
2. Electrospin pure chitosan from an acetic acid solution of varying concentrations in an attempt to replicate the work by Vrieze [86].
3. Study the effects of different blend ratios, solution parameters and operating parameters of the resultant scaffolds of chitosan/PVA blends and characterise the fibres.
4. Create fibres from a water based chitosan/PVA system with the addition of hydroxybenzotriazole to negate the need to the use of acetic acid as a solvent and compare the morphologies of the resultant fibres to those produced using the more traditional solvent system.
5. Compare the production yields of PHB produced from the *R. eutropha* strain of bacteria using rapeseed oil and olive oil as carbon sources to the more conventional glucose carbon source.
6. Electrospin the PHB from all three carbon sources to determine whether nanofibres can be produced.

7. Examine the properties of the PHB produced using oils and compare it to the PHB produced using glucose to determine if the oils are suitable as a viable replacement for glucose.
8. Study the effect of the carbon source on the resultant electrospun fibres in terms of both morphology and thermal properties.
9. Attempt to reduce the average fibre diameter of electrospun PHB below 1 µm, which is the common size found in the literature [172], through the addition of the salt Benzyl triethylammonium chloride.

1.7.2. **Justification**

The field of electrospinning research has grown exponentially over the last decade however despite this there is still a lack of coherence with regards to the consistency of the results, with conflicting reports on the effects of solution parameters and operating parameters. This is likely due to the dynamic nature of the electrospinning process whereby small changes in parameters can have dramatic effects on the properties and the morphologies of the produced fibres.

Electrospun materials are known to have potential applications in the fields of energy, environmental engineering and biomedicine. These are fields where an understanding and high degree of control over the fibre properties are essential. Alterations in fibre diameters will affect the porosity and potential filtration properties as well as the tensile strength and potentially drug delivery efficiency due to a decreased surface area to volume ratio. The effects of altering parameters on the crystalline properties are also very important to understand as the degree of crystallinity will affect such properties as degradation rate and mechanical strength.

By studying the effect of altering parameters on crystallinity it may be possible to then tailor the process in order to obtain a desired crystallinity value.

Due to the amount of research presently taking place into electrospinning studies looking into the effect of these parameters has already taken place, but inconsistencies arise because everyone is using slightly different electrospinning setups. Due to this, recreating identical repetitions of experiments by different research groups is almost impossible. There are isolated reports of certain parameters that allow chitosan to be electrospun in its pure form, without the addition of another polymer, however there are many more publications which claim this is not possible [54, 80, 81].

This study aims to rule out some of these inconsistencies by performing the same detailed characterisation studies on the effects of electrospinning parameters on a number of different polymers and polymer blends in order to get an undistorted view of the effects of the electrospinning process where the differences between the blend behaviours or different polymer behaviours could not simply be explained by the use of different equipment. This should yield some overarching results which detail the effects of altering parameters on the electrospinning process.

PHB has been shown to be a promising biomaterial with a wide range of applications; however its application has been hindered due to the high cost associated with the synthesis. These costs are incurred due to the fermentation and extraction processes but also due to the carbon substrate required [173].This study aims to look into the effect on the material properties of using two different carbon sources for PHB production, olive oil and rapeseed oil as compared with glucose. Glucose was chosen as a control substrate as it is a very common carbon source

used in the production of PHB from bacterial cells and is one of the most researched [161]. Oils were chosen to be studied as a potential alternative to the more traditional glucose as a bacterial mechanism takes place when oils are utilised which converts the fatty acids present in the oil to PHB. Plant oils contain many more carbon atoms per gram as compared to alternative substrates used in PHB production such as glucose so they will potentially yield a much greater amount of PHB [174].

The two oils studied were selected for various reasons. It is hypothesised that although olive oil is more expensive per tonne than glucose it may produce a greater yield of PHB therefore undercutting the overall cost of using glucose to produce a given amount of PHB. Rapeseed oil has a comparable cost to glucose, however once again due to the increased number of carbon atoms it should produce a much greater yield of PHB. Rapeseed oil is also present in most cooking oils and it has been proposed that waste cooking oil could be used as a low cost carbon source for use in PHB production [161]. The bacterial species *R.eutropha* has been selected as the bacterial strain for PHB production in the present work as it is a cost effective bacterium which has been shown to accumulate as much as ~90% w/w PHB [175]. Additionally a wide range of carbon sources, including olive oil, rapeseed oil and glucose have previously been successfully utilised to produce PHB using *R. eutropha* [161].

As previously discussed in section 1.6.4 electrospinning is one process which could be utilised to process as produced PHB into a scaffold ready for application. In the current literature, reports on electrospinning bacterially produced PHB do not discuss the source or properties of the PHB and is commonly purchased from a commercial supplier. This work differentiates itself as the PHB synthesis has been carried out by

a known source and therefore differences in properties can be accounted for from alterations in the synthesis all the way to scaffold production with analysis of the effects of different carbon sources and parameters.

2. MATERIALS AND METHODS

2.1. Electrospinning

A model ES1a electrospinning machine, manufactured by Electrospinz, New Zealand, was used for the initial series of experiments. The ES1a set-up is shown in Figure 9. The header tank contains the polymer solution and is connected to the needle tip by capillary tubing. This set-up uses a gravity-feed based system. The flow rate of the solution is controlled by raising or lowering the header tank. This set-up also allowed for varying the distance between the needle tip and the collecting plate by way of a sliding mechanism from 0-20 cm. Applied voltage can be altered on the power supply ranging from 0-30 kV. The needle tips used with this system were Axygen T-200-4 which had an internal diameter at the tip of 0.8 mm. In this setup electrospinning is achieved horizontally.

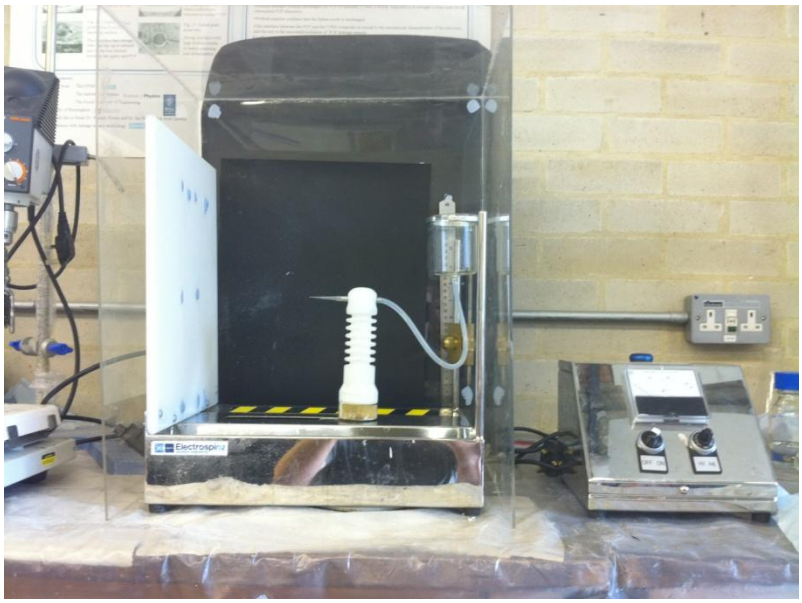

Figure 9: Optical image of an ES1a Electrospinning machine.

The second set-up used was a more conventional system aligned in a vertical orientation with the needle located above the collecting plate and was used to provide more control over the flow rate of the solution to the needle tip. This set-up consisted of a DC power supply (Model 73030P, Genvolt, UK) capable of providing a

voltage range of 0-30 kV and a NE-300 syringe pump (Pump systems inc.) with a dispensing accuracy of ± 1% and a 10 ml syringe (BD, New Jersey) with a blunted 25G stainless steel needle (BD, New Jersey). The collecting plate consisted of a sheet of stainless steel covered with aluminium foil to collect fibres on. This steel sheet was placed on a jack allowing needle tip distance to be varied up to a maximum distance of 30 cm. An image of this electrospinning set-up is shown in Figure 10.

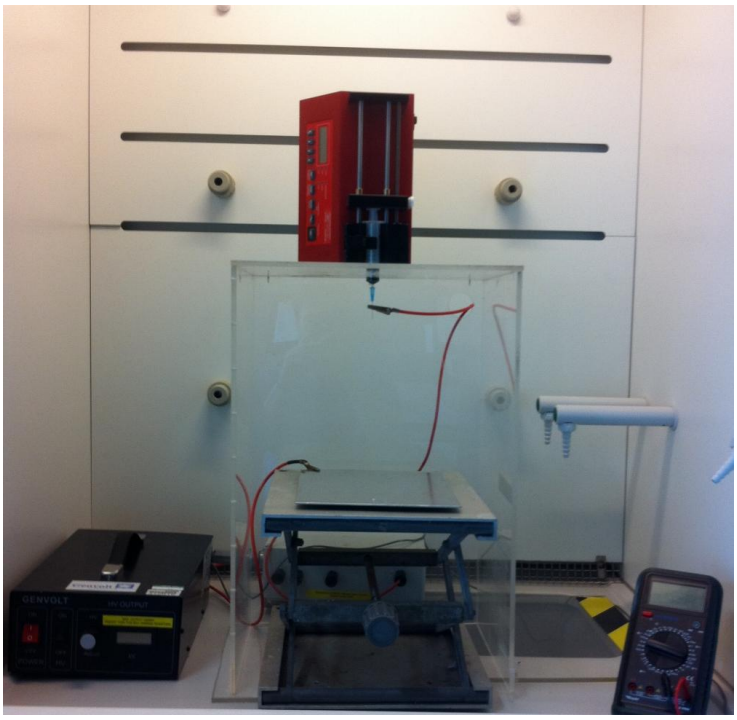

Figure 10: Optical image of the Custom built electrospinning machine.

The exact parameters used for electrospinning varied for each series of experiments and will be detailed in subsequent sections. The parameters varied were the applied voltage, needle tip distance, and flow rate. All other parameters were kept constant, with a room temperature maintained at 22^{o}C.

The experimental protocol was as follows; before carrying out each experiment the electrospinning machine was washed out by passing distilled water through it, to ensure there were no blockages and to rinse away old solutions which may still have been present from previous use. The electrospinning machine was placed inside a Perspex box inside the fume cupboard. The machines parameters were adjusted to the desired values (details of which are outlines in subsequent sections). Aluminium foil was attached to the collecting plate on which the produced fibres were collected. Solution was added to the header tank or drawn into the syringe depending on which machine was used. The solution was allowed to flow to the end of the needle tip in order to remove all air from the system. The header tank on the ES1a machine was covered with parafilm in order to prevent evaporation of the solution while electrospinning took place that cause solution concentration changes. The perspex box was then sealed ready for the high voltage supply to be turned on to carry out electrospinning.

The process was allowed to run for five hours in order to produce enough material for thermal analysis. Care was taken to monitor the electrospinning process while it was running to identify any polymer solidifying at the needle tip which could either partially block of fully block the needle tip and effect the resultant scaffold. If such a blockage was observed the process would be halted and the blockage removed before electrospinning commenced again. Once completed the foil sheet covering the collecting plate was removed and placed in a desiccator for at least 24 hours to allow the residual solvent and moisture to evaporate.

2.2. Scanning Electron Microscopy (SEM)

Scanning electron microscopes work by tracing an electron beam over the specimen you wish to view. When the beam hits the specimen secondary electrons are dislodged from the surface in unique patterns. A secondary electron detector is used to collect these electrons and registers different levels of brightness on a monitor. An image of the specimen can then be built up pixel by pixel as the microscope beam scans over it [176].

Two scanning electron microscopes were used during the course of this work. Initially a Phillips XL-30 SEM was used for the first series of experiments however in later work a Phillips XL-30 FEG ESEM (Environmental Scanning Electron Microscope) was utilised in order to obtain higher resolution micrographs.

After electrospinning each sample was dried in a desiccator for 24 hours. Small sections were cut out of the foil from all over the fibre deposition area and were attached to SEM stubs using adhesive carbon film. The samples were then coated with platinum using an Emscope SC500 (Emscope laboratories, Kent, UK) sputter coater. Coating was performed for 3 minutes at a current of 25 mA.

Average fibre diameters were determined from the SEM micrographs by using Image J software (National Institutes of Health, USA) to measure 200 individual fibre diameters from at least 5 micrographs taken of sections spread across the deposition area for each scaffold.

2.3. FTIR

Fourier transform infrared spectroscopy (FTIR) is an analytical technique which can be used to identify chemical bonds based on their infrared absorption behaviour.

This information can be using to identify unknown substances based on which chemical bonds are present in the sample [176].

A Nicolet FTIR spectrometer (Magna-IR 850) was used to obtain FTIR spectra of the scaffolds using a golden gate single reflection diamond Attenuated Total Reflectance (ATR) attachment. Each spectrum was made up from 100 scans with a resolution of 4 cm^{-1} and a wave number range or 650-4500 cm^{-1}.

2.4. Differential Scanning Calorimetry (DSC)

DSC is a very useful thermal analysis technique which is able to look at how a material's heat capacity in changed by temperature. It is suitable for many materials including polymers. A sample's mass is accurately measured before being heated and cooled while monitoring the changes in the heat flow and therefore heat capacity in comparison to a reference (typically an empty pan). This technique allows for the detection of different transitions such as melting, glass transition and crystallisation viewed as exothermic or endothermic peaks on the trace produced.DSC provides a much more accurate method of measuring the melting temperature of a material than the traditional melting point apparatus and allows for the calculation of the crystallinity of the sample, the method of which will be described below.

DSC was used to obtain information on the phase transitions in the samples. A Perkin-Elmer DSC7 machine was used. Approximately 5mg of material was peeled off the collecting foil and packed into a covered aluminium pan. The reference pan was also covered but left empty. The samples were subjected to a temperature scan of 25^{o}C to 225^{o}C at a heating rate of 10^{o}C /min for the first heating cycle. The temperature was then held at 225^{o}C for 2 minutes before cooling back down to 25^{o}C

at a rate of 10^{o}C /min. After this first cycle and subsequent heating scan was made again from 25^{o}C to 225^{o}C at 10^{o}C /min.

These scans were used to determine the glass transition temperature (T_g), the melting temperature (T_m) and the crystallisation temperature (T_c) of the samples. ICTAC (International Confederation for Thermal Analysis and Calorimetry) standards dictate that the T_m for metals and organics should be taken as the onset of the melting peak, while the peak value should be used in the case of other polymers. As the materials studied in the present work are all organic polymers the T_m shall be taken as the onset of the melting peak, however peak values of melting shall also be recorded in order to represent the temperature at which complete melting has taken place. The T_g of PHB is known to be around 2^{o}C [177] and therefore it should not be present in the DSC scans as our temperature range starts at 25^{o}C. T_c will be observed on cooling of the samples and not on the heating sequence as all the polymers being studied are semi-crystalline and are therefore already crystallised, but T_c for re-crystallisation will be observed on cooling.

The degree of crystallinity was calculated from data obtained in the DSC traces using the equation below [178]

$$X_c(\%) = \frac{\Delta H_f^m}{\Delta H_f^{100\%}} \times 100$$

Where X_c = percentage crystallinity (%), ΔH_f^m = Heat of fusion (J.g^{-}1) and $\Delta H_f^{100\%}$ = the heat of fusion for 100% crystalline material (J.g^{-1}). The value for $\Delta H_f^{100\%}$ was found in the literature for each material studied.

$\Delta H_f^{100\%}$ for PVA = 155 J.g^{-1} [179] $\Delta H_f^{100\%}$ for PHB = 146 J.g^{-1} [180]

2.5. Gel Permeation Chromatography (GPC)

Gel permeation chromatography is a technique which is used to measure the molecular weight (M_n) of organic-soluble polymers. This is a chromatographic method by which particles are separated based on their hydrodynamic volume, or in layman's terms their size. An organic solvent is required as an eluent and acts as the mobile phase while the stationary phase is made up of beads of porous polymeric material with a range of known pore sizes which are contained within a column. When the polymer solution is injected into the column, different sized particles will filter through at different rates, as small particles will enter into the pores of the stationary phase polymer while larger particles will not [181].

GPC was used to measure the molecular weight of the PHB produced by *R. Eutropha* using the three different carbon sources. It was also carried out on the PHB after it had been electrospun from G-PHB, O-PHB and R-PHB at concentrations of 1.5 %, 2 % and 2.5 %. The weight-average molecular weight (M_w) and number-average molecular weight (M_n) were obtained from the GPC. These values were subsequently used to determine the polydispersity (PD) by the ratio of M_w to the M_n.

2.6. Chitosan/PVA

2.6.1. **Materials**

Polyvinyl alcohol (PVA) (Mw ≈ 72,000 Daltons with a degree of hydrolysation ≥98%) was purchased from Merck, Germany. Chitosan from shrimp shells ≥75%-85% de-acetylated with a molecular weight ≈ 200,000 Daltons and Chitosan from shrimp shells ≥75%-85% de-acetylated with a molecular weight ≈ 110,000 Daltons,

Hydroxybenzotriazole hydrate wetted (HOBt.H2O) and Acetic acid 96% puriss were purchased from Sigma-Aldrich UK.

2.6.2. **Electrospinning of PVA**

PVA solutions were prepared by dissolving PVA powder in deionised water for 2 hours at 80 ^{o}C with constant stirring from a magnetic stirrer in order to produce a homogeneous solution. Solutions were then allowed to cool to room temperature. Four solutions with different concentrations were made, 6 %, 8 %, 10 % and 12 % weight/volume (w/v) whereby 10 g of PVA powder would be added to 100 ml of deionised water in order to make a 10 % solution for example.

The prepared solutions were electrospun using the gravity feed electrospinning set-up (Figure 9) at four different voltages; 10 kV, 15 kV, 20 kV and 25 kV. For this series of experiments the effect of applied voltage on fibre formation and crystallinity of produced scaffolds for different solution concentrations was the area of interest and therefore all other parameters were kept constant. A needle tip distance of 10 cm was maintained and the header tank was kept at a height of 25 cm, with the height being directly proportional to the flow rate.

2.6.2.1. SEM

Samples were prepared for SEM analysis using the method described in section 2.2. The prepared samples were then viewed under a Phillips XL-30 SEM. Average fibre diameters were determined from the SEM micrographs by using Image J software.

2.6.2.2. DSC

Samples were prepared and DSC was carried out as described in section 2.4.

2.6.3. **Chitosan**

Chitosan solutions were made up in a variety of configurations:

a) Low molecular weight chitosan (≈110,000 Da) dissolved in a 2 % acetic acid solution under gentle magnetic stirring at room temperature for 2 hours. The concentration was varied between 1-5 wt %
b) Higher molecular weight chitosan (≈200,000 Da) dissolved in a 2 % acetic acid solution under gentle magnetic stirring at room temperature for 2 hours. The concentration was varied between 1-5 wt %
c) Low molecular weight chitosan dissolved in a concentrated 90 % acetic acid solution under gentle magnetic stirring at room temperature for 2 hours. The concentration was varied between 1-5 wt %
d) Higher molecular weight chitosan dissolved in a concentrated 90 % acetic acid solution under gentle magnetic stirring at room temperature for 2 hours. The concentration was varied between 1-5 wt %

Once solutions had been made up, they were electrospun using the custom made electrospinning setup (Figure 10). The electrospinning parameters were varied throughout their whole range of values. The voltage was varied from 0-30 kV, the needle tip distance from 5-25 cm and the flow rate from 0.3-2 ml/hr.

The collected deposits were coated with platinum and viewed under the Phillips XL-30 FEG ESEM to observe the morphology and determine whether fibre formation had been successful.

2.6.4. **Electrospinning of Chitosan-PVA blends**

Chitosan-PVA blends were prepared by initially preparing individual Chitosan and PVA solutions. PVA solutions were prepared by dissolving PVA in appropriate concentrations in deionised water. This was carried out at 80^{o}C under magnetic stirring for a period of 2 hours. The solution was allowed to cool before being added to the chitosan solution. The chitosan solution was prepared by dissolving chitosan in 2% acetic acid at room temperature under magnetic stirring for 2 hours. Once both solutions were prepared and appeared to be homogenous they were added together and magnetically stirred for a further 2 hours.

The chitosan and PVA solutions were combined in a number of different blend ratios. Table 8 shows the details of the different blends including the overall solution concentrations, the relative % of each polymer and the blending ratio used. Overall solution concentrations were varied from 5-8 %. These concentrations meant the PVA concentration present was lower than in the previous series of experiments where PVA was electrospun on its own. This was the case because the addition of even small percentages of chitosan greatly added to the solutions viscosity. The viscosity limits for electrospinning would have been exceeded if the optimum PVA concentration was used with chitosan added.

Table 8: Solution concentrations and blend ratios of chitosan-PVA solutions and the effective concentration of each polymer in solution.

Overall solution concentration (%)	Blend Ratio PVA:chitosan	PVA concentration within solution (%)	Chitosan concentration within solution (%)
5	90:10	4.5	0.5
	80:20	4	1
	70:30	3.5	1.5
	60:40	3	2
	50:50	2.5	2.5
6	90:10	5.4	0.6
	80:20	4.8	1.2
	70:30	4.2	1.8
	60:40	3.6	2.4
	50:50	3	3
7	90:10	6.3	0.7
	80:20	5.6	1.4
	70:30	4.9	2.1
	60:40	4.2	2.8
	50:50	3.5	3.5
8	90:10	7.2	0.8
	80:20	6.4	1.6
	70:30	5.6	2.4
	60:40	4.8	3.2
	50:50	4	4

Each of the chitosan-PVA blend solutions were subjected to two electrospinning studies.

The first study focused on the effect of the applied voltage on the morphology and thermal characteristics of the electrospun fibres. All of the operating parameters were fixed other than the applied voltage which was varied at 5, 10, 15, 20 and 25 kV. Three series of experiments were performed with the range of voltages at a needle tip distance of 7.5 cm, 10 cm and 12.5 cm. Flow rate was kept constant at 1 ml/hr for all three series.

The second study was concerned with the effect of the needle tip distance on the morphology and thermal characteristics of the electrospun fibres. The needle tip distance was varied at 7.5 cm, 10 cm and 12.5 cm. Electrospinning was carried out at these three needle tip distances with an applied voltage of 15, 20 and 25 kV.

For both of these studies the produced samples were characterised using SEM, DSC and FTIR.

2.6.4.1. SEM

Samples were prepared for SEM analysis using the method described in section 2.2. The prepared samples were then viewed under a Phillips XL-30 FEG ESEM. Average fibre diameters were determined from the SEM micrographs by using Image J software.

2.6.4.2. DSC

Samples were prepared and DSC was carried out as described in section 2.4

2.6.4.3. FTIR

FTIR was carried out on all the electrospun polymer blends and compared to the electrospun samples formed from just one polymer to confirm that the resultant scaffolds were indeed blends of the constituent parts. This was to rule out the possibility that the polymers had not blended in solution and the electrospun product contained just one of the polymers.

A small section of the deposition on the collecting plate was peeled away from the foil and placed under a golden gate single reflection diamond Attenuated Total Reflectance (ATR) attachment on the FTIR. Each spectrum was made up from 100 scans with a resolution of 4 cm^{-1} and a wave number range or 650-4500 cm^{-1}.

2.6.5. **Electrospinning of Chitosan-Hydroxybenzotriazole aqueous solution**

Hydroxybenzotriazole was weighed out with chitosan and added to water in a 1:1 and 2:1 chitosan:HOBt (w/w) ratio, the solutions were left overnight, subjected to magnetic stirring at room temperature to allow time for full dissolution. Solutions were made up in concentrations of 1, 2, and 3 %. The prepared solutions were electrospun under various operating parameters, applied voltage ranged from 0-30 kV, needle tip distance from 5-25 cm and flow rate from 0.3-2 ml/hr.

The collected deposits were coated with platinum and viewed under the Phillips XL-30 FEG ESEM to observe the morphology and determine whether fibre formation had been successful.

2.6.6. **Electrospinning of Chitosan-Hydroxybenzotriazole/PVA aqueous solution**

Hydroxybenzotriazole was weighed out with chitosan and added to water in a 1:1 and 2:1 chitosan:HOBt (w/w) ratio. The solutions were left overnight and subjected to magnetic stirring at room temperature to allow time for full dissolution. The prepared solutions were then added to a PVA solution to make up an overall solution concentration of 7% with a blend ratios of 90:10, 80:20 and 70:30 PVA:chitosan. Solutions were then electrospun with an applied voltage of 15 kV and 20 kV with a needle tip distance of 10 cm.

The collected deposits prepared as described in section 2.2 and viewed under the Phillips XL-30 FEG ESEM to observe the morphology and determine whether fibre formation had been successful.

2.7. PHB

Media preparation, fermentation and extraction were carried out by Dr Soroosh Bagheriasl at Wolverhampton University while the subsequent electrospinning and characterisation was carried out as part of the present work. The exact methodology used for the PHB production is detailed in Bagheriasl's thesis [182].

2.7.1. **Materials**

Chloroform and hexane were obtained from Sigma Aldrich, UK. *R. eutropha* cells were supplied by the National Collection of industrial and Marine Bacteria, Aberdeen, UK.

2.7.2. **Production of PHB**

2.7.2.1. Media Preparation

Tryptone soya agar (TSA), tryptone soya broth (TSB) and Basal salt medium (BSM) were all supplied by Lab M Ltd. The respective mediums were prepared by following the manufacturer's instructions. Once prepared the media were sterilised by placing in an autoclave for 15 minutes at 121^{o}C.

2.7.2.2. Carbon Sources

PHB was produced using three carbon sources. The carbon sources were Glucose, purchased from Lab M Ltd. Olive oil, purchased from ASDA and rapeseed oil purchased from Tesco.

2.7.2.3. Starter culture preparation

R. Eutropha was inoculated into 50 ml conical flasks along with 20 ml of TSB medium. The flasks were then placed in a rotary incubator (New Brunswick Scientific, UK) for 24 hours at a temperature of 30^{o}C and speed of 150 rpm. These could then be used as starter cultures for the subsequent fermentations.

2.7.2.4. Fermentations

Aseptic techniques were used to inoculate the fermentation media with the starter culture. The inoculation ratio was 8% v/v. The fermentations were performed in 500 ml Erlenmeyer flasks and were carried out using each of three carbon sources. A Bandelin electronic, UW 2200, sonicator was used for rapeseed oil and olive oil in order to make an emulsion with BSM. This was required as the oils were not miscible in BSM. For glucose the use of the sonicator was not required as glucose

was easily soluble in the BSM. BSM, starter culture and either glucose, olive oil or rapeseed oil were added to the flasks and then put into the rotary incubator for 48 hours at 30^{o}C and 150 rpm.

2.7.2.5. Extraction

After the fermentation has taken place the samples were centrifuged in a Hermle Labortechnik, Z300K at 6000 rpm for 15 minutes. The biomass was then removed from the supematant and placed in a freezer for 12 hours at -20^{o}C. Following this the biomass was freeze dried for 72 hours using an Edwards Freeze drier (Modulyo). The dried biomass was then extracted by the Soxhlet extraction method using chloroform. Soxhlet extraction was allowed to run for 5 hours.

Once the extraction process was complete the remaining chloroform from the extraction process was transferred to a 250 ml beaker and n-hexane was added drop wise in equal volumes to chloroform to precipitate the PHB. A magnetic stirrer was used to provide light agitation to the solution to aid the precipitation process. The precipitation product was removed from the solution and allowed to dry in a desiccator.

2.7.3. **Electrospinning of PHB chloroform solution**

Each series of experiments carried out on electrospinning PHB was replicated exactly for the three different carbon sources the PHB was produced with, PHB produced using olive oil (O-PHB), PHB produced using rapeseed oil (R-PHB) and PHB produced using glucose (G-PHB). The PHB samples were weighed out and dissolved in chloroform in three different concentration, 1.5 %, 2 % and 2.5 % w/v. Solutions were stirred at room temperature using a magnetic stirrer for 2 hours.

For electrospinning of PHB the electrospinning parameters used were

A) Applied voltage of 7 kV
B) Needle tip distance of 12.5 cm
C) Flow rate of 1 ml/hr

These parameters were determined after a series of experiments (results not shown) whereby the objective was to find operating parameters that were capable of yielding fibres from all of the different PHB solutions at different concentrations and from different carbon sources. These were therefore not the optimum parameters for any one solution but a compromise to allow results to be comparable.

2.7.3.1. SEM

Samples were prepared for SEM analysis using the method described in section 2.2. The prepared samples were then viewed under a Phillips XL-30 FEG ESEM. Average fibre diameters were determined from the SEM micrographs by using Image J software.

2.7.3.2. DSC

Samples were prepared and DSC was carried out as described in section 2.4

2.7.3.3. FTIR

After the extraction process from *R. Eutropha* a FTIR spectra was of the precipitant was obtained. This was compared to the spectra of commercial PHB (Sigma-Aldrich) to confirm that the product extracted was indeed PHB. The commercial samples of PHB were treated with hexane and chloroform for 24 hours to ensure an accurate comparison could be made.

2.7.3.4. GPC

The molecular weights and polydispersities before and after electrospinning were compared to determine what effect the electrospinning process has on molecular weight and chain length distributions.

GPC was carried out at Smithers-Rapra, Shawbury, UK. 20 mg of sample was dissolved in 10 ml of chloroform acting as the eluent. Once dissolved the solution was filtered through a 0.2 µm polyamide membrane. Analysis was carried out at a flow rate of 1.0 ml/min using PLgel guard columns. 2 mixed bed-B columns with a nominal flow rate of 1.0 ml/min at 30^{o}C.

2.7.4. **Electrospinning of PHB solution in chloroform with addition of BTEAC as ionising salt**

Solutions with a concentration of 2% were made up by dissolving PHB from each of the three carbon sources in chloroform as described previously. Once the solutions were prepared the salt BTEAC was added in 0.5% increments up to 2% with a control left with no BTEAC present.

The resultant solutions were electrospun under the same parameters as the previous series of experiments with PHB; applied voltage of 7 kV, needle tip distance of 12.5 cm and flow rate of 1 ml/hr so that results would be comparable.

The resultant fibres were soaked in methanol in order to remove any residual BTEAC remaining in the fibres. The scaffolds were then viewed under SEM in order to observe fibre morphologies and FTIR was performed to confirm that no BTEAC was present and the chemical structure of the PHB remained unchanged.

3. RESULTS AND DISCUSSION

3.1. Introduction to Results

The results presented in this chapter are split into two sections. The first section concerns the work carried out using PVA and chitosan and their various blends. The second section concerns the production and electrospinning of PHB.

3.2. Electropsun Polyvinyl alcohol (PVA)

As-received PVA was successfully made-up into 8 and 10 % solutions and subsequently electrospun at an applied voltage of 10, 15, 20 and 25 kV. SEM micrographs of the fibres produced from electrospinning the 8 % PVA solution at each of the four voltages can be seen in Figure 11. Two micrographs of each sample are presented, showing different magnifications, 2000x and 9000x. On the higher magnified micrograph some of the fibre diameters have been marked for illustration purposes.

From Figure 11 it can be seen that there is not a great difference in the morphology of the fibres produced from the 8% solution when applied voltage was changed from 10-25 kV. Under all applied voltages the formation of uniform, straight nanofibres was achieved. There were a few beads present in all of the scaffolds, but such a small amount that this was not deemed to be significant. The sample electrospun at 10 kV was considered to be the closest to being bead-free. In the samples electrospun at higher voltages, particularly 25 kV, there are small areas where the fibres appear to be connected or webbed. This is believed to be caused by the higher applied voltage in certain instances causing too much solution to be ejected from the needle tip, the temporarily thicker jet does not have enough time for the solvent to completely evaporate so the fibres arrive on the collecting plate still wet

and not fully formed, causing a blob in the area they land where some fibres may fuse together producing a webbing effect [183].

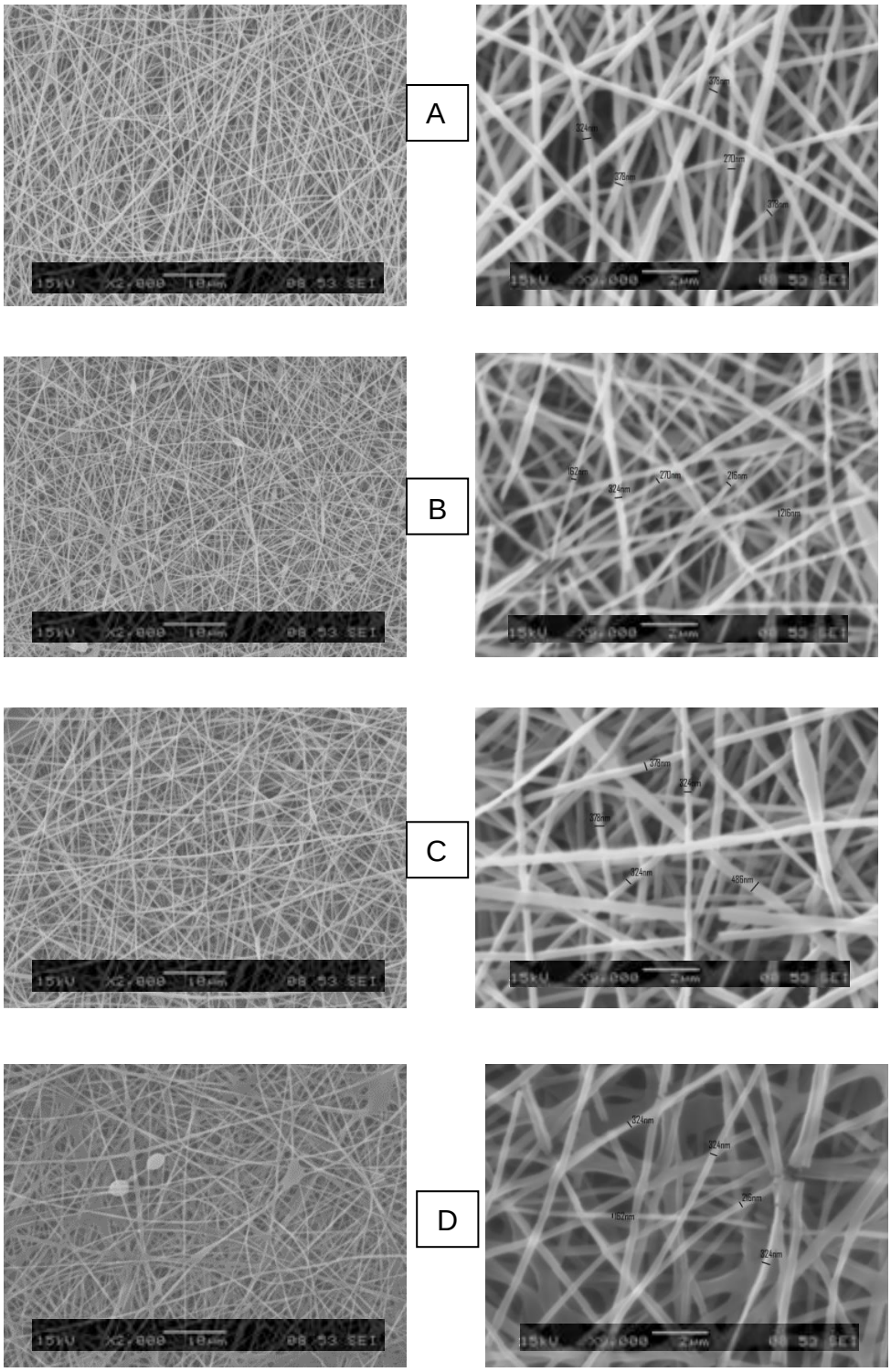

Figure 11: SEM micrographs of PVA nanofibres produced by electrospinning from an 8% solution at two different magnifications and electrospun with different applied voltages (A) 10 kV (B) 15 kV (C) 20 kV (D) 25 kV

This webbing effect could be controlled or prevented by having a greater control over the amount of solution allowed to flow to the end of the needle tip. This could be achieved either through using a needle tip with a smaller internal diameter or by using a syringe pump capable of controlling the rate the solution is supplied to the end of the needle tip. The apparatus used for the present series of experiments used a gravity feed system whereby the flow rate could easily be controlled. In subsequent experiments a different set up was used which incorporated a syringe pump allowing complete control over the flow rate.

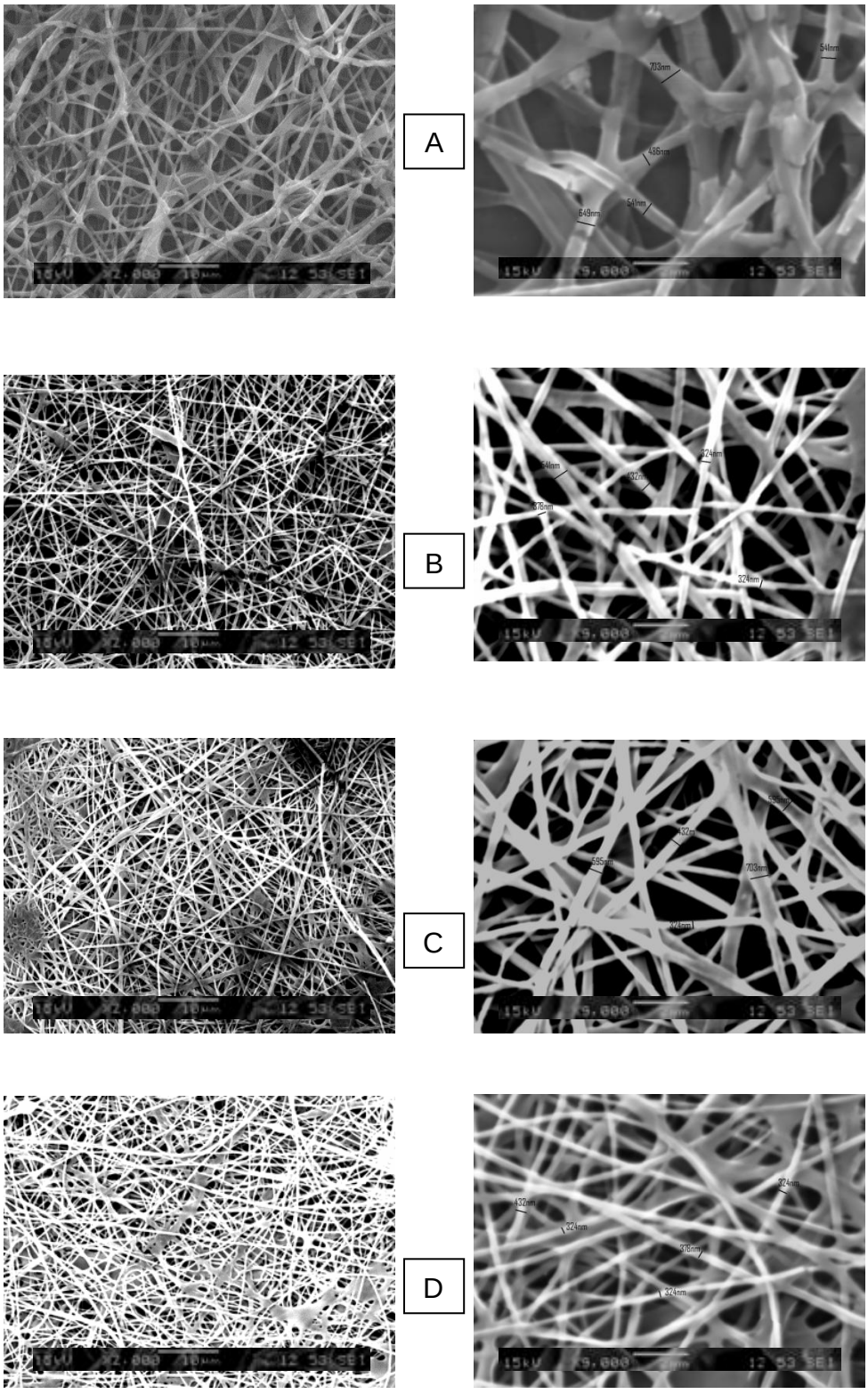

Figure 12: SEM micrographs of PVA nanofibres produced by electrospinning from a 10% solution at two different magnifications and electrospun with different applied voltages (a) 10 kV (b) 15 kV (c) 20 kV (d) 25 kV

SEM micrographs of the fibres produced from electrospinning the 10 % PVA solution at each of the four voltages can be seen in Figure 12. Once again two micrographs of each sample are presented at different magnifications, 2000x and 9000x, with some of the fibre diameters marked on the higher magnification image.

The fibre morphologies obtained from the 8 % PVA solution appear to be quite different to those obtained from the 10 % solution. While the former are straight and uniform in their dimensions, the latter show more branching and varying fibre diameters. This is likely due to the increased viscosity associated with a higher solution concentration resulting in greater chain entanglements which resist the stretching effect of the applied voltage and work to prevent fibre formation [30]. We can see as the voltage is increased from 10 kV to 25 kV that the fibres do become straighter and more uniform suggesting that higher voltages are necessary for electrospinning the 10 % solution.

The SEM micrographs were obtained using a Phillips XL-30 SEM. This was adequate to view the produced fibres at low magnifications however, when the magnification was increased for micrographs to be taken for the purpose of measuring fibre diameters it was not capable of providing a higher enough resolution to achieve satisfactory micrographs. In further work a higher quality Phillips XL-30 FEG ESEM was used in order to obtain higher quality micrographs.

The average fibre diameters from the scaffolds produced for the 8% and 10% solution were measured and are presented in Figure 13.

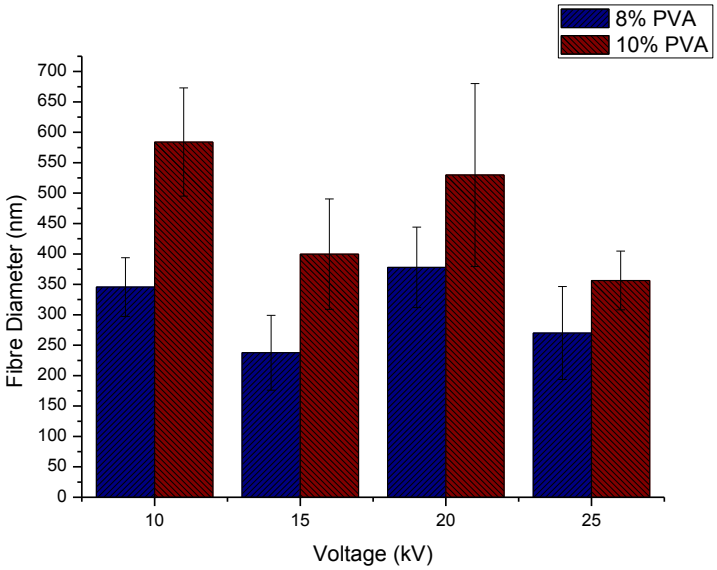

Figure 13: Average fibre diameter of PVA electrospun from 8% and 10% solutions with varied voltage.

The error bars in the Figure 14 depict the fibre distribution range. For example the scaffold produced from a 10% PVA solution electrospun at 10 kV contained an average fibre diameter of 582 nm with some of the fibres being as small as 495 nm and some as large as 773 nm. When producing an electrospun scaffold it is desirable to be able to produce fibres which have uniform dimensions across their whole length and all of similar dimensions. This allows for much more accurate predictions to be made on the properties and the function of the scaffold. The fibre diameter has an effect on the porosity of the scaffold [184], if a specific porosity is required for a particular application, for instance if the scaffold was being used as a filtration material, it would be unsuitable if some regions consisted of the desired porosity while others were either too porous or not porous enough. We would therefore like to produce scaffolds with as little fibre size distributions as possible.

The results show that under all four applied voltages the use of the 10% PVA solution resulted in the formation of fibres with larger diameters than those formed using the 8% solution. At an applied voltage of 15 kV the average fibre diameter was 238 nm from the 8% solution and 399 nm from the 10% solution. This finding is in keeping with previous literature and is explained by the effect the concentration has on increasing the viscosity. In a higher viscosity solution there are more chain entanglements which oppose the stretching forces placed on the jet as it travels from the needle tip to the collecting plate, this leads to less stretching occurring and therefore larger fibre diameters collected [185].

One of the most important parameters in controlling fibre morphology is thought to be the applied voltage; however the results from the present study do not appear to show the voltage having a significant effect on the average fibre diameter. The 10% solutions appear to be influenced more heavily than the 8% solution, with a general trend of the average fibre diameter decreasing when the applied voltage was increased, however due to the relatively large fibre size distribution we are unable to statistically confirm this trend. Standard T test was carried out on the sample range produced from the two solution concentrations. $p = 0.098$ for the 8% solution and $p = 0.063$ for the 10% solution. As $P > 0.05$ in both cases the difference was not determined to be statistically significant. This result was unexpected as it is well documented that the applied voltage has significant effects on the mechanics taking place during the electrospinning process [186, 187]. It is thought that the higher columbic forces generated as a result of a higher applied voltage would result in more stretching of the fibres resulting in smaller fibre diameters however this does not appear to have been the case. There are studies which suggest that when a higher voltage is used more solution is ejected from the needle tip and the

acceleration of the solution is much greater, reducing flight time and therefore also reducing the time in which the polymer is stretched, this would result in larger fibre diameters as the voltage is increased [44].

In the present study we do not see an overall trend of increasing or decreasing fibre diameter as the applied voltage is increased from 10 to 25 kV, however if we look at changes between 10-15 kV, 15-20 kV and 20-25 kV we are able to see trends which are present in fibres produced from both solution concentrations. Average fibre diameter decreases when voltage is changed from 10 kV to 15 kV, then increases when further increased to 20 kV, and then decreases once again when increased to 25 kV. It can be hypothesised from this result that both mechanisms detailed in the literature may be taking place, but either one may be more dominant at a given voltage. When the voltage is increased from 10 kV-15 kV the effect of the increased voltage on the columbic forces may outweigh the decreased flight time caused by faster acceleration and result in smaller fibre diameters. However, on further increases of voltage to 20 kV, the reduced flight time becomes more of a factor than the increased stretching forces causing larger fibre diameters.

The fibre diameter distribution from the 8% solution is much smaller than the 10% solution with fibres only varying by ~ ± 50 nm whereas the distribution from the 10% solution was as high as ~ ± 120 nm. The greater fibre distribution combined with the overall larger average fibre diameter would suggest that the 8% solution is the more suitable concentration for electrospinning PVA. As there is no significant difference in fibre distribution or average fibre diameter caused by altering the applied voltage, we are unable to further eliminate operating parameters to hone in on the optimum parameters for PVA fibre formation, which will have to be determined by further characterisation such as by the thermal characteristics.

3.2.1. **Thermal analysis of PVA**

3.2.1.1. DSC of 8% PVA solutions

DSC traces of PVA electrospun from 8% solution are presented in Figure 14 and are compared to the heating trace of PVA powder as it was received from the manufacturer. There is a large endothermic peak observed approaching 100^{o}C in all of the traces however it is better defined in the electrospun samples. This broad peak is caused by water evaporation [92]. While steps were taken to dry the samples in a desiccator after electrospinning it is possible that some of the residual solvent (water) still remained in the scaffold. The PVA powder obtained from the manufacturer was tested 'as received' and was not dried before handling. This powder also showed an endothermic peak approaching 100^{o}C however this peak was smaller than that of the electrospun samples. This was due to the moisture in the air and the storage environment being absorbed by the polymer. Reheating traces were also carried out on electrospun PVA which did not contain the peak at 100^{o}C confirming that water had evaporated and was therefore no longer present in the reheated sample.

The T_g of PVA is known to be around 85^{o}C [188]. The endothermic peak associated with the T_g can be seen in three of the traces occurring at around 45^{o}C The shift of the T_g to this lower temperature is believed to be due to the presence of moisture within the sample [189]. The T_g of a polymer is known to be affected by the water content within the polymer. Water can cause plasticising of the polymer whereby the water molecules block some of the attractive forces between the polymer chains or increase the distance between the polymer chains. These two factors allow the polymer chains to move more freely resulting in a lower $T_{g,}$ Other studies have

shown that the change in T_g due to plasticising by water can be quite significant, with Lee et al. [189] showing that the T_g of their PVA sample was reduced from 68°C in an anhydrous state to 48°C in the presence of water.

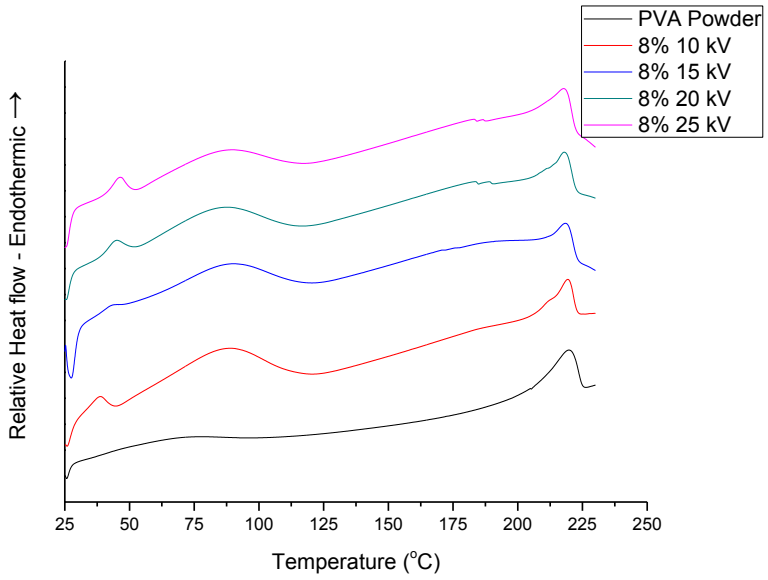

Figure 14: DSC traces of PVA powder and PVA electrospun from an 8% solution at different voltages

The T_m was measured based on the temperature at the height of the endothermic melting peak as can be seen in Figure 14 and is quantified in Table 9. It occurred at the same temperature in all samples, both the electrospun and as-received, at ~218°C. PVA has a melting temperature of 230°C when fully hydrolysed during synthesis and 180°C when partially hydrolysed [190] as described in section 1.5.5. As the PVA used in the present work was ≥98% hydrolysed this was within the expected range. T_m is strongly affected by the molecular weight of a polymer. The higher the M_w the longer the polymer chains and therefore the greater number of bonds required to be broken during melting [191]. This means polymers with a higher M_w will require more energy to melt and will have a higher T_m. Since the

electrospinning process does not have an effect on the molecular weight of the polymer [192] a change in T_m was not expected.

Table 9: Thermal analysis results of PVA powder and PVA electrospun from an 8% solution and different voltages

PVA	T_g	T_m	Crystallinity (%)
Powder	Not visible	219	26.6
8% 10 kV	38	219	14.1
8% 15 kV	42	218	13.4
8% 20 kV	43	217	18.9
8% 25 kV	46	217	22.5

The crystallinity was determined using the formula presented in the 'Materials and Methods' section 2.4 and the values calculated are presented in Table 9. The crystallinity of the as-received PVA powder was calculated to be 26.6% while the crystallinity of electrospun PVA was found to be considerable lower, ranging from 13.4%-22.5%. Under all applied voltages the PVA's crystallinity was reduced by the electrospinning process. This effect is thought to be due to the rapid solidification that takes place during electrospinning while the jet travels toward the collecting plate and the solvent evaporates. This takes place over a very short space of time and may not allow enough time for complete crystallisation to occur. It was also observed that while the crystallinity of electrospun PVA could never equal that of the as-received material, the values did get closer when the voltage was increased with the crystallinity of PVA electrospun at 25 kV having a crystallinity only ~4% lower

than the as-received material , compared to over 17% lower when electrospun at 10 kV.

It is possible that while the electrospinning process in general reduces the crystallinity for the reason stated above, there are parameters within the process that can be changed in order to reduce or increase the crystallinity. In the present study, it is shown that crystallinity can be increased by increasing the applied voltage. Zhao et al. [45] explained that the phase of the electrospinning process when molecular orientation and crystallisation occur is as the jet travels through the air towards the collecting plate. It therefore stands to reason that parameters which effect this phase of the process, such as an increased electric field strength brought on by increasing the applied voltage would lead to greater molecular orientation due to an increase in the number of charges within the polymer jet.

It has been proposed that crystallinity shares an 'inverted U' relationship with the applied voltage, whereby an increase in applied voltage would lead to an increase in the crystallinity up to a point and then any further voltage increase would cause the crystallinity to be reduced again [141]. This is explained by Ramakrishna et al. [8] who explained that crystallinity was not just a result of the molecular orientation but is also influenced by the flight time of the jet. When the voltage is increased the acceleration of the jet is higher and reduces the flight time which leaves less time for crystallisation to take place. Experimental evidence has shown that there is an optimum voltage at which electrospinning will yield the highest crystallinity and above or below this crystallinity will be reduced and this optimum voltage is unique to each polymer [141]. In the present work the crystallinity continued increasing when compared to the lower voltage all the way to the highest voltage tested (25 kV), it is

therefore proposed that the optimum voltage to yield the highest crystallinity in the PVA samples tested may be greater than 25 kV.

3.2.1.2. DSC of 10% PVA solutions

The results of the DSC scans from the 10% solution show much the same results as the 8% solution. They exhibit a large endothermic peak around 100^{o}C attributed to water evaporation and display an endothermic peak representing T_m at approximately 220^{o}C which remained unchanged after electrospinning, regardless of the voltage applied. The DSC traces carried out on the samples produced from the 10% solution are presented in Figure 15 and the T_m's derived from these scans presented in Table 10.

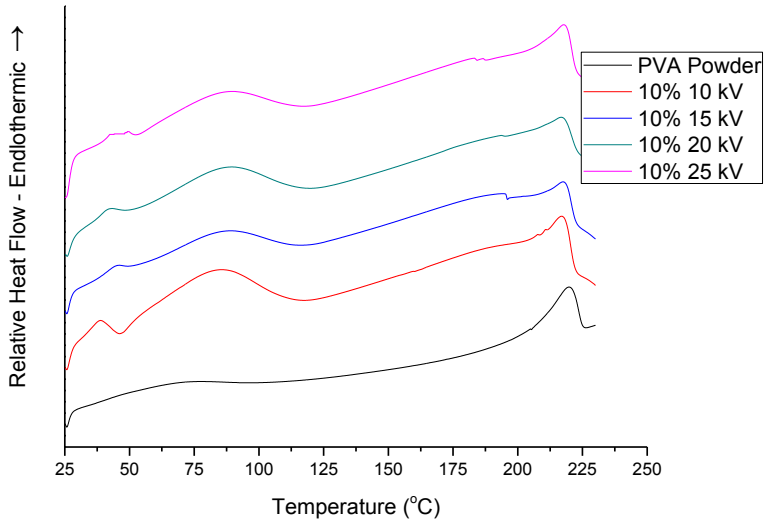

Figure 15: DSC traces of PVA powder and PVA electrospun from a 10% solution at different voltages.

The % crystallinity calculated for PVA electrospun from 10% solutions at different voltages are presented in Table 10. They show the same trends as the samples produced from 8% solutions. The crystallinity is decreased by the electrospinning

process at all voltages when compared to as-received PVA powder. While the crystallinity increases as the voltage is increased, it is not increased enough to be greater than the non-electrospun material.

Table 10: Thermal analysis results of PVA powder and PVA electrospun from an 10% solution and different voltages.

PVA	T_g	T_m	Crystallinity (%)
Powder	Not visible	219	26.6
10% 10 kV	38	217	14.1
10% 15 kV	45	218	14.5
10% 20 kV	44	217	22.7
10% 25 kV	43	218	23.5

3.2.1.3. Effect of solution concentration of crystallinity

When the % crystallinity of PVA fibres spun from an 8% solution are compared with those from a 10% solution it can be seen that the higher solution concentration results in a higher degree of crystallinity. A summary of these comparisons is shown in Table 11. This trend was present in all cases except when electrospinning with an applied voltage of 10 kV. This was an unexpected result as it was thought that since polymers in solution at a lower concentration contain less chain entanglements [30], the chains would be more mobile and as such would be more susceptible to molecular orientation when the voltage is applied. Furthermore Inai et al. [193] showed that the solidification process is slower in low concentration polymer

solutions which could also lead to higher molecular orientation and increased crystallinity.

Table 11: Comparison of crystallinity values obtained after electrospinning PVA from different solution concentrations while altering the applied voltage.

PVA solution concentration (%)	Crystallinity when electrospun at different voltages (%)			
	10 kV	**15 kV**	**20 kV**	**25 kV**
8%	14.1	13.4	18.9	22.5
10%	14.1	14.5	22.7	23.5

3.2.2. **Conclusions from this section**

From this series of experiments we are able to see the effect solution concentration and voltage have on the morphology and thermal properties of electrospun PVA and determine which parameters are the most suitable to use as a starting point for creating chitosan-PVA blend fibres. The 8% solution produced a more uniform scaffold with smaller diameter fibres, and although the crystallinity of the PVA was higher when electrospun from the 10% solution, the 8% solution scaffolds would be of more use in a potential application due to their morphology. The voltage did not have as great an effect on the diameter of the produced fibres as expected however the present work showed the higher the voltage, the higher the crystallinity. Therefore high voltage will be used in future work without it being too high to cause jet instability.

3.3. Electrospinning chitosan

The electrospinning of pure chitosan without the addition of another polymer to make up a blend was unsuccessful in the present work. Solutions were prepared with varying chitosan concentrations ranging from 1 – 4% in both a weak 5% acetic acid and strong 90% acetic acid. These solutions were subsequently electrospun under various operating parameters, with the applied voltage varied from 5 – 25 kV, the needle tip distance varied from 5 – 20 cm and the flow rate varied from 0.1 - 3 ml/hr. No combination of these operating parameters resulted in the successful formation of nanofibres. Table 12 depicts the solution concentrations attempted as well as the solvent used and the proposed reason why electrospinning could not take place.

There are numerous references in the literature relating to the unsuitability of chitosan as an electrospinning material without the addition of another polymer to form a blend [81, 104]. The inability of chitosan to be spun into nanofibres appears to be due to two main reasons. The first is the high viscosity of chitosan in solution [54]; the implications of too high a viscosity in electrospinning were discussed in detail in section 1.4.3.1.1.

Table 12: Different chitosan solutions and their electrospinability along with the proposed reason for any negative result.

Chitosan solution		**Electrospinnability with voltages ranging from 5 – 25 kV and Needle tip distance ranging from 5 – 20 cm**	**Reason for not electrospinning**
Concentration	**solvent**		
1%	5% acetic acid	Negative	Stable jet could not be formed
	90% acetic acid	Negative	Stable jet could not be formed
2%	5% acetic acid	Negative	Solution too viscous
	90% acetic acid	Negative	Solution too viscous
3%	5% acetic acid	Negative	Solution too viscous
	90% acetic acid	Negative	Solution too viscous
4%	5% acetic acid	Negative	Solution too viscous
	90% acetic acid	Negative	Solution too viscous

When the solution concentration was greater than 3%, the viscosity was too high to allow the solution to flow through the syringe to the end of the needle tip therefore electrospinning was impossible. 18G needles with larger internal diameters were trialled as replacements to the standard 22G needles being used, however solution flow was still not achieved. The viscosity of solutions was unchanged when different acidic concentrations were used as the solvent.

Solutions with a concentration ranging from 1-3 % exhibited a sufficiently low viscosity to allow the solution to flow through the needle tip in the electrospinning apparatus. The electrospinning parameters were altered with combinations of different applied voltages, needle tip distances and flow rates. Under no parameters was a stable jet formed. Droplets were observed to be ejected from the needle tip and landed on the collecting plate as liquid droplets. Vrieze et al. [86] was successful at electrospinning pure chitosan at a solution concentration of 3%, and acetic acid concentration of 90%, an applied voltage of 20 kV, flow rate of 0.3 ml/hr and needle tip distance of 10 cm. These parameters were replicated in the present work but electrospinning was not possible. An SEM micrograph of the collected material obtained while operating under Vrieze et al.'s operating parameters is shown in Figure 16 while Figure 17 shows an SEM micrograph of the material Vrieze et al. produced. It can be seen from this image that no fibre formation has taken place and that the material is arranged in bundles as the solution has been ejected from the needle tip in droplets and subsequently solidified on the collecting plate.

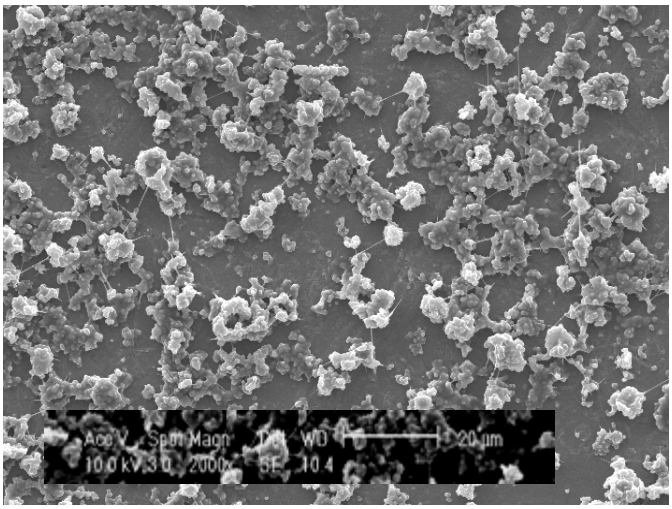

Figure 16: SEM micrograph of chitosan deposit on the collecting plate when electrospun from a 3% solution in 90% acetic acid under an applied voltage of 20 kV, needle tip distance of 10 cm and a flow rate of 0.3 ml/hr.

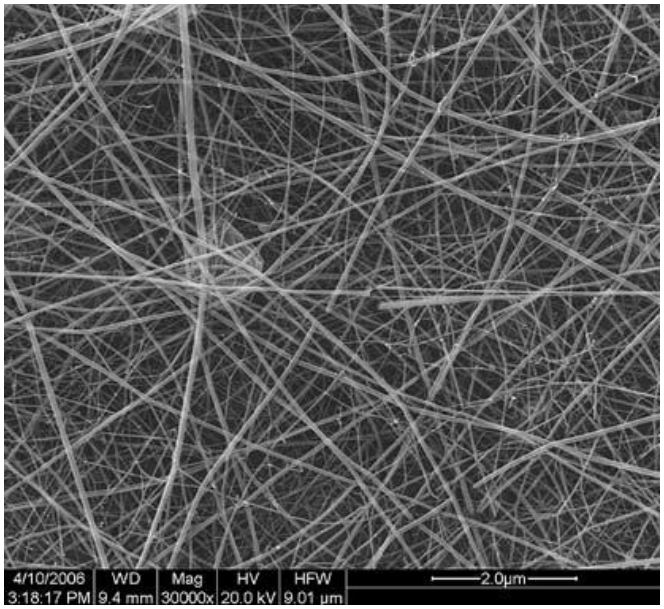

Figure 17: SEM micrograph of chitosan nanofibres courtesy of Vrieze et al. when electrospun from a 3% solution in 90% acetic acid under an applied voltage of 20 kV, needle tip distance of 10 cm and a flow rate of 0.3 ml/hr [86].

The difficulty in electrospinning chitosan has been a topic of discussion in many journal articles with a common consensus that the intermolecular forces caused by the ionic groups in the polymer backbone repelling each other and preventing fibre formation. Geng et al. [87] showed that by dissolving chitosan in a more concentrated acetic acid, the overall surface tension of the solution was reduced while the net charge density of the solution was increased. These two changes in properties increase the likelihood of fibre formation due to reducing the critical voltage needed to overcome the surface tension and providing more charged ions to create a larger whipping instability. These changes in solution properties were not measured in the present work, however the results of the SEM show the properties were clearly not influenced in such a way that would allow fibre formation.

3.4. Electrospinning of Chitosan-PVA blends

In an attempt to create an electrospinnable solution, PVA was added to the chitosan in acetic acid in different blend ratios and at different concentrations. Fibres were successfully produced from electrospun polymer solutions with an overall concentration ranging from 5 - 8% with different mass ratios of chitosan to PVA. Table 13 shows which polymer solutions were capable of producing fibres and the degree to which beads were present. It was found that the chitosan content could be increased from 10% up to 40% when the overall polymer solution concentration was lowered sufficiently to prevent viscosity from becoming too high. Chitosan is known for being highly viscous when in solution. The NH_2 and OH groups of the chitosan molecule interact strongly, producing hydrogen bonds between the polymer chains [194]. These interactions are somewhat reduced by the addition of PVA as the PVA molecules disrupt the intermolecular interactions between the polymer chains. This

is evidenced by the fact that when a 2% pure chitosan solution was made the viscosity was too high for it to flow through the needle tip of the electrospinning machine, however a 5% 60:40 PVA/chitosan solution, which contains 3% PVA and the same 2% chitosan, produced a free flowing solution.

Table 13: Fibre formation and bead structure in scaffolds produced from different chitosan-PVA solutions made using 2% acetic acid.

Solution concentration (%)	PVA:Chitosan ratio	Fibre production	Presence of beads
5	90:10	Yes	Many
5	80:20	Yes	Many
5	70:30	No	-
5	60:40	No	-
6	90:10	Yes	Some
6	80:20	Yes	Some
6	70:30	No – Solution too viscous	-
7	90:10	Yes	Very few
7	80:20	Yes	Very few
7	70:30	No – Solution too viscous	-
8	90:10	Yes	Very few
8	80:20	Yes	Very few
8	70:30	No – Solution too viscous	-

Despite the viscosity being reduced by lowering the polymer solution concentration this does not appear to be the only factor limiting the chitosan content in electrospun chitosan/PVA blends. Although the 5% 70:30 and 60:40 PVA/chitosan solutions were able to flow through the capillary tubing and out of the needle tip, producing fibres from these solutions was unsuccessful. Figure 18 shows an SEM micrograph of the scaffold produced from a 5% 70:30 PVA/chitosan blend, it can be seen that while there do appear to be a small amount of interconnecting fibres, the scaffold is

predominantly made up of beads of solution which have not sufficiently been formed into fibres. This is concurrent with a previous study which was also unsuccessful in producing fibres from polymer solutions with chitosan contents above 20% [99]. It is thought that this could be due to the way PVA facilitates the production of fibres, as mentioned previously, the PVA molecules moderate the repelling interactions between chitosan's polycationic molecules. In solutions with chitosan content greater than 30% there may not be sufficient PVA molecules to reduce the repulsive forces which would prevent sufficient chain entanglements and inhibit the formation of continuous fibres [195].

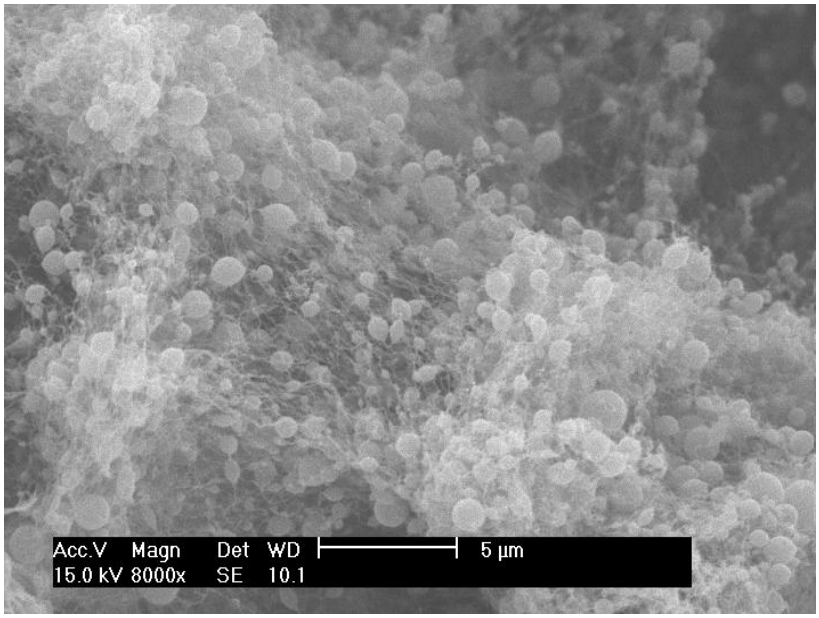

Figure 18: SEM micrograph showing a scaffold produced from a chitosan-PVA blend solution with a ratio of 70:30 PVA:chitosan and an overall solution concentration of 5%.

3.4.1. **Effect of concentration on fibre morphology**

Lower concentration solutions were seen to produce much more beading on the produced fibres, this effect was most markedly observed in the fibres produced from a 5% 90:10 PVA/chitosan solution where there are beads apparent on almost every fibre. A small amount of beading can be expected in electrospun polymer scaffolds due to the nature of the process, however high amounts of beading such as those found in the 5% 90:10 PVA/chitosan solution will have a severe impact on the use of the scaffold. An electrospun scaffold for use in application will be tailored to have very specific properties necessary for the particular application. For example it may be required to have certain porosity so that some molecules are able to pass through it, such as those in the drugs used for wound treatment while not allowing bacteria to pass through it. These properties are determined in part by the fibre diameter, however when there are beads present this adds an 'unknown' to the scaffold whereby its properties cannot be accurately predicted due to the random distribution of the beads. These beads may act as a source of weakness and have a negative impact on the surface area to volume ratio of the produced scaffold.

Beading is more likely to occur in low concentration solutions because there are less polymer chains present in relation to the amount of solvent, which increases the likelihood of solvent molecules aggregating to form beads [8]. The beading phenomenon is seen to reduce when polymer concentration is increased, with fibres being practically bead-free in solutions over 7%. Figure 19 presents SEM micrographs of PVA/chitosan scaffolds produced from 5, 6, 7 and 8% solution concentrations. In image (a) from a 5% concentration beads are clearly visible on the majority of fibres. Image (b) from a 6% solution shows less than half the fibres

have beads present while image (c) and (d) from 7% and 8% solutions, respectively show almost no beads at all.

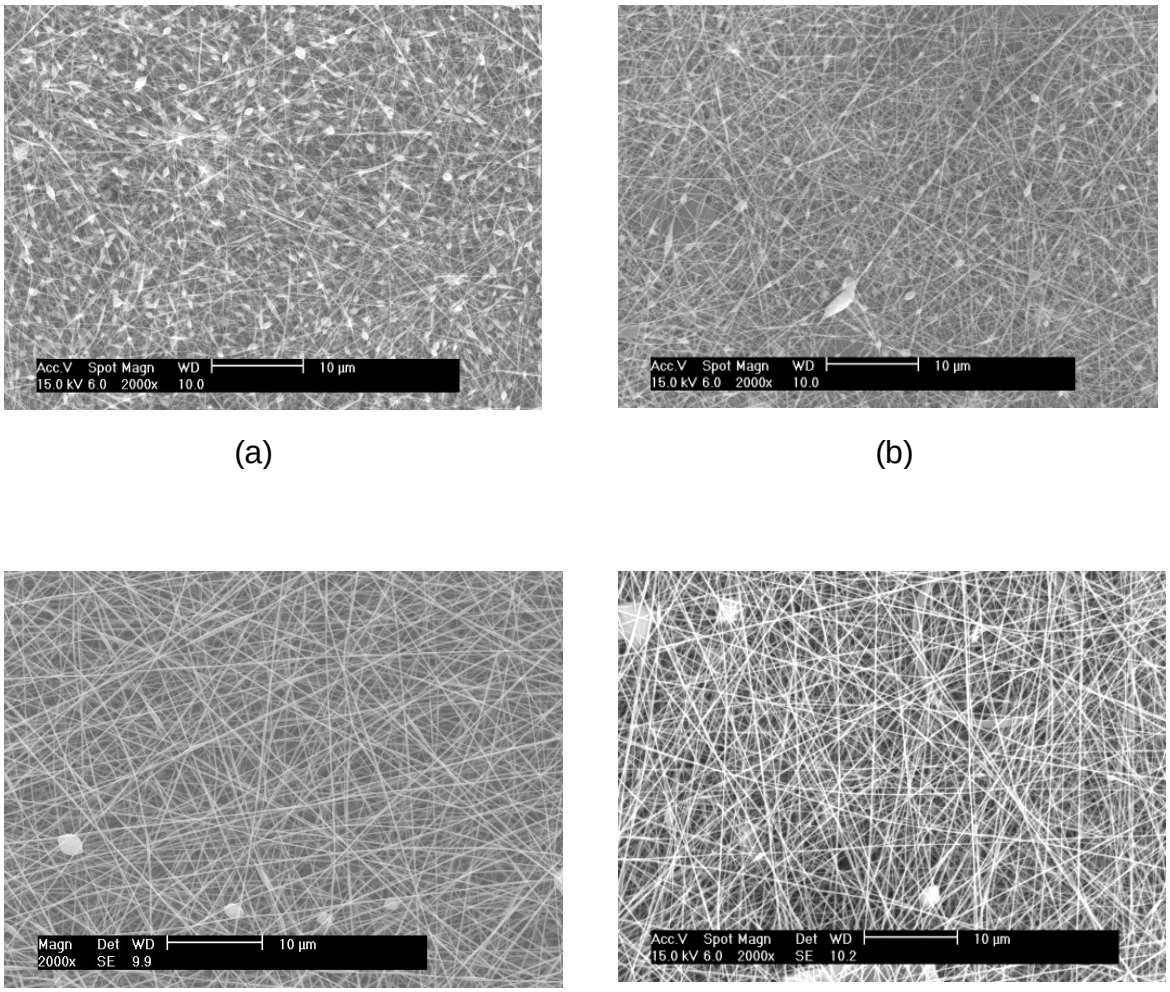

(a) (b)

(c) (d)

Figure 19: SEM micrographs of PVA/chitosan nanofibres electrospun from (a) 5% (b) 6% (c) 7% (d) 8% concentration acetic acid solutions with blend ratios of 90:10 at an applied voltage of 20 kV, needle tip distance of 10 cm and flow rate of 1 mL/hr.

While Table 13 shows the solutions that were successfully electrospun, it was not always the case that each solution could produce fibres under all of the variable parameters tested in this study. It was common for some solutions not to produce

fibres at the extremes of the variable conditions, for example, at the shortest needle tip distance and the highest voltage, or at the longest needle tip distance and the lowest voltage. This is due to either the electric field strength being too low to overcome the surface tension of the solution and form a Taylor cone or being too high and surpassing the critical value. This will be discussed in more detail in section 3.4.4.

3.4.2. **Effect of polymer solution concentration on average fibre diameter**

Irrespective of the blend ratio of chitosan to PVA in the solution, the average diameter of the fibres obtained increased when the overall solution concentration was increased. Figure 20 shows the average diameter of fibres within scaffolds produced from solutions of different concentrations with a PVA:chitosan blend ratio of 90:10 electrospun at an applied voltage of 15 kV and needle tip distance of 10 cm. This relationship was also displayed under all operating parameters, with fibre diameter increasing with increased concentration at 15, 20 and 25 kV and needle tip distances of 7.5, 10 and 12.5 cm and at all combinations of the two.

Figure 20 and Figure 21 show the average fibre diameters of the scaffolds produced from different concentration solutions with the same blend ratio. It can clearly be seen from the graph that the average fibre diameter increases with increased concentration. In the 90:10 blend ratio scaffolds produced with an applied voltage of 15 kV (shown in Figure 20) the average fibre diameter is seen to increase from 113 nm for the 5% solution to 303 nm for the 8% solution. In the 80:20 blend ratio scaffolds produced with an applied voltage of 20 kV (shown in Figure 21) the average fibre diameter is also seen to rise from 100 nm to 200 nm from 5% to 8% solution concentrations, respectively. This is consistent with previous results found

in the literature for electrospinning [31, 58, 196] as well as the results found earlier in the present study when electrospinning PVA without forming a blend with chitosan. This effect is due to a greater number of polymer chains within the solution at higher concentrations which lead to a greater number of chain entanglements. These entanglements resist the stretching caused by the repellent forces acting on the jet as it travels through the air reducing the stretching effect and resulting in larger fibre diameters [8].

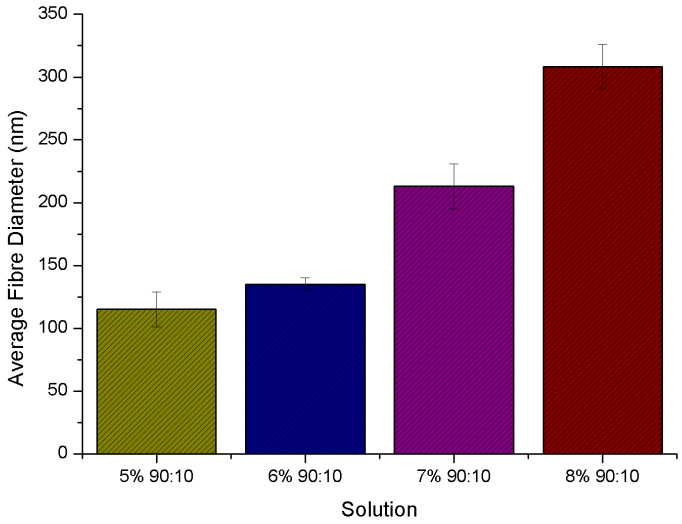

Figure 20: Effect of concentration of PVA/chitosan blend solutions with a blend ratio of 90:10 on the average diameter of fibres produced by electrospinning at an applied voltage of 15 kV.

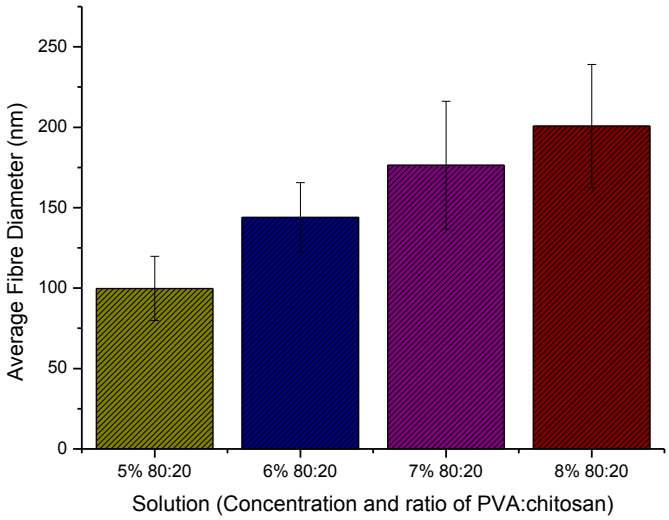

Figure 21: Effect of concentration of PVA/chitosan blend solutions with a blend ratio of 80:20 on the average diameter of fibres produced by electrospinning at an applied voltage of 20 kV.

3.4.3. **Effect of blend ratio**

Figure 22 shows the average diameter of fibres produced from 5, 6, 7 and 8 % solution concentrations, comparing the blend ratios 90:10 and 80:20 at these four different overall concentrations. It was thought that increasing the chitosan content within the solution while maintaining the same overall concentration would lead to a significant reduction in fibre diameter. Chitosan contains ionisable amino groups which mean it is highly conductive. Park et al. [195] showed that the conductivity of a chitosan blend solution increased with increased chitosan content. Returning back to the theory behind electrospinning, increased conductivity results in greater repulsive forces between the polymer chains within the solution which promotes greater stretching and should therefore lead to smaller diameter fibres [8]. The results of the present study did not show a significant decrease in average fibre

diameter when the blend ratio was changed from 90:10 to 80:20 PVA:chitosan. With an applied voltage of 20 kV, the average fibre diameter difference for 90:10 ratio compared to 80:20 were 3 nm, 3 nm, 4 nm and 5 nm for 5, 6, 7 and 8% solution concentrations, respectively.

It is thought, that while the conductivity of the solution most likely increased due to the greater chitosan content in the 80:20 ratio solutions compared to 90:10, this may not have been significant enough to offset the large increase in solution viscosity caused by the additional chitosan, which as mentioned before promotes larger fibre diameters. These two factors working in opposition to each other along with the fact that the two blend ratios are both relatively similar, explaining the results seen in the present work that the chitosan content did not have a significant effect on the average fibre diameter.

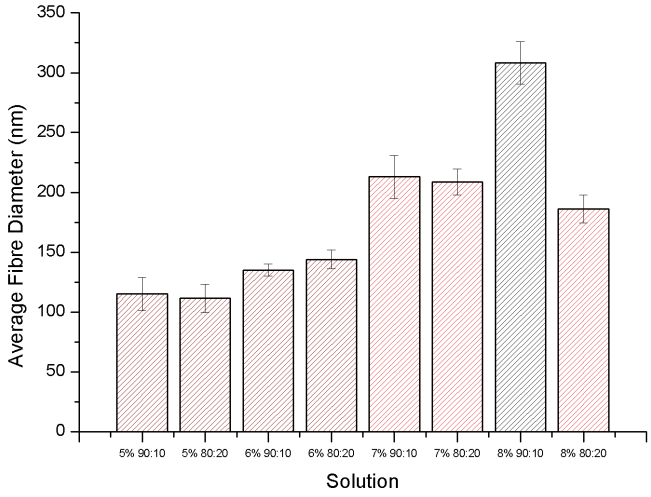

Figure 22: Effect of blend ratio of PVA:chitosan on the average fibre diameters produced by electrospinning.

3.4.4. **Effect of needle tip distance**

Figure 23, Figure 24, and Figure 25 show the effect of needle tip distance on fibre diameters at different applied voltages, and Figure 26 shows the overall average fibre diameters produced from all experiments at each needle tip distance. From Figure 26, it can be seen that there is a general tendency across all solutions, with the exception of 8% 80:20 that the fibre diameter increases when the needle tip distance increased from 7.5 cm to 12.5 cm. When the needle tip distance increased the electric field strength was reduced so the effect is similar to reducing the applied voltage. This means there are less repulsive forces acting on the jet and so there will be less stretching of the solution.

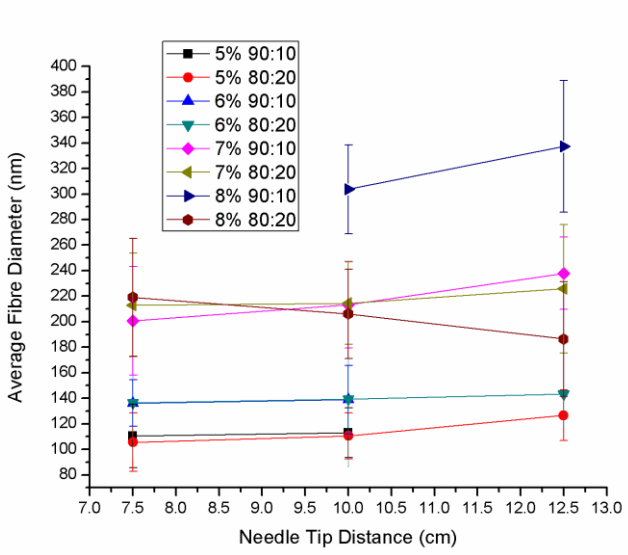

Figure 23: Effect of needle tip distance on the average fibre diameter of fibres produced from different concentrations and blend ratios of PVA:chitosan in solution by electrospinning at a fixed applied voltage of 15 kV

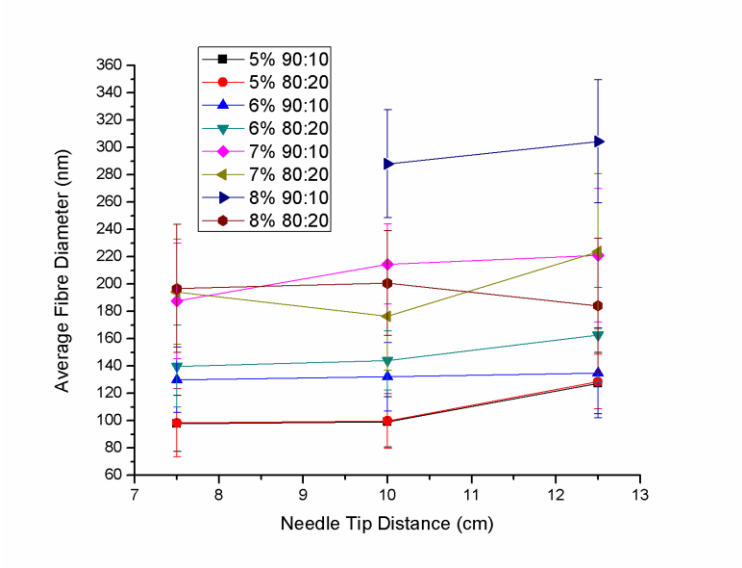

Figure 24: Effect of the needle tip distance on average fibre diameter of fibres produced from different concentrations and blend ratios of PVA:chitosan in solution by electrospinning at a fixed applied voltage of 20 kV.

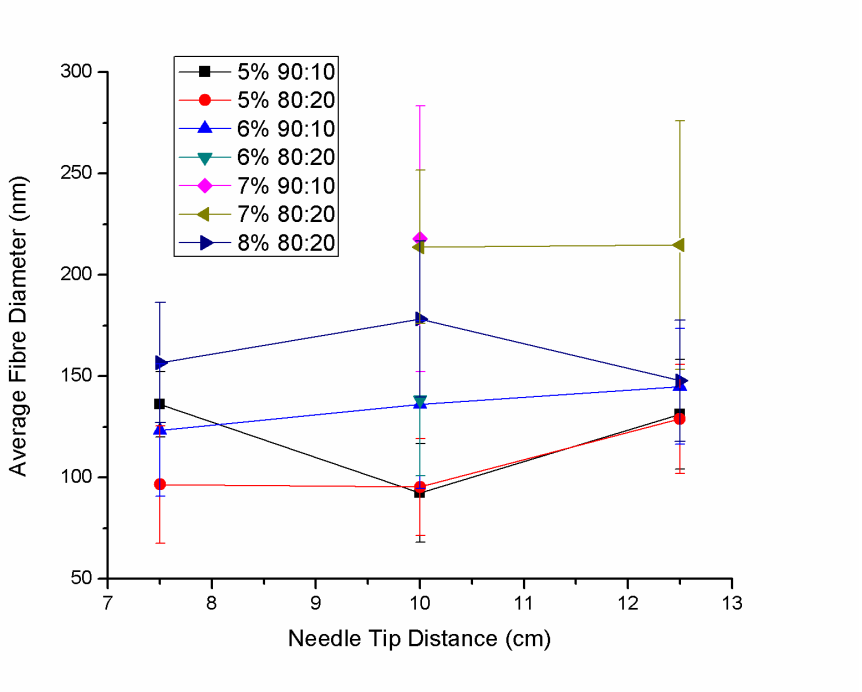

Figure 25: Effect of the needle tip distance on average fibre diameter of fibres produced from different concentrations and blend ratios of PVA:chitosan in solution by electrospinning at a fixed applied voltage of 25 kV.

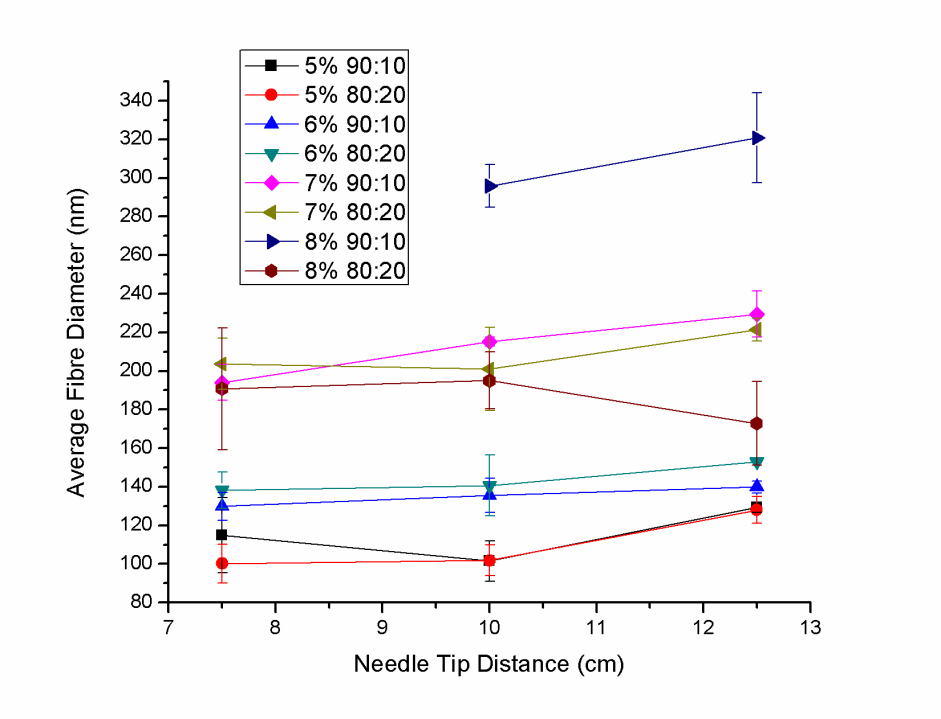

Figure 26: Effect of the needle tip distance on the average fibre diameter of fibres produced from different concentrations and blend ratios of PVA:chitosan in solution by electrospinning across all tested applied voltages (15, 20, 25 kV).

It is this reduction in electrostatic force, which is believed to have prevented the 7% 90:10 solution from producing fibres at a needle tip distance of 12.5 cm and a voltage of 15 kV. That combination of parameters may not have created a strong enough electric field to overcome the solutions surface tension and produce a jet. The opposite was true at the shortest distance and highest applied voltage of 25 kV. Only 3 out of the 8 fibre producing electrospun solutions were succesfully electrospun under these conditions due to the electric field strength being too high and surpassing the critical value, resulting in instability of the jet and the taylor cone receeding into the needle tip [31, 197].

Although an overall trend is observed accross all the experiments carried out, when we look at the graphs for individual voltages, we see that there are different responses by some solutions to the change in needle tip distance. The 8% 80:20 solution shows a decrease in fibre diameter when the distance is increased from 7.5 cm to 12.5 cm, this could be due to a secondary effect of increasing the needle tip which is an increased flight time for the jet as it has further to travel before hitting the collecting plate. The polymer jet therefore has more time to elongate and stretch resulting in thinner fibres [198].

At the shortest distance of 7.5 cm there appeared to be a tendancy for some of the polymer solution to be present in the form of globules on the scaffolds. An example of this can be seen in Figure 27. This is likely because the very short flight time of the jet due to the short distance between the needle tip and the collecting plate does not allow enough time for all of the solvent to evaporate before the fibres hit the collector. It may also be due to some solutions being ejected from the needle tip as droplets. This can sometimes occur during electrospinning when there is instability in the Taylor cone and if the needle tip distance is small some of these droplets may reach the collecting plate. This is not desirable as excessive residual solvents in the scaffolds could be harmful if intended for application to human skin [62].

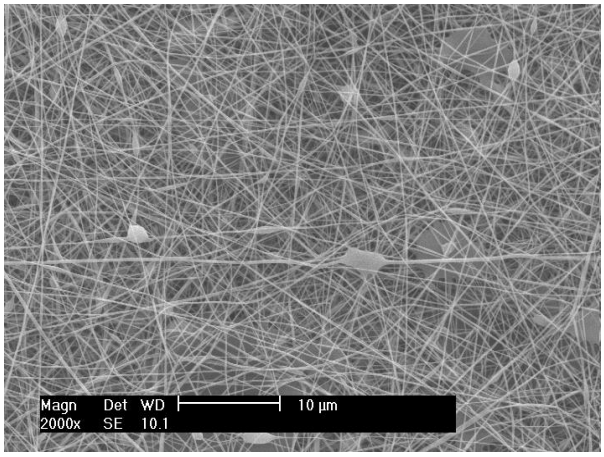

Figure 27: SEM micrograph of fibres produced from a 7% 90:10 PVA/chitosan blend solution electrospun with an applied voltage of 20 kV and a needle tip distance of 7.5 cm.

3.4.5. **Effect of voltage**

Voltage was varied from 10-25 kV however it was found that 10 kV was not suffient to create a jet to produce fibres. Figure 28, Figure 29 and Figure 30 show the effect of applied voltages varied from 15-25 kV on average fibre diameters at different needle tip distances and Figure 31 shows the overall effect of applied voltage accross all tested needle tip distances. There is a general trend of decreasing average fibre diameter with increased voltage. This is concurent with previous findings by Lee et al. [48]. The present results show only a slight reduction which in the case of some solutions was not statistically significant. This supports the findings of other studies such as those by Demir et al. [58] Zhao et al. [198] and Zhao et al. [196] who suggested that fibre diameter could increase with voltage as the increased voltage causes the jet to accelerate from the needle tip to the collector faster, reducing flight time and therefore reducing stretching. More solution is also ejected out of the tip of the needle resulting in a thicker jet which also leads to thicker

fibres [44]. It is likely that both of these mechanisms are occuring to different extents with increased repulsive forces being marginally more dominant resulting in the small reduction in fibre diameters.

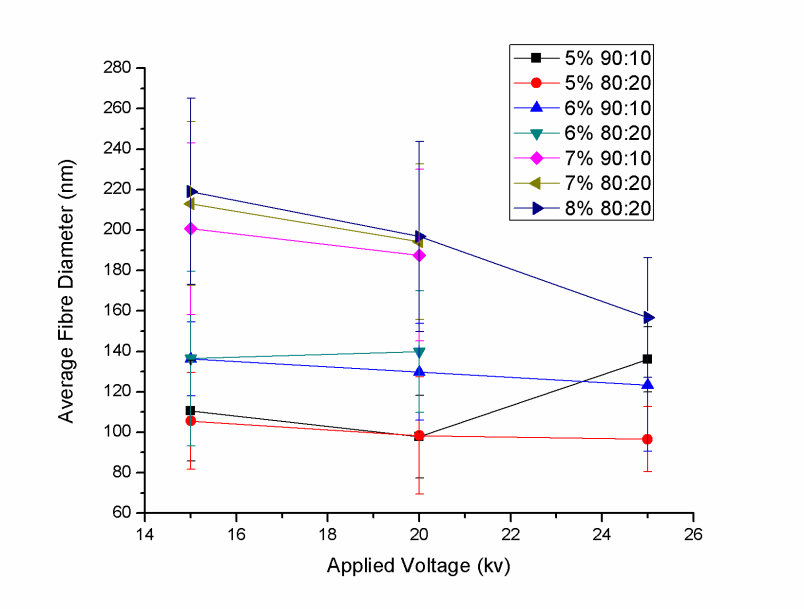

Figure 28: Effect of applied voltage on average fibre diameter of fibres produced from different concentrations and blend ratios of PVA:chitosan in solution by electrospinning at a fixed needle tip distance of 7.5 cm

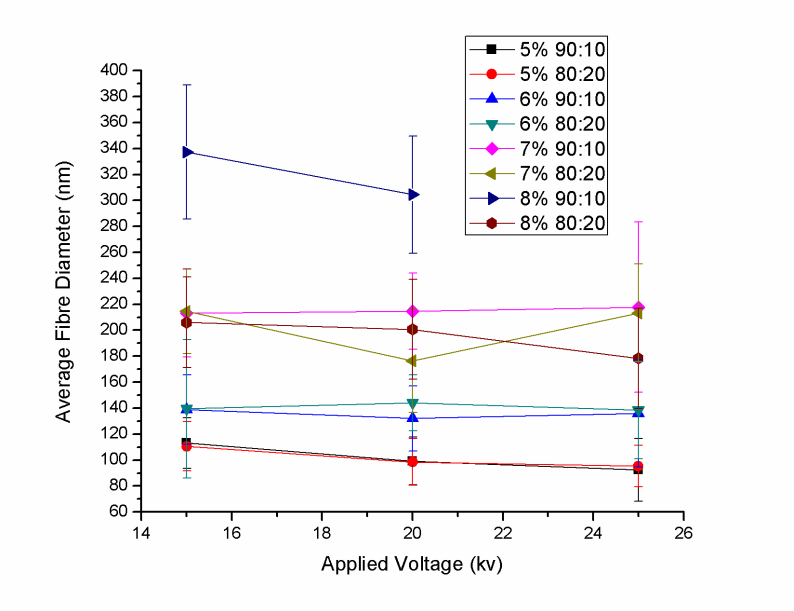

Figure 29: Effect of applied voltage on average fibre diameter of fibres produced from different concentrations and blend ratios of PVA:chitosan in solution by electrospinning at a fixed needle tip distance of 10 cm

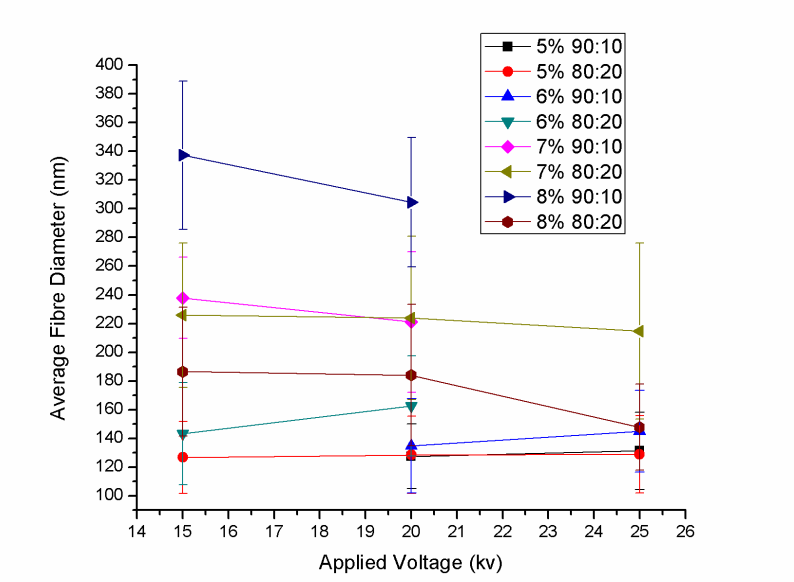

Figure 30: Effect of applied voltage on average fibre diameter of fibres produced from different concentrations and blend ratios of PVA:chitosan in solution by electrospinning at a fixed needle tip distance of 12.5 cm

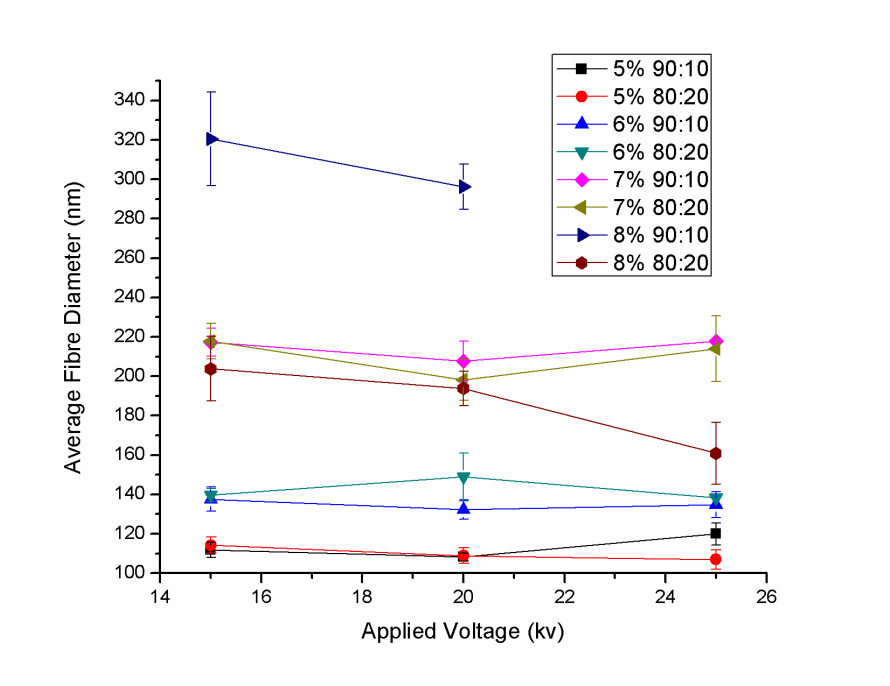

Figure 31: Effect of applied voltage on average fibre diameter of fibres produced from different concentrations and blend ratios of PVA:chitosan in solution by electrospinning averaged across all tested needle tip distances (7.5, 10, 12.5 cm)

What is more interesting with respect to the applied voltage is the effect it has on the stability of the jet, the shape of the Taylor cone and the rate of fibre production. At high voltages of 25 kV, the jet was regularly unstable, ejecting droplets from the needle tip and this resulted in solution solidifying and blocking the needle which became high maintainance as the tip had to be manually unblocked. This would be unnacceptable when used in industry. The unstable jet also produced fibres of largely varying fibre diameters, which were non-uniform, shown in Figure 32, whereas at lower voltages of 15 kV and 20 kV, the jet is very stable and fibres appear more uniform, example shown in Figure 33.

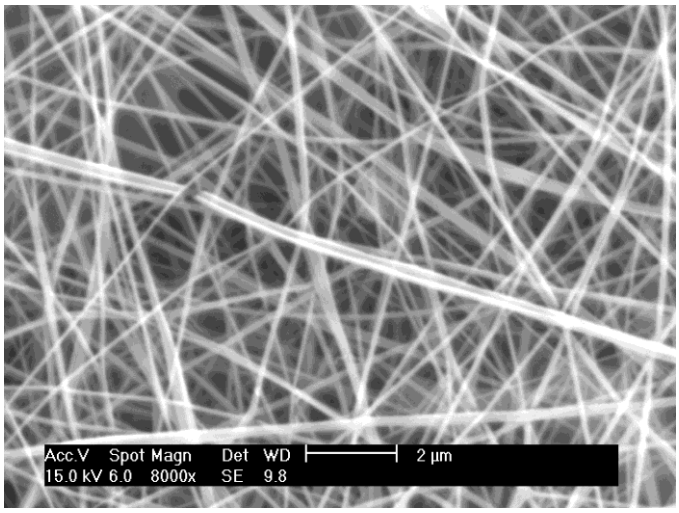

Figure 32: SEM of fibres produced from an 8% 80:20 PVA/chitosan blend solution electrospun with an applied voltage of 25 kV and a needle tip distance of 10 cm

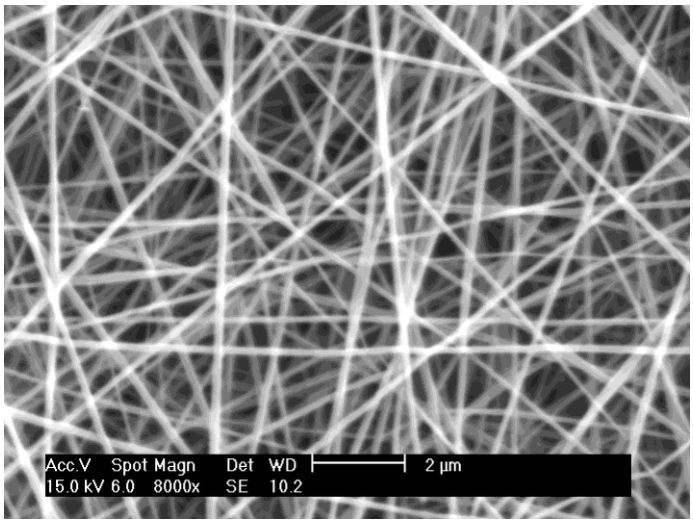

Figure 33: SEM of fibres produced from an 8% 80:20 PVA/chitosan blend solution electrospun with an applied voltage of 15 kV and a needle tip distance of 10 cm

Since fibre diameter appears to remain relatively constant between 15 kV and 20 kV and both voltages can produce uniform fibres at 7% and 8% concentration solutions, this leads to other criteria being needed to determine which would be the most suitable. At the higher voltage, fibres are produced at a faster rate which is

beneficial from a manufacturing perspective, however the reduced flight time resulting from the faster jet leaves less time for crystallisation to take place. Thermal analysis of the two parameters is required to determine if there is a significant difference in crystallinity between fibres produced by the two applied voltages.

3.4.6. **FTIR**

FTIR scans were carried out to confirm the presence of both chitosan and PVA in the chitosan/PVA blend scaffolds. Spectra were obtained of PVA and chitosan separately in their as-received powder form in order to identify their individual characteristic peaks.

3.4.6.1. FTIR – PVA Powder

Figure 34 shows the FTIR spectra of as-received PVA powder.

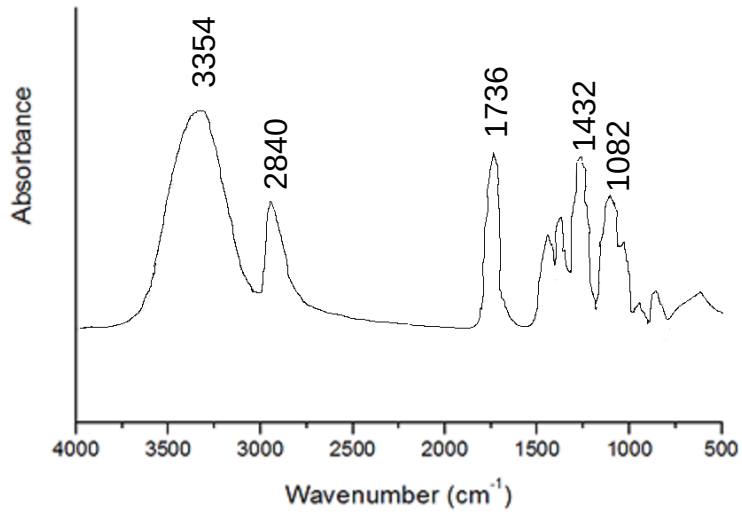

Figure 34: FTIR spectra of as-received PVA powder

PVA shows an absorbtion peak at 3354 cm^{-1} which is attributed to the intermolecular hydrogen bonding as well as –OH stretching vibrations [199]. The band observed at 2840 cm^{-1} is associated with C-H stretching in alkyl groups while the absorption peak at 1082 cm^{-1} corresponds to –C-O stretching [200]. The peak at 1736 cm^{-1} is attributed to stretching of C=O and C-O from residual acetyl groups remaining in the material as the PVA used was only 98% hydrolysed. The absorbance peak at 1432 cm^{-1} represents CH_2 bending [201]. These characteristic peaks and their respective assignments are summarised in Table 14.

Table 14: FTIR characteristic peak assignments of PVA

Characteristic peak (cm^{-1})	**Assignment**	**Reference**
3354	-OH stretching	[199]
2840	C-H from alkyl groups	[200]
1736	Acetyl groups C=O and C-O	[201]
1432	CH_2 bending	[201]
1082	C-O	[200]

3.4.6.2. FTIR - Chitosan Powder

Figure 35 shows the FTIR spectra of as-received chitosan powder

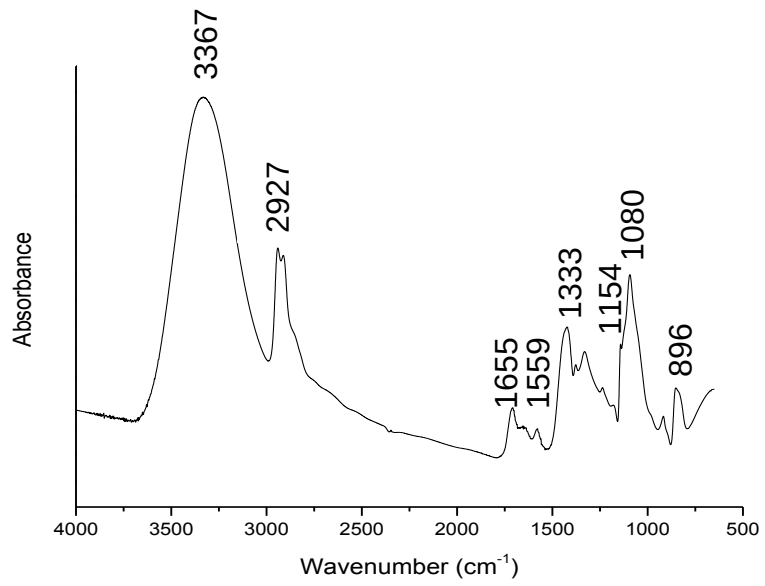

Figure 35: FTIR spectra of as-received chitosan powder

Chitosan shows two peaks around 893 cm^{-1} and 1156 cm^{-1} which are attributed to the saccharide structure of chitosan [202]. Peaks characteristic to chitosan at 1655 cm^{-1} and 1322 cm^{-1} are reported to be primary amides and tirtiary amides respectively. The broad peak at 3367 is typical of O-H stetching and also -NH stretching, the –OH band overlaps the –NH band. The peak at 2927 cm^{-1} is the typical C-H stretching. The peak at 1080 cm^{-1} is attributed to the C-O stretching in chitosan. A summary of these peaks is shown in Table 15.

Table 15: FTIR characteristic peaks observed from chitosan.

Characteristic peak (cm-1)	Assignment	Reference
3367	Amine NH symmetric vibration with overlapping –OH stretching	[203]
2927	C-H vibration	[203]
1655	Primary amide C=O	[204]
1559	Amino group	[204]
1333	Amide III	[203]
1154	Saccharide structure	[202]
1080	C-O-C	[203]
896	Saccharide structure	[202]

3.4.6.3. FTIR – Electrospun Chitosan/PVA

FTIR spectra were subsequently obtained using the Golden Gate Single Reflection Diamond on samples of the electrospun scaffolds produced at different blend ratios. As has previously been discussed, the electrospinning process does not have an impact on the chemical structure of the material, so no difference in FTIR spectra was expected between samples electrospun under different operating parameters but containing the same blend ratio of PVA:chitosan.

Figure 36 shows the FTIR spectra of electrospun PVA:chitosan 90:10 and Figure 37 shows the FTIR spectra of electrospun PVA:chitosan 80:20. It can be seen in these spectra, that characteristic peaks of both chitosan and PVA are present.

In the spectra for PVA-chitosan blends, the band attributed to hydroxyl stretching has shifted to lower wave numbers from 3354 cm^{-1} in the pure PVA powder spectra to 3337 cm^{-1}. Zhang et al [104] suggested that this shift of the hydroxyl band in PVA-chitosan blends occurs due to hydrogen bonds acting between –OH groups in the PVA and $–NH_2$ groups in the chitosan.

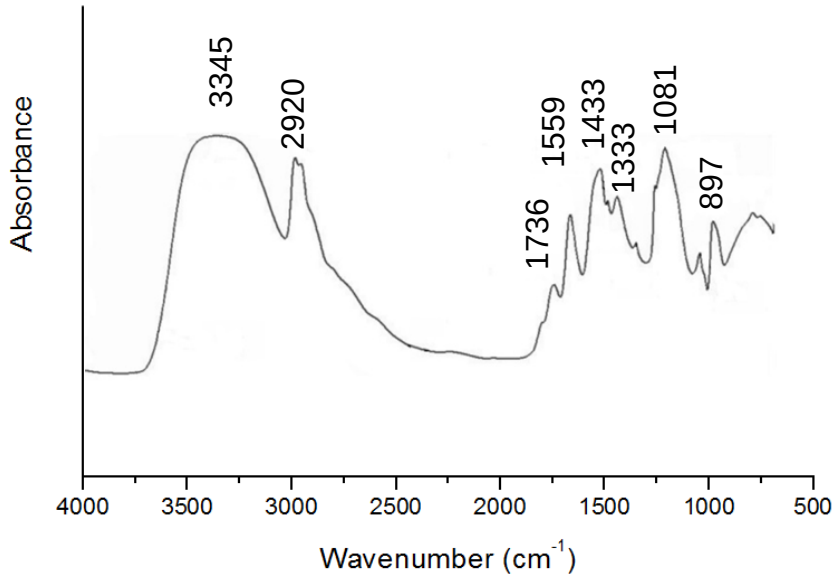

Figure 36: FTIR spectra of PVA:chitosan electrospun fibres obtained from a 7% 90:10 solution.

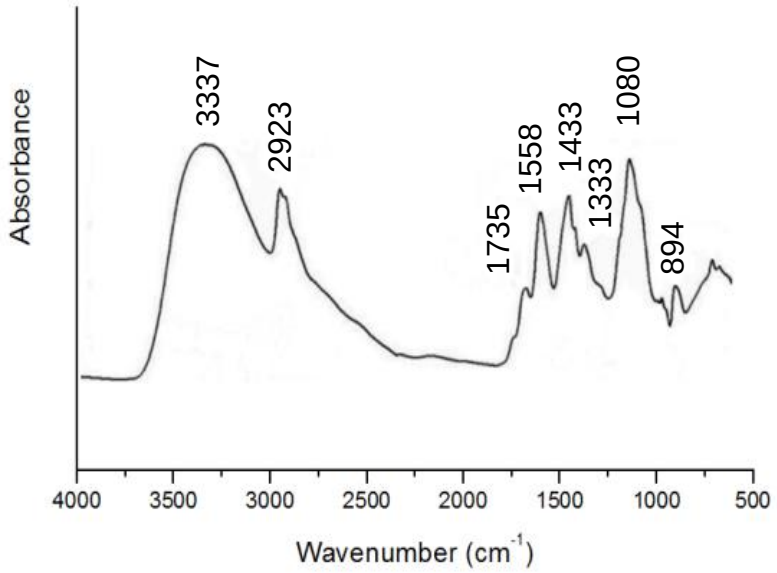

Figure 37: FTIR spectra of PVA:chitosan electrospun fibres obtained from a 7% 80:20 solution.

3.4.7. **DSC**

DSC was carried out on powder samples of the as-received chitosan and PVA as well as on the electrospun PVA/chitosan blend scaffolds in order to observe the effect the blend ratio would have on the thermal properties as well as the effect altering the operating parameters (voltage and needle tip distance) would have.

3.4.7.1. DSC - Chitosan

Like most polysaccharides, chitosan does not melt, but instead degrades when heated above a critical temperature. This degradation process is reported to begin at approximately 250^{o}C [205, 206]. As such, the DSC scan of chitosan powder heated from 25^{o}C to 225^{o}C show in Figure 38 does not exhibit any endothermic peak relating to $T_{m.}$ Care was taken not to approach the degradation temperature too closely so that material degradation would not affect subsequent heating runs.

There is a broad endothermic peak occurring around 100^{o}C in the first heating cycle of the chitosan powder. This is attributed to moisture evaporation since chitosan is known to be susceptible to absorbing moisture. This endothermic peak is very broad and may mask more subtle changes in enthalpy, as such a second heating run was carried out and it can be seen in the reheating trace shown in Figure 39 the endothermic moisture evaporation peak is no longer present. The baseline step associated with the T_g of chitosan is usually very small due in part to the fact that chitosan is semi-crystalline and only the amorphous regions undergo a glass transition. Another cause of the above is also the presence of the rigid 2-amino-2-deoxy-D-glucopyranose (or glucosamine residues) in the chitosan molecules [206]. A small deviation in the inclination of the baseline can be observed at approximately 140^{o}C, which can be attributed to the T_g of chitosan and is in agreement with a study by Dong et al. [207].

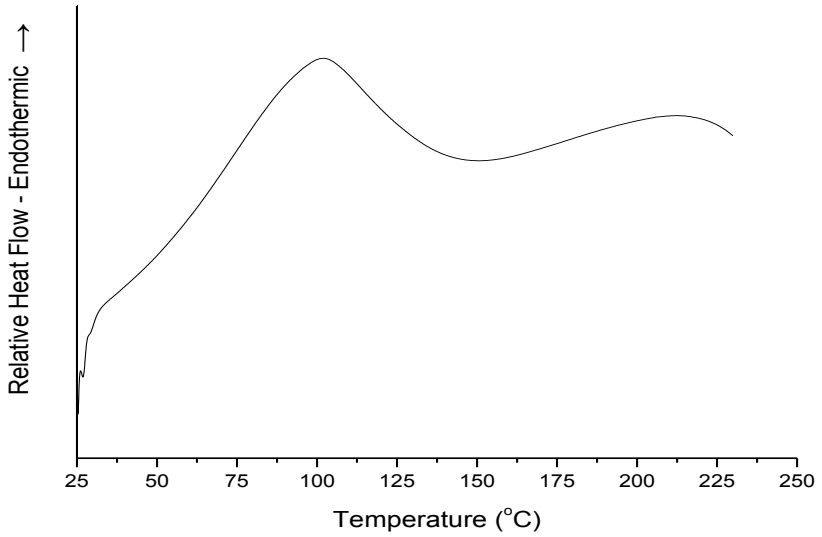

Figure 38: DSC scan for the heating of chitosan powder

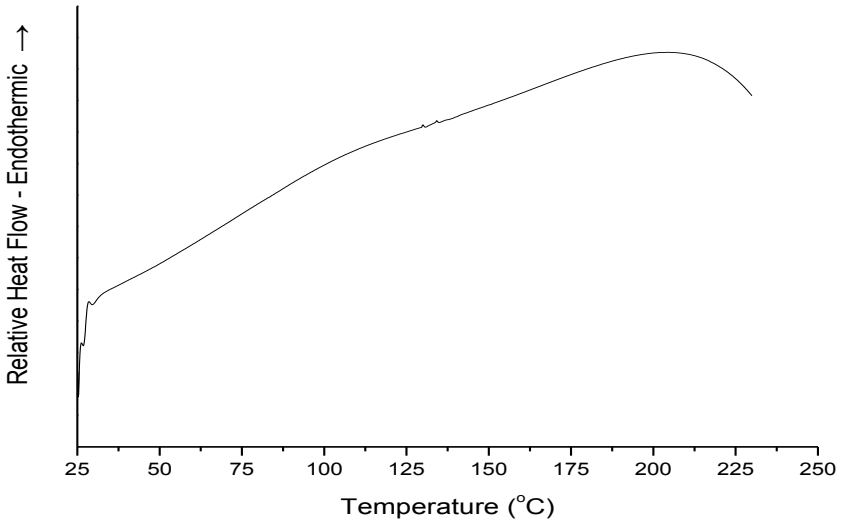

Figure 39: DSC scan for the reheating of chitosan powder

3.4.7.2. DSC - PVA

The DSC scans of pure PVA have been discussed previously in section 3.2.1 however another representation of the PVA powder DSC trace is shown in Figure 40 for clarity. PVA exhibited a T_g at 45°C and a T_m at 218°C.

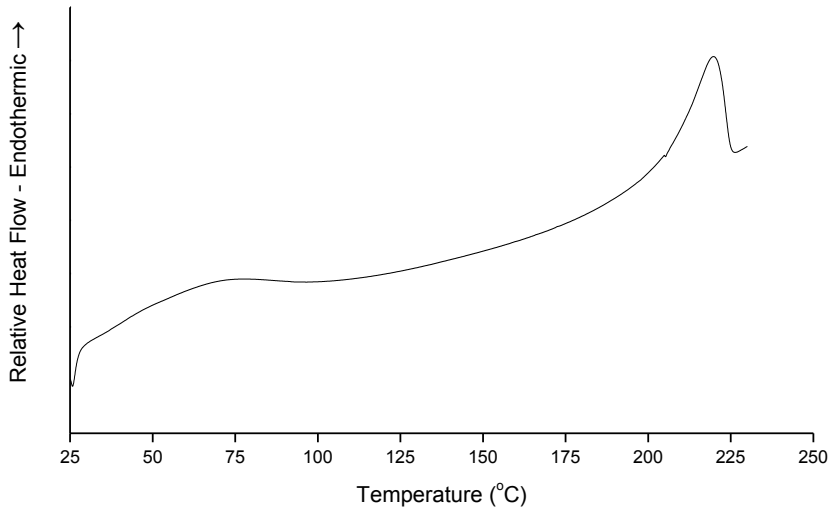

Figure 40: DSC trace of PVA powder

3.4.7.3. DSC – PVA/chitosan

3.4.7.3.1. Effect of blend ratio

DSC traces were obtained from fibre samples produced by electrospinning at an applied voltage of 15 kV, a needle tip distance of 10 cm and flow rate of 1 ml/hr from PVA/chitosan solutions of blend ratios 90:10 and 80:20. These traces are presented in Figure 41.

From Figure 41, it can be seen that as the chitosan content in the polymer solution is increased, the T_m is shifted towards a lower temperature. Furthermore, when the T_m

values of the electrospun PVA/chitosan blends are compared to PVA powder, it can be seen that the T_m of the blends is much lower. While the electrospinning process has been shown in the work presented in section 3.2.1 to have an effect on the peak intensities and therefore the crystallinity, it does not have an effect on the T_m values. It can therefore be reasoned that the reduction in the T_m is attributed to the addition of chitosan.

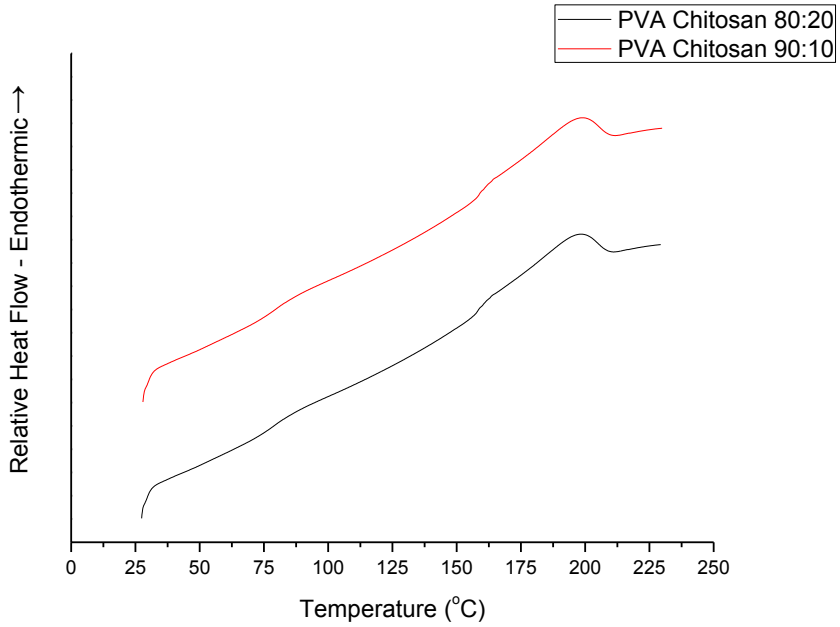

Figure 41: DSC heating trace of PVA/chitosan blend ratio electrospun at 20 kV with a needle tip distance of 10 cm

The peak intensity is also seen to reduce as compared to the PVA powder, which exhibits a sharp endothermic peak, the peak for PVA:chitosan blends are broader and less well defined. Upon calculating the crystallinity, it is shown that increased chitosan content decreases the % crystallinity of the samples suggesting that the

crystalline microstructure could not be developed as well in the blended samples. Table 16 shows the thermal analysis results of electrospun PVA/chitosan from different blend ratios.

Table 16: Thermal analysis results of electrospun PVA:chitosan from a 7% solution with different blend ratios electrospun at 20 kV

PVA:Chitosan Ratio	T_m (^oC)	C (%)
90:10	204	17.4
80:20	201	16.7

The reduction in T_m is attributed to the molecular interactions which occur between the PVA and chitosan blends [99]. This result is in keeping with results shown in papers focused on non-electrospun PVA/chitosan blends [208] and glutaraldehyde-chitosan/PVA blend films [209]. The T_m is determined by the amount of energy required to break bonds to make the phase transition from solid to liquid. PVA and chitosan individually both have a large amount of hydrogen bonds acting between the polymer chains which require energy to break. When the two polymers are blended the alignment between the chains is disrupted resulting in less intermolecular interactions. This means less energy is required due to there being fewer bonds to break and the T_m will be lower.

It has already been discussed in section 1.6.2, that the electrospinning process has a detrimental impact on the crystallinity of the produced fibres due to the fast solidification time. However, when the PVA:chitosan blend fibres are compared to

PVA fibres electrospun under the same operating parameters, it can be seen that crystallinity is lower in the blended fibres. This suggests that crystallinity is being reduced not only by the electrospinning process but by the addition of chitosan to the blend.

The explanation for the reduced crystallinity is similar to the explanation for the reduced T_m value as a reduction in T_m is normally indicative of a lower crystallinity. When the chitosan and PVA are blended, intermolecular bonds are broken and the order and alignment of the polymer chains is disrupted. This inhibits the formation of bonding between polymer chains and a more amorphous structure will be present.

3.5. Electrospinning of Chitosan-hydroxybenzotriazole

With the addition of hydroxybenzotriazole, chitosan was successfully dissolved in water. The dissolution was complete when the blend ratio of chitosan:HOBt was 1:1. However, complete dissolution could not be achieved with the 2:1 blend ratio even with the addition of heat when stirring. Chitosan could successfully be dissolved at room temperature with a 1:1 blend. This is in keeping with the study conducted by Fangkangwanwong et al. [210] who proposed the mechanism of the reaction between chitosan-HOBt and water as shown in Figure 42.

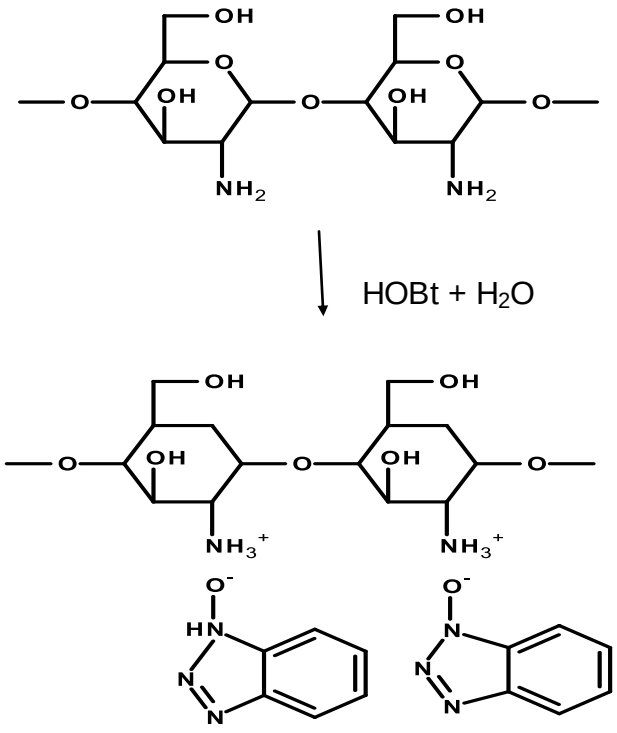

Figure 42: Mechanism of chitosan reacting with HOBt in order to dissolve in water

Attempts were then made to electrospin the chitosan-HOBt solutions produced with a 1:1 blend ratio at solution concentrations of 1, 2 and 3 %. Fibre production from these solutions was unsuccessful. A stable jet could not be achieved despite extensive alterations of the operating parameters of the electrospinning equipment. Instead of a jet formation droplets were ejected from the needle tip with globular deposits collected on the collecting plate. This result was the same as what was observed when attempting the electrospin pure chitosan in acetic acid solutions.

3.6. Chitosan-hydroxybenzotriazole/PVA

In the same way that the addition of PVA facilitated the formation of fibres from chitosan in an acetic acid solution, it also facilitated the formation of fibres when added to chitosan-HOBt-water solutions.

Figure 43 shows SEM micrographs comparing the morphology of fibres produced from an acetic acid chitosan/PVA solution and a chitosan-HOBt/PVA water solution. The solutions were made up to the same concentration and blend ratio (7% solution concentration with a blend ratio of 90:10 PVA:chitosan) and were electrospun under the same operating parameters of 15 kV applied voltage and needle tip distance of 10 cm. It can be seen from these micrographs, that the morphology is not affected by the use of a HOBt-water solution compared to the traditional acetic acid solution. Uniform bead free fibres were produced in both cases with average fibre diameters 205 nm and 187 nm, respectively.

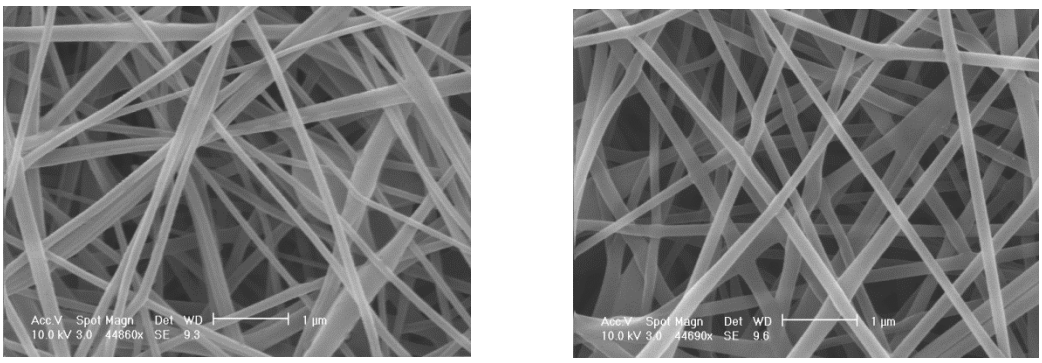

Figure 43: SEM micrographs of Electrospun fibres produced from (A) Chitosan/PVA acetic acid solution (B) Chitosan-HOBt/PVA water solution

Fibre production from blend ratios of 90:10 and 80:20 were both successful, however when the chitosan content was increased to 70:30, the viscosity of the solution became too great to electrospin. It has previously been reported, that fibres could not be produced from chitosan/PVA blends when the proportion of chitosan exceeded 30% [99].This was due to insufficient interactions with PVA to inhibit the repulsive forces acting between the ionic groups in the chitosan backbone, which

obstruct the formation of fibres. It was then suggested by Charernsriwilaiwat et al. [117], that when the HOBt-water system was utilised as opposed to the use of acetic acid, the chitosan content could be as high as 50% whilst still successfully yielding fibres. This result could not be replicated in the current study at a 7% solution concentration as the viscosity became too great to electrospin when the chitosan content was increased above 20%. This may be due to the use of PVA with a greater M_w in the present work than in the previous study, the M_w of PVA used in the previous paper is not given. If the M_w of PVA was higher this would cause an increase if viscosity. It could also be due to a different electrospinning set-up being used in the previous study with a larger needle diameter which allowed solutions with greater viscosity to flow through it.

3.7. Polyhydroxybutyrate

3.7.1. **Yields of PHB produced with different carbon sources**

PHB yields were determined as part of previous work conducted by Bagheriasl [182] who produced the PHB and are presented in Table 17. These values were used to derive the percentage of PHB.

Table 17: Cell dry weight, PHB produced and % PHB produced from the three different carbon sources after fermentation [182].

Carbon source	Average CDW (g/l)	Average PHB cell (g/l)	PHB (%)
Glucose	1.07	0.13±(0.01)	12
Olive oil	3.45	1.26 ±(0.2)	37
Rapeseed oil	2.9	1.06 ±(0.1)	37

The results show that when glucose was utilised as a carbon source the accumulated yield of PHB was much lower, only 0.13g/l (12%), compared to when either of the two oils were used, 1.06g/l (37%) and 1.26g/l (37%) for rapeseed oil and olive oil respectively.

As all experimental conditions were kept constant, the difference in the yield of PHB can only be due to the effect of changing the carbon source. For a given mass, plant oils such as rapeseed oil and olive oil contain more carbon atoms than sugars like glucose [211]. The results shown here therefore fall in line with the hypothesis that a greater number of carbon atoms will result in a greater yield of PHB.

3.7.2. **Characterisation of produced PHB**

In order to confirm that the substance produced was in fact PHB, FTIR analysis was carried out. The peak assignments of PHB were determined by performing a FTIR trace on a commercial sample of PHB purchased from Sigma Aldrich. The peaks observed in this trace which are characteristic to PHB are summarised in Table 18.

Table 18: FTIR peak assignments of commercial PHB

Characteristic peak (cm^{-1})	**Assignment**	**Reference**
~2900	C-H vibration	[212]
1720	C=O stretching	[212]
1457	CH_3 asymmetric deformation	[213]
1379	CH_3 symmetric deformation	[213]
1280	C-O-C stretching	[213]
1263	C-O-C stretching and CH deformation	[213]
1228	C-O-C stretching	[212]
1178	C-O-C stretching	[213]
1130	CH_3 rocking	[213]
1097	C-O-C stretching	[213]
1054	C-O stretching	[213]
1042	C-CH_3 stretching	[213]

The FTIR spectra of the suspected PHB samples produced from the three different carbon sources where then compared to this control spectra obtained from the commercial PHB. These traces can be seen in Figure 44.

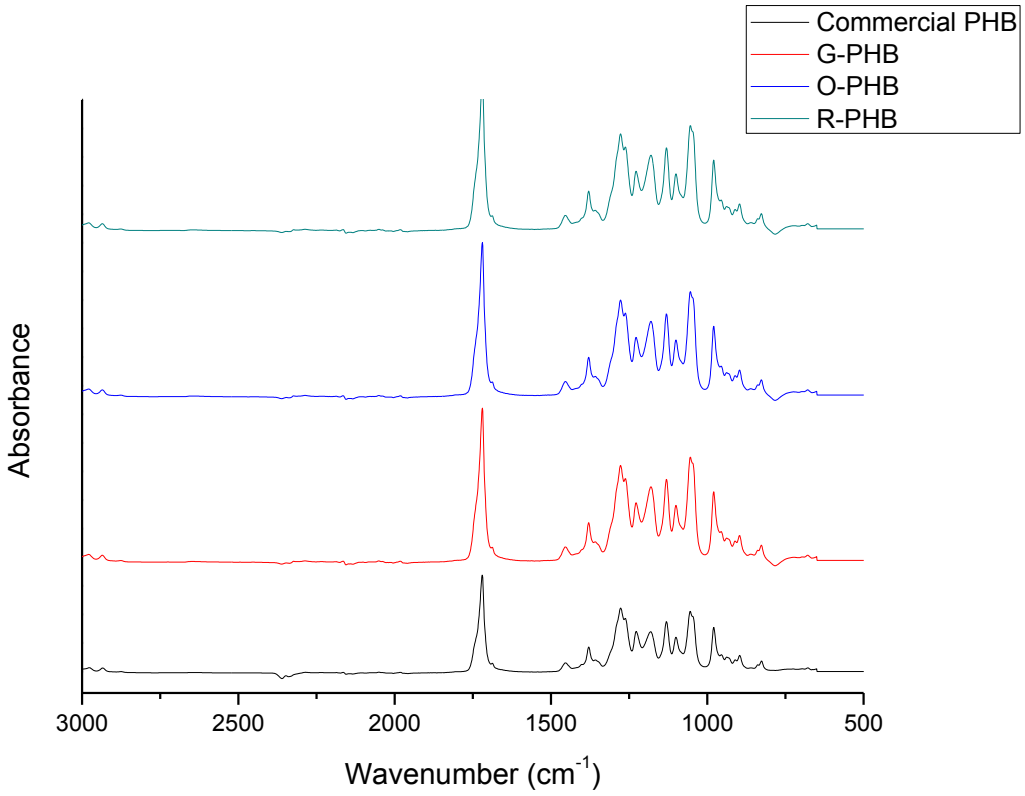

Figure 44: FTIR spectra comparing commercial PHB with PHB produced from *R. eutropha* using three different carbon sources.

As can be seen in the graph the spectra obtained were close to identical. The ester carbonyl band observed at 1720 cm^{-1} in the commercial PHB is present in all three samples. The peaks at wavenumbers 1379 and 1455 cm^{-1} characteristic of methyl (CH_3) and methylene (CH_2) deformations respectively and were visible in all PHB samples. The specific wave numbers and their respective assignments obtained from PHB produced from *R. Eutropha* are presented in Table 19 and compared to commercial PHB

.

Table 19: Peak placement and assignments from FTIR spectra of PHB produced from *R. eutropha* using three different carbon sources and compared to commercial PHB.

Characteristic Peak (cm^{-1})				Assignment
G-PHB	**O-PHB**	**R-PHB**	**Commercial PHB**	
2900	2900	2900	2900	C-H vibration [212]
1720	1720	1720	1720	C=O stretching [212]
1452	1460	1452	1457	CH_3 asymmetric deformation [213]
1381	1381	1381	1379	CH_2 symmetric deformation [213]
1276	1276	1276	1280	C-O-C stretching [213]
1260	1260	1260	1263	C-O-C stretching and CH deformation [213]
1226	1230	1226	1228	C-O-C stretching [212]
1179	1179	1179	1178	C-O-C stretching [213]
1135	1130	1135	1130	CH_3 rocking [213]
1103	1103	1103	1097	C-O-C stretching [213]
1051	1055	1051	1054	C-O stretching [213]
1043	1043	1043	1042	C-CH_3 stretching [213]

3.7.3. **Electrospinning of PHB**

Nanofibres were successfully produced by electrospinning each of the three PHB samples synthesised using glucose, olive oil and rapeseed oil from solution concentrations of 1.5%, 2% and 2.5%. Commercial PHB was also electrospun from a higher concentration solution of 13%.

3.7.3.1. G-PHB

Electrospinning of G-PHB from 1.5% w/v solutions at operating the parameters of 7 kV applied voltage and 12.5 cm needle tip distance resulted in the smallest average fibre diameter of 580 nm however the fibres produced were not uniform in diameter and contained a considerable amount of beading due to the low viscosity of the solution [32]. The beading problem was alleviated when the solution concentration was increased, with the 2% and 2.5% solutions not displaying the same beading phenomenon. Average fibre diameter showed an increase when solution concentration was increased, as depicted in Figure 45. Average fibre diameter increased from 580 nm to 990 nm and 1050 nm for 1.5%, 2% and 2.5%, respectively. This result is in keeping with the previous research showing that electrospun nanofibres show a tendency to increase in diameter when solution concentrations are increased due to an increase in viscosity and more chain entanglements resisting the stretching forces imposed on the jet by the electric field [55]. This is also in keeping with the previous work carried out in this study, with both PVA and PVA/chitosan blends showing an increase in fibre diameter when solution concentration was increased. As the fibres obtained from 1.5% solutions contained beads, the smallest fibres suitable for application produced from G-PHB were from the 2% solution at 990 nm. T test statistical analysis $p < 0.05$ showed there is a significant difference between the average fibre diameter of fibres produced from 1.5% G-PHB solutions and 2% G-PHB solutions with $p = 0.000001$ but the difference between 2% and 2.5% was not statistically significant.

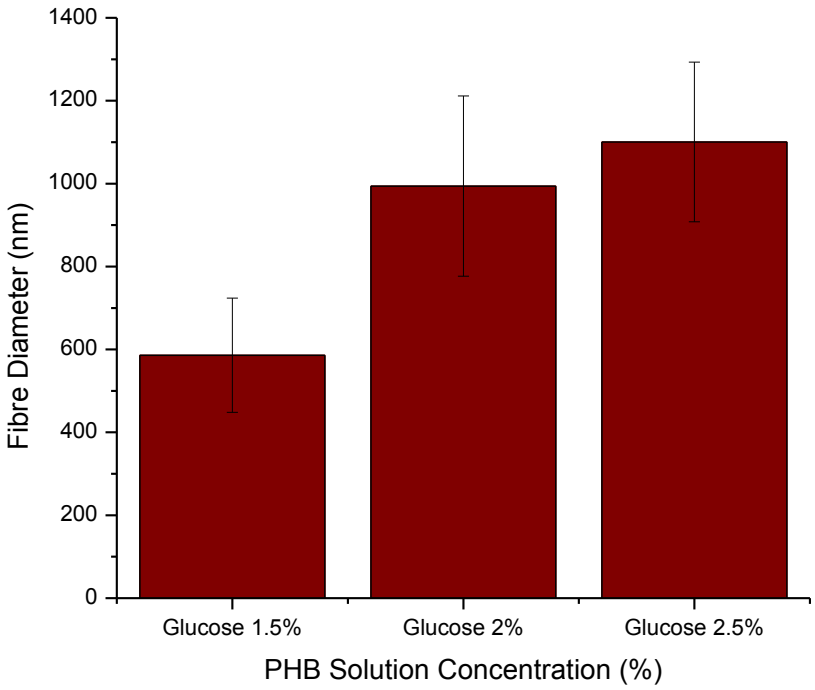

Figure 45: Average fibre diameter of electrospun nanofibres produced from G-PHB at solution concentrations of 1.5%, 2% and 2.5% w/v

SEM micrographs of fibres produced from each solution as well as histograms displaying the fibre diameter distribution are presented in Figure 46.

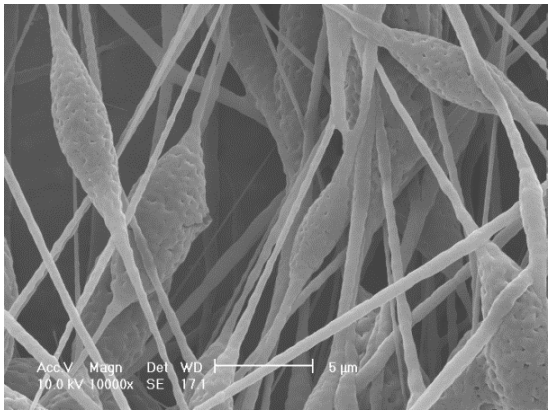

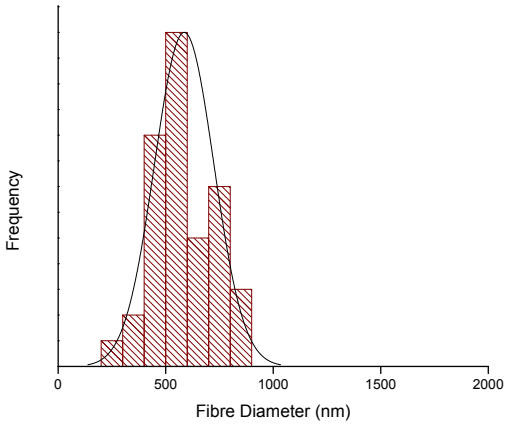

1a

1b

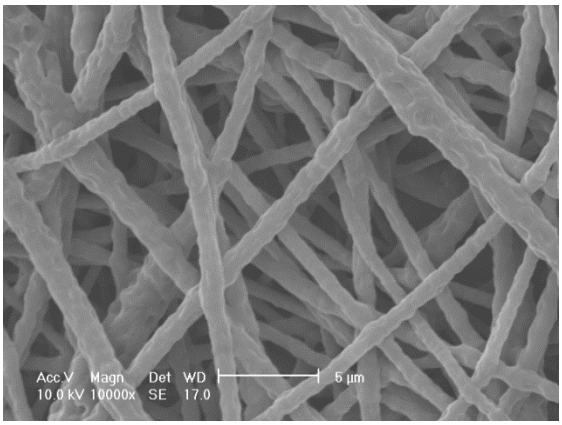

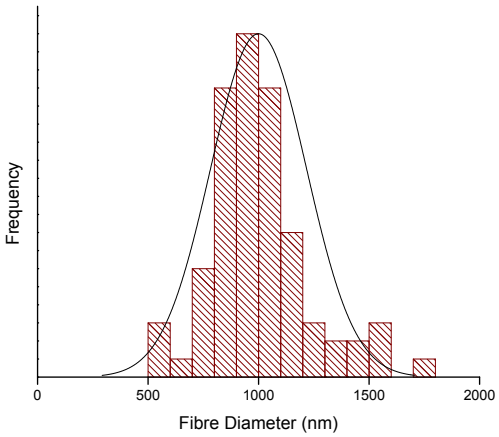

2a

2b

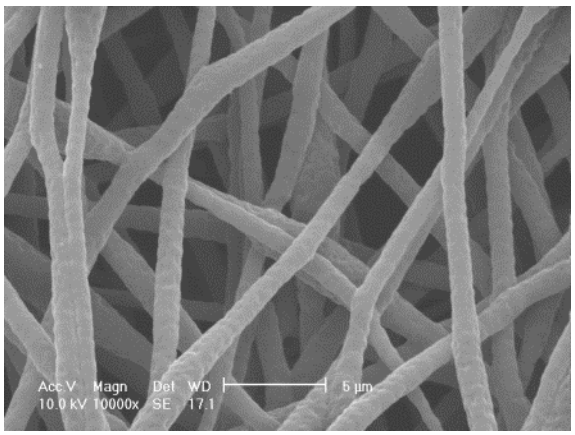

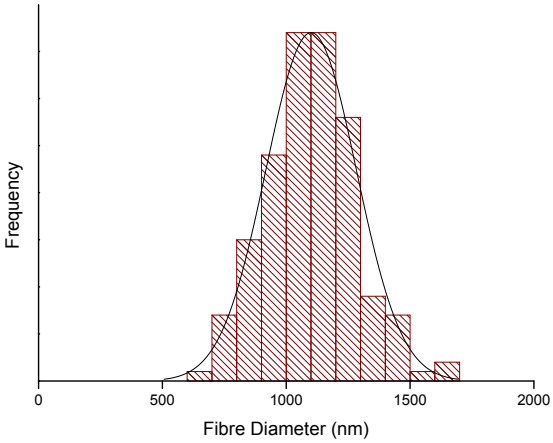

3a

3b

Figure 46: SEM micrographs (a) and histograms (b) depicting the fibre diameter distribution obtained after electrospinning G-PHB from (1) a solution concentration of 1.5% w/v (2) a solution concentration of 2% w/v and (3) a solution concentration of 2.5% w/v

3.7.3.2. O-PHB

Electrospinning of O-PHB was successful from all three solution concentrations 1.5%, 2% and 2.5% however once again the morphology of the fibres varied depending on the concentration. SEM micrographs of fibres produced from each solution as well as histograms displaying the fibre diameter distribution are presented in Figure 47.

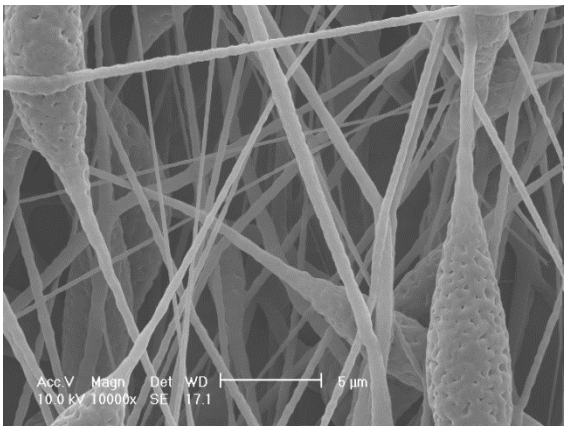

1a

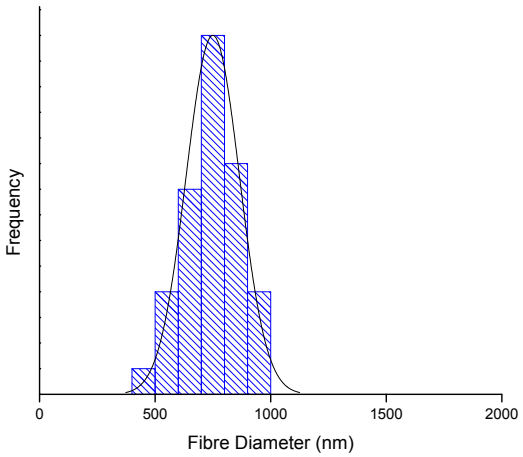

1b

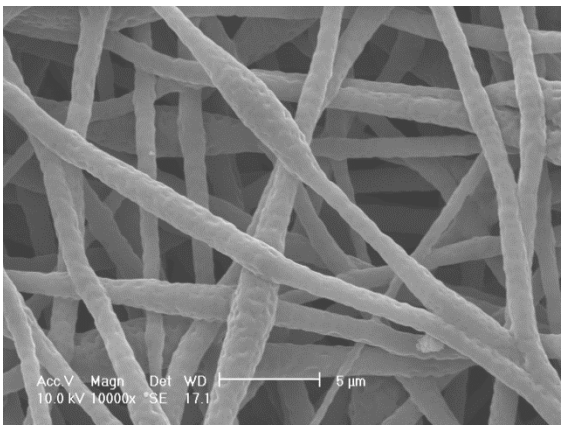

2a

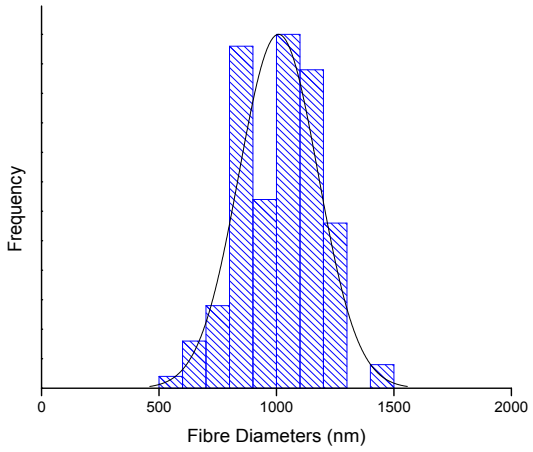

2b

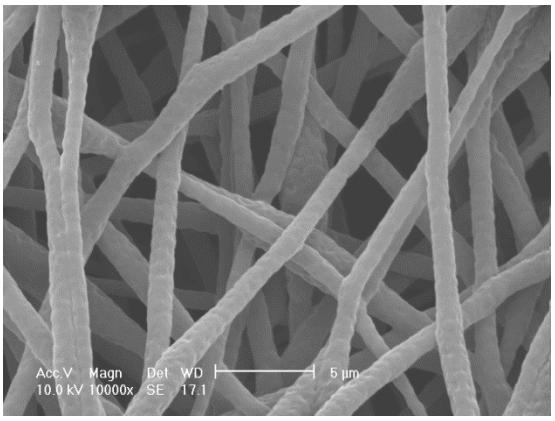

3a

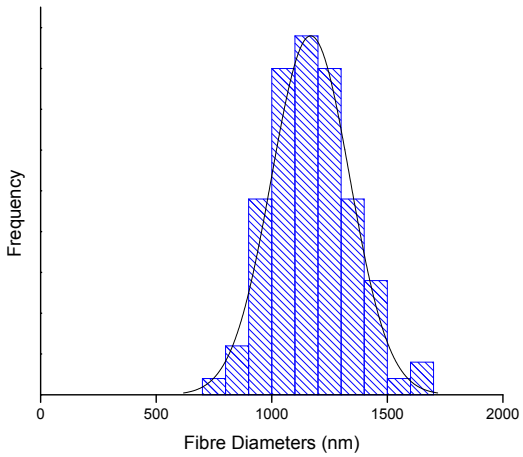

3b

Figure 47: SEM micrographs (a) and histograms (b) depicting the fibre diameter distribution obtained after electrospinning O-PHB from (1) a solution concentration of 1.5% w/v (2) a solution concentration of 2% w/v and (3) a solution concentration of 2.5% w/v.

The 1.5% O-PHB solution resulted in the smallest average fibre diameter of 750 nm however there were many beads present on these fibres so the average fibre diameter figure is not an accurate representation of the quality and uniformity of the fibres produced. Average fibre diameter increased to 980 nm and 1150 nm for 2% and 2.5% solution concentrations respectively. Beading was reduced in the fibres produced from the 2% solution but there were still present. The fibres produced from the 2.5% solution were completely bead free. Figure 48 shows the effect of solution concentration on resultant fibre diameters after electrospinning. Performing a T test, $p = < 0.05$, for statistical analysis revealed $p = 0.0000001$ between the average fibre diameter fibres produced from 1.5% O-PHB solutions and 2% O-PHB solutions, showing there is a significant difference. The difference between 2% and 2.5% was not statistically significant.

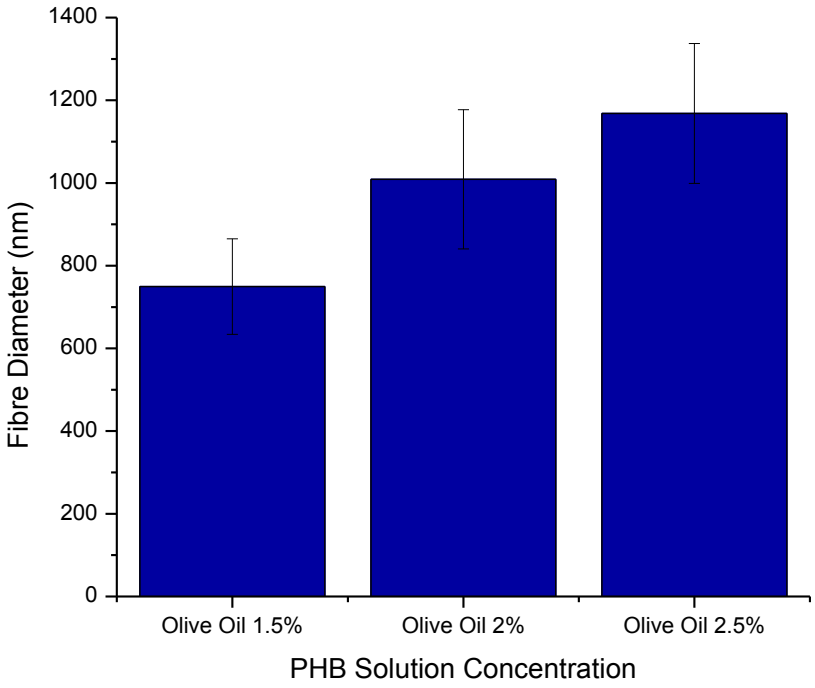

Figure 48: Bar graph showing the average fibre diameter of electrospun nanofibres produced from O-PHB at solution concentrations of 1.5%, 2% and 2.5% w/v.

3.7.3.3. R-PHB

Electrospinning of R-PHB was successful from all three solution concentrations; 1.5%, 2% and 2.5%. A bar graph showing the average fibre diameters obtained from R-PHB from different concentration solutions is shown in Figure 49.

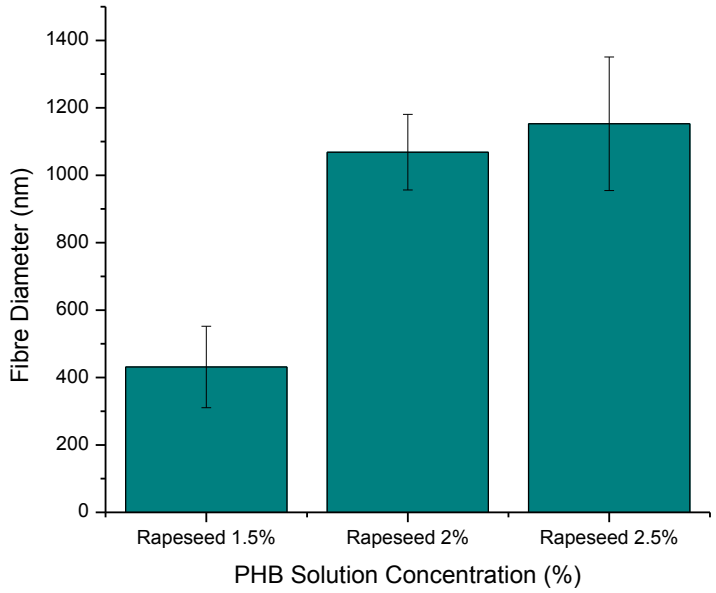

Figure 49: Average fibre diameter of electrospun nanofibres produced from R-PHB at solution concentrations of 1.5%, 2% and 2.5% w/v.

The average fibre obtained from the 1.5% R-PHB was ~425 nm which was the lowest of the three carbon sources by over 100 nm. While the average fibre diameter was the lowest from the 1.5% R-PHB solution the histogram of fibre diameters shows it also had the largest spread of fibre diameters with a range of ~150 nm -~750 nm. Ideally a scaffold would be made up of fibres all of the same size and shape so that its properties are consistent throughout the scaffold. If some

fibres are larger than others or there is an area made up of predominantly larger fibres then this will have an impact on the porosity of the scaffold in this area and may be less efficient at filtration for example [184]. As shown in O-PHB and G-PHB beads are again present from the lowest concentration. The beads are no longer present in the scaffolds produced from 2% and 2.5% concentrations. Average fibre diameter increases as solution concentration increases, up to ~1000 nm for 2% and ~1100 nm for 2.5%. The histograms show that diameter distribution is the lowest for the 2% solution with the majority of fibres falling within a diameter range of 400 nm compared to a 1000 nm range from 2.5% and 550 nm from 1.5%

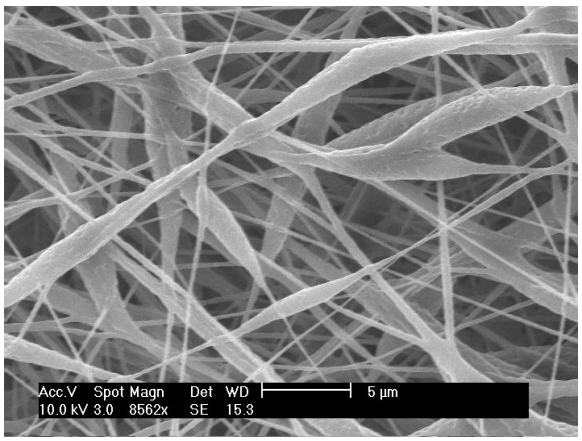

1a

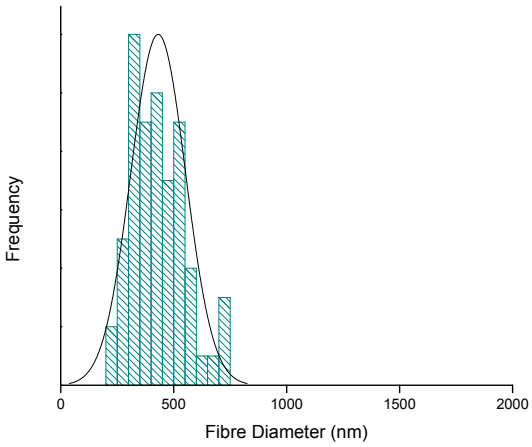

1b

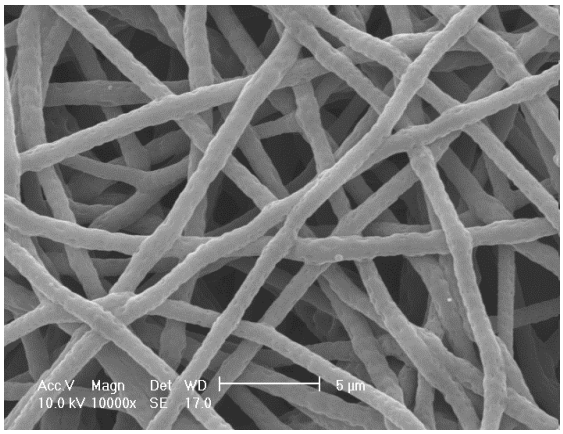

2a

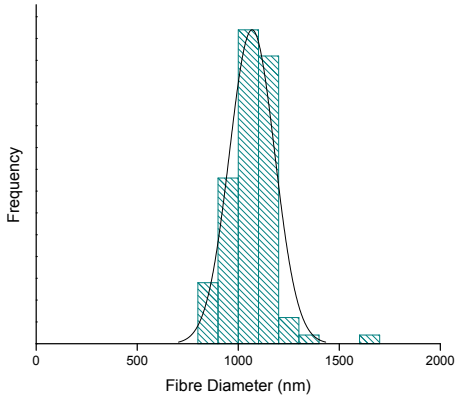

2b

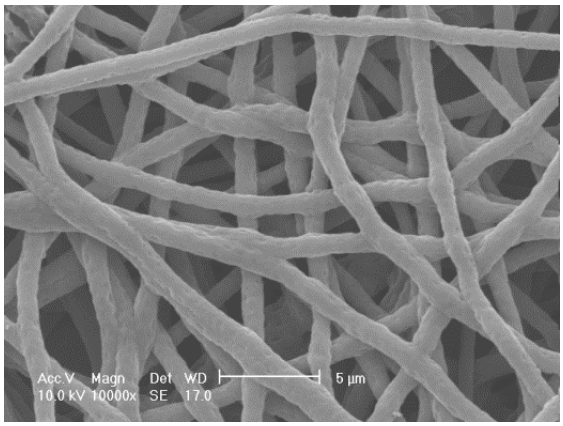

3a

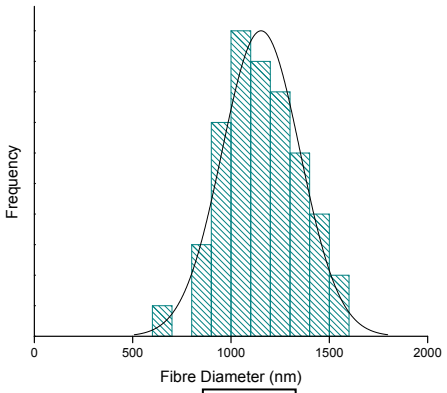

3b

Figure 50: SEM micrographs (a) and histograms (b) depicting the fibre diameter distribution obtained after electrospinning R-PHB from (1) a solution concentration of 1.5% w/v (2) a solution concentration of 2% w/v and (3) a solution concentration of 2.5% w/v

3.7.4. **Discussion of Electrospinning PHB from different carbon sources**

We can see from these results that the PHB produced from each of the carbon sources show the same trends when electrospun from varying concentration solutions. 1.5% results in the smallest overall average fibre diameter however the % size variation between the fibres is the greatest, so there are not all of a similar diameter as desired. The prevalence of beads is also greatest in the 1.5% solutions due to the lower viscosity which is inherently attributed to low concentration solutions. A solution with a low concentration of polymer present will have fewer polymer chain entanglements and will therefore exhibit a lower viscoelastic force when electrospinning [31]. The viscoelastic force works to oppose the Coulombic forces and electric field, which are both acting to stretch the solution as it travels in the jet. If the viscoelastic force is greatly exceeded by the coulombic forces then the stretching forces will be too great and the parts of the jet may break up. The formation of beads then occurs due to the elasticity of the stretched polymer chains recoiling back towards their original length before solidifying, resulting in small areas of fibres with larger diameters, which are known as beads [35]. This is also thought to be the cause of the larger deviation in fibre diameters, the low viscoelastic forces causing irregular splitting of some chain entanglements and not others resulting in some areas of the jet stretching more than others.

When the solution concentration is increased, the viscosity is also increased, so the viscoelastic forces are greater and there is less chance of jet splitting and bead formation. This is believed to be the case with the current work. As the concentration is increased from 1.5% to 2% fewer beads are present in the PHB fibres from all three carbon sources. A few beads are still present from this

concentration but with far less frequency. The effect is demonstrated further when the concentration is increased to 2.5% no beads were found in the scaffolds at all.

The average fibre diameters obtained from PHB in this series of experiments were quite large by electrospinning standards at around 1µm for bead free uniform fibres. It is possible to create polymeric fibres with diameters as small as 1 nm [214]. It can therefore be concluded it is not the process that is leading to the larger diameters, but the material/solution used or the operating parameters implemented. The applied voltage has been shown to be a key parameter in achieving small fibre diameters. The applied voltage used in this study was 7 kV which is significantly lower than others studies, with voltages of up to 25 kV typically used. Increasing the applied voltage has been shown by some, to decrease fibre diameter [48, 58]. 7 kV was chosen as a parameter for this study as it was suitable for successfully producing fibres from a range of different concentrations while allowing direct comparison to be made. However future work could be carried out to optimise the parameters for each solution in order to produce smaller fibres.

While the produced fibre are considered large by electrospinning standards, when the sizes of the fibres produced in the current study are compared to those in the literature it can be seen that the fibres obtained in this study are smaller. Suwantong et al. [171] and Sombatmankhong et al. [169] obtained PHB fibres with diameters of 3.7 ± 1.7 µm. The parameters used in these experiments were different however, with a solution concentration of 14% w/v and an applied voltage of 12 kV. The reason for the much greater solution concentration was that the Mw of the PHB used was much lower, at 300,000 g/mol compared to the PHB used in the present study, at >700,000 g/mol, as will be discussed in section 3.7.7.

3.7.5. **Addition of Salt to PHB Solutions for Electrospinning**

Benzyl triethylammonium chloride (BTEAC) was added to 2% PHB solutions at concentrations of 0.5, 1 and 1.5%. The addition of greater than 1.5% BTEAC appeared to be too much as a stable jet could not be produced, however fibres were successfully produced with the addition of 0.5% and 1% salt. The average diameter of these fibres was significantly smaller than those produced without the addition of BTEAC while all other variable parameters were kept constant. Figure 51 shows SEM micrographs along with fibre diameter histograms of fibres produced from 2% solution from PHB samples synthesised with each of the three carbon sources.

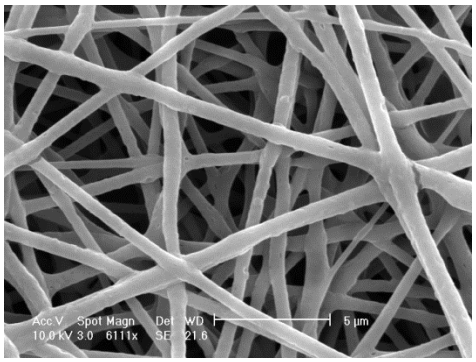

1a

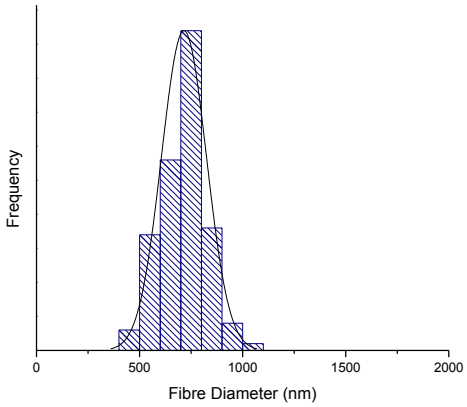

1b

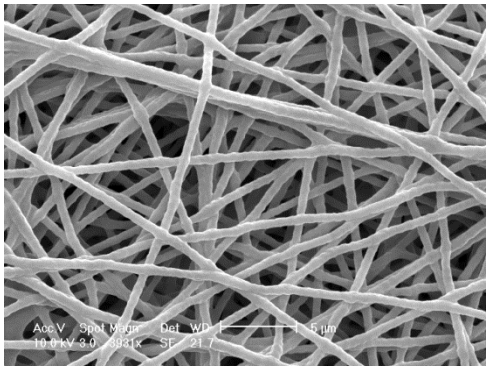

2a

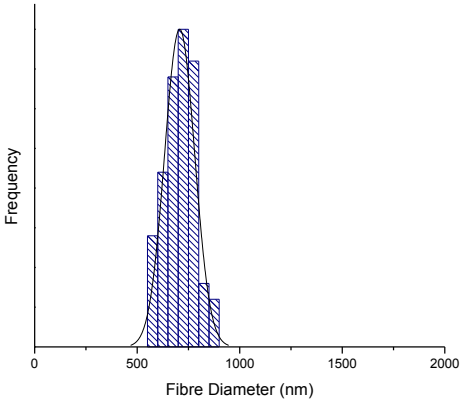

2b

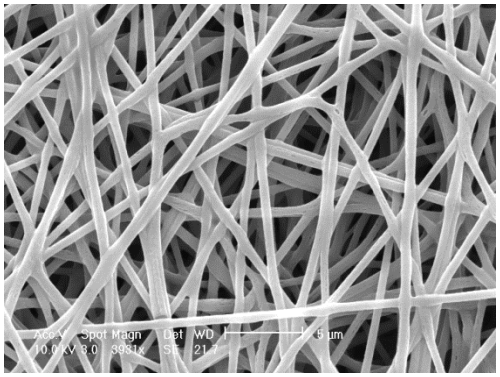

3a

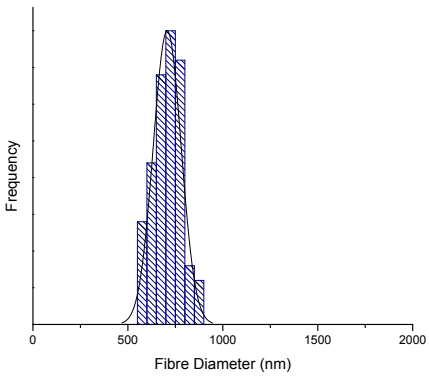

3b

Figure 51: SEM micrographs (a) and histograms (b) depicting the fibre diameter distribution obtained after electrospinning 2% PHB solutions with the addition of 1% BTEAC in the solution from (1) G-PHB (2) O-PHB (3) R-PHB

As well as the significant decrease in fibre diameter achieved by the addition of BTEAC we can also see differences in the morphology of the fibres by comparing the SEM micrographs shown in Figure 51 to those shown in Figure 46 Figure 47 and Figure 50. Firstly, there was not a single bead present in any of the samples produced when 1% BTEAC was added to the solution. Secondly, the surface of the fibres was smoother. This can be attributed to the same factor that leads to the decreased fibre diameter, the conductivity of the polymer solution. Choi et al. [172] have shown that the conductivity of a PHB chloroform solution is increased by the addition of BTEAC. Because there is greater charge density acting on the jet due to the increased conductivity, the elongation forces are also greater as the charged ions repel each other and act to stretch the fibres more than they would be in a less conductive jet. The increased stretching results in smaller, straighter, smoother fibres [214].

Table 20 presents a comparison between the average fibre diameters obtained when PHB samples produced using different carbon sources were electrospun with the addition of varying amounts of BTEAC.

Table 20: Comparison between the fibre diameters obtained from PHB samples produced using different carbon sources with varying amounts of BTEAC added to the solution prior to electrospinning.

PHB solution	**BTEAC %**			
	0	**0.5**	**1**	**1.5**
	Average Fibre Diameter (nm)			
2% G-PHB	994	680	685	675
2% O-PHB	1009	663	640	653
2% R-PHB	1068	692	684	672

We can see from these results that there is a >30% decrease in average fibre diameter with the addition of BTEAC. A reduction in fibre diameter was achieved by the addition of 0.5% BTEAC; however further addition of BTEAC up to 1% and 1.5% do not result in further reduction in fibre diameter. When BTEAC concentrations greater than 2% were added the solution was rendered unspinnable. In this instance the formation of a stable Taylor cone was not possible and multiple jets were sprayed from the needle tip. It therefore seems that the effect of conductivity on fibre diameter is only beneficial up to a critical value, above which, no additional benefit can be gained until eventually it is detrimental. It has been shown previously that while increases in conductivity can improve electrospinning, too high conductivity is unsuitable as it causes a reduction in the tangential electric field resulting in the electrostatic force running along the surface of the solution to diminish significantly, which works against Taylor cone formation [43]. The effect BTEAC has on the

conductivity of the solution should be related to the viscosity of the solution. As such if the PHB concentration in the solution is increased, then it would be expected that a greater amount of BTEAC would be required to see a reduction in fibre diameter. It is also expected that the critical amount of BTEAC before electrospinning was not longer possible would also be increased.

Scaffolds produced with BTEAC present were treated with methanol to remove the BTEAC. FTIR was carried out after the treatment to ensure the BTEAC had been removed. The graph in Figure 52 shows a comparison of fibres obtained with a 2% PHB solution with no BTEAC present and fibres from a 2% PHB solution with 1% BTEAC after methanol treatment. These are approximately identical and there are no signs of characteristic peaks from BTEAC present.

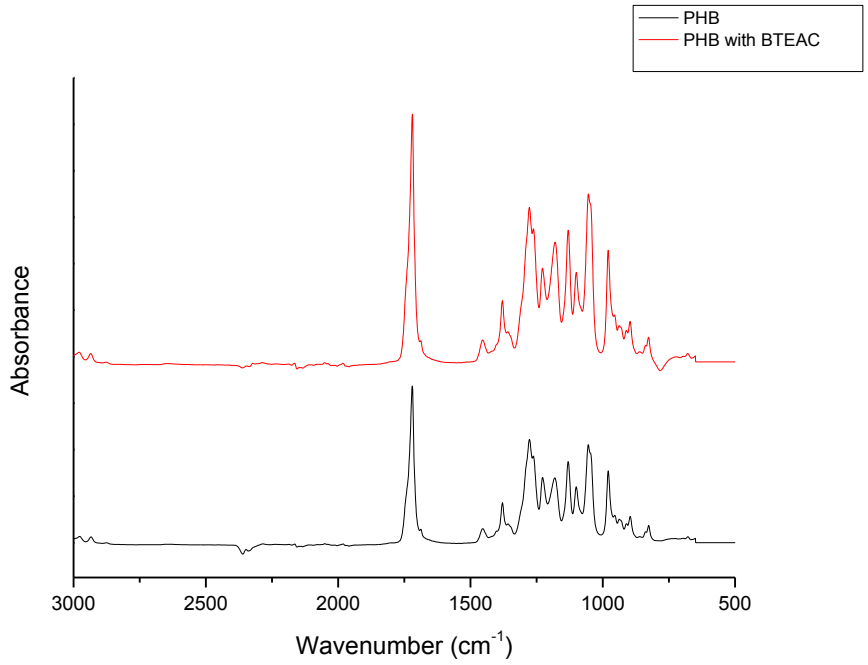

Figure 52: FTIR spectra showing electrospun G-PHB compared with electrospun G-PHB which had BTEAC present in the solution before electrospinning

3.7.6. **Commercial PHB**

In order to compare the PHB produced from the three different carbon sources a commercial PHB sample was also electrospun. This sample was different to the produced PHB and as such the solution concentration had to be altered in order for successful electrospinning to be performed using the same operating parameters used throughout the rest of this study (applied voltage of 7 kV and needle tip distance of 12.5 cm flow rate of 1ml/hr). This difference was due to the molecular weight of the PHB being considerably lower than that of the G-PHB, O-PHB and R-PHB. The solution concentration had to be increased from 1.5-2.5% in the earlier series of experiments to ~10% in order to produce a solution with comparable viscosity. The solutions were very difficult to electrospin and the fibres that were produced were highly beaded. An SEM image of fibres produced from commercial PHB is shown in Figure 53.

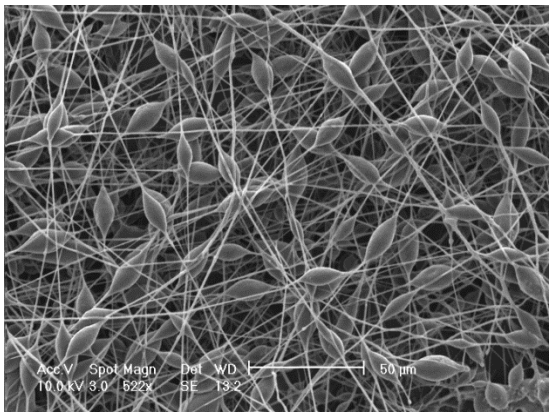

Figure 53: SEM micrograph of commercial PHB electrospun from a 10% w/v solution

3.7.7. **GPC analysis**

Gel permeation chromatography was carried out on the produced PHB samples from all three carbon sources, both before and after electrospinning, in order to determine the molecular weight (M_w), molecular mass (M_n) and the polydispersity (PD). The results from GPC for electrospun and non-electrospun PHB are shown in Table 21. There were no significant differences in the M_w of PHB produced using the two oils, olive oil and rapeseed oil with values of 7.14 $x10^5$ g/mol and 7.10$x10^5$ g/mol respectively, or PHB produced using glucose as a carbon source which exhibited an M_w only slightly higher at 7.61$x10^5$ g/mol.

Table 21: Weight average molecular weight (M_w), number average molecular mass (M_n) and polydispersity (PD - M_w/M_n) of non-electrospun and electrospun PHB samples produced using olive oil, rapeseed oil and glucose as carbon sources.

PHB	**M_w ($x10^5$ g/mol)**	**M_n ($x10^5$ g/mol)**	**Polydispersity (PD)**
G-PHB	7.61	6.29	1.21
G-PHB (electrospun)	7.35	6.07	1.23
O-PHB	7.14	4.95	1.42
O-PHB (electrospun)	5.92	4.15	1.43
R-PHB	7.10	4.89	1.45
R-PHB (electrospun)	5.79	3.94	1.47

The GPC data obtained shows that PHB produced using glucose has a greater uniformity in its molecular weight as demonstrated by a lower PD value of 1.21

compared with 1.42 and 1.45 from olive oil and rapeseed oil, respectively. When comparisons are made between PHB samples before and after electrospinning it can be seen that the PD remains unchanged by the electrospinning process. M_w and M_n are seen to reduce marginally, but not by a significant amount so we can conclude that the electrospinning process does not have an effect on the molecular weight of the polymer, this is in keeping with previous literature which has not shown solution electrospinning to have an effect on molecular weight. Although high stress conditions are present during electrospinning, the magnitude of the elongational flow is not sufficient to cause chain scission which would result in a lower M_w [192]. There are however examples of where molecular weight has decreased after melt electrospinning of poly(ethylene terephthalate) attributed to thermal degradation experienced within the melt reservoir [215] and in PLA attributed to a combination of thermal degradation and mechanical scission caused by the polymer melt being forced through the needle tip [216]. There are subtle differences between the molecular characteristics of PHB produced using glucose and PHB produced using the two oils. Previous literature has suggested that the M_w of PHB produced using plant oils is hindered by the presence of glycerol which can act as a chain transfer agent which hinders chain elongation and as a result reduces the M_w [217]. It has also been reported that fructose produced PHB had a higher M_w compared with PHB produced with virgin sesame oil and soybean oil [218, 219]. The oils studied in the present work show no such disadvantages or effects on M_w when compared to the use of glucose.

3.7.8. **DSC of PHB**

The melting temperature (T_m) and percentage crystallinity (C) results derived from the DSC scans of the PHB samples produced using the three different carbon sources are presented in Table 22.

Table 22: Thermal analysis results of PHB produced by *Ralstonia eutropha* using olive oil, rapeseed oil and glucose as carbon sources

PHB	T_m (^oC)	C (%)
O-PHB	173.2	54.2
R-PHB	172.2	52.2
G-PHB	172.5	53.5

The glass transition temperature (T_g) of PHB has been shown to be in the range of 0-5^{o}C [220]. The DSC traces in the present study were carried out in a temperature range of 25 ^{o}C – 200^{o}C so as expected a T_g peak was not present in any of the traces. Thermal analysis results show that there were no significant differences between PHB samples produced using the different carbon sources. T_m was approximately 172.5^{o}C. All three percentage crystallinity values were within ± 1% of 53 %. The values obtained for the T_m were in line with values found in previous literature for PHB [221]. This result shows that there is no detrimental effect on thermal characteristics of PHB produced using *Ralstonia Eutropha* when the carbon source is substituted from glucose with either of the two oils trialled in the present study.

3.7.8.1. DSC of electrospun G-PHB

DSC traces of PHB produced using glucose and then electrospun from solution concentrations of 1.5, 2 and 2.5 % w/v were compared to the as-produced PHB which had not undergone electrospinning. Figure 54 shows the DSC traces obtained from G-PHB samples before and after electrospinning from different concentrations

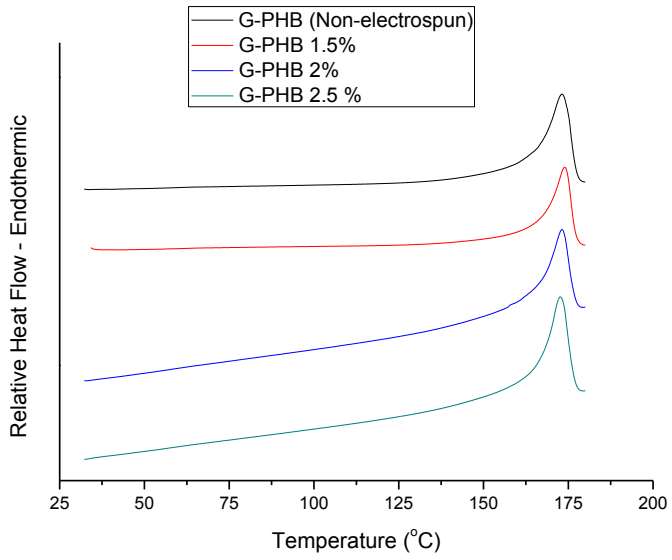

Figure 54: DSC traces of G-PHB electrospun from different concentrations solutions as compared to non-electrospun G-PHB

It can be seen from the DSC traces that the endothermic peak associated with the T_m of the samples all occurred at a similar temperature which was consistent with the T_m values seen in the literature [222]. The breadth of these peaks was also similar between all three samples. This result is as expected; the breadth of the

endothermic melting peak is primarily determined by the polydispersity of the polymer being tested. A large polydispersity whereby many different chain lengths are present in the polymer will lead to a much broader melting peak brought on by shorter chains melting before longer ones. Conversely when a polymer has a small polydispersity, all of the chains will be a similar length and a very narrow peak will be exhibited as all the chains will melt at approximately the same temperature [223]. The GPC data presented in section 3.7.7 showed that the polydispersity between non-electrospun PHB and PHB electrospun from a 2% solution remained unchanged, with both values at approximately 1.22. This result is confirmed by the similar breadths observed in the melting peak. The T_m values of G-PHB also did not change significantly, with the T_m still occurring at around 172^oC after electrospinning, except for the sample produced from the 2.5% concentration solution which was a little lower at 166.4^oC. No crystallisation peak was seen upon heating G-PHB as PHB is already semi-crystalline [137]. Crystallinity values were calculated using the heat of fusion values obtained from the area under the melting peak using the equation detailed in section 2.4. The crystallinity values for electrospun G-PHB were all lower that the G-PHB sample which had not been electrospun. It was also observed that crystallinity increased when the solution concentration was increased.

The values for T_m and C for electrospun G-PHB are summarised in Table 23.

Table 23: Thermal analysis results of electrospun G-PHB electrospun from different solution concentrations

PHB	Solution concentration					
	1.5		2		2.5	
	T_m (^oC)	C (%)	T_m (^oC)	C (%)	T_m (^oC)	C (%)
G-PHB	173.2	50.2	171.5	51.1	166.4	52.6

3.7.8.2. DSC of electrospun O-PHB

DSC traces of PHB produced using olive oil and then electrospun from solution concentrations of 1.5, 2 and 2.5 % w/v were compared to the as-produced PHB which had not undergone electrospinning. Figure 55 shows the DSC traces obtained from PHB samples before and after electrospinning from different concentrations

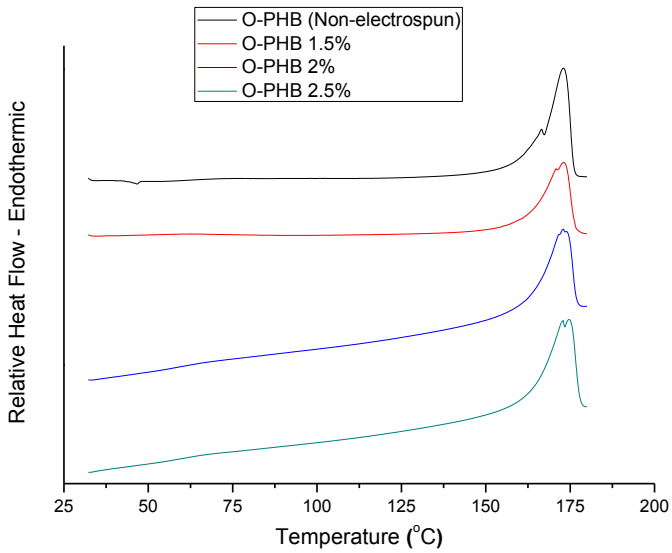

Figure 55: DSC traces of O-PHB electrospun from different concentrations solutions as compared to non-electrospun O-PHB

It can be seen from the DSC traces in Figure 55 that the T_m of both the non-electrospun and electrospun samples occurred at a similar temperature. It can also be seen that O-PHB exhibited a double melting peak. This may occur as a result of the crystalline structure of the sample. PHB has previously been shown in some cases to exhibit double, or even multiple melting peaks. This has been attributed to secondary crystallisation that has been shown to occur during melting and can also take place during storage at room temperature [224-226]. As with G-PHB there were no differences observed in the breadths of the endothermic melting peaks due to the samples all having the same PD values.

The thermal characteristics and crystallinity values calculated for O-PHB are shown in Table 24. The crystallinity of O-PHB was lower after electrospinning than the non-electrospun material. The greatest reduction was observed with the 1.5 % solution, compared to the non-electrospun material, whereby the crystallinity decreased from 54.2 % to 45.8 %. Crystallinity also decreased in the fibres obtained from higher concentration solutions, but not by such a significant amount, with a drop to 52.2 % for the 2% solution and 53.4 % for the 2.5 % solution.

Table 24: Thermal analysis results of electrospun O-PHB electrospun from different solution concentrations

PHB	**Solution concentration**					
	1.5		2		2.5	
	T_m (^oC)	C (%)	T_m (^oC)	C (%)	T_m (^oC)	C (%)
O-PHB	173.1	45.8	173.1	52.2	174.1	53.4

3.7.8.3. DSC of electrospun R-PHB

DSC traces of PHB produced using rapeseed oil and then electrospun from solution concentrations of 1.5, 2 and 2.5 % w/v were compared to the as-produced PHB which had not undergone electrospinning. Figure 56 shows the DSC traces obtained from PHB samples before and after electrospinning from different concentrations

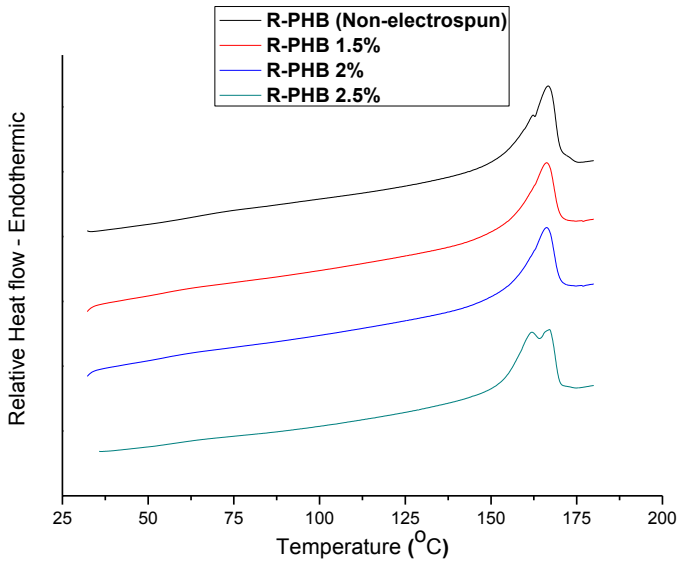

Figure 56: DSC traces of R-PHB electrospun from different concentrations solutions as compared to non-electrospun R-PHB

As with the other two PHB samples the R-PHB T_m value remained unchanged after electrospinning from all three solution concentrations at ~172°C. No significant differences were observed in the breadths of the melting peaks however a double melting peak was present in the R-PHB produced from the 2.5% solution. Once again this is attributed to secondary crystallisation that has been shown to take place within PHB during storage [224], resulting in some bimodal melting where some, slightly less ordered, secondary crystalline regions melt before the other crystalline regions.

The thermal characteristics and crystallinity values calculated for O-PHB are shown in Table 25. Crystallinity was seen to decrease in all three electrospun samples when compared to the non-electrospun material. The greatest reduction was with the 1.5% solution where the crystallinity decreased from 52.2 % in the as-produced material, to 41.9% in the electrospun sample. The crystallinity of the PHB from the 2% solution was comparable to the 1.5% solution at 42.1% however the crystallinity was found to be increased to 47.1% from the 2.5% solution; however this is still lower than the non-electrospun sample.

Table 25: Thermal analysis results of electrospun R-PHB electrospun from different solution concentrations

PHB	**Solution concentration**					
	1.5		**2**		**2.5**	
	T_m (^oC)	C (%)	T_m (^oC)	C (%)	T_m (^oC)	C (%)
R-PHB	171.9	41.9	171.2	42.1	173.4	47.4

A summary of the % crystallinity values obtained from thermal analysis of PHB samples both before and after electrospinning are shown in Table 26. It can be seen that PHB produced from all three carbon sources show a decrease in crystallinity once they have undergone the electrospinning process. The greatest difference is observed between the non-electrospun PHB and the PHB electrospun from a 1.5% solution, with R-PHB showing the most significant decrease from 52.2% to 41.9%. It is quite common for the crystallinity of electrospun material to be reduced when compared to the raw material. This is attributed to the fast deposition rate between

the jet being ejected from the needle tip, the solvent evaporating and reaching the collector [53]. This short time does not allow enough time for crystallisation and therefore a lower degree of crystallinity is observed. A case has been put forward that the electric field present during electrospinning can cause molecular orientation and alignment of polymer chains which would lead to an increased crystallinity [45]. This does not appear to be the case in this instance but this might be attributed to the fact that a relatively low voltage of 7 kV was being used for this series of experiments which may not have provided strong enough forces to encourage an increased crystallinity. This hypothesis suffers however due to the fact that the crystallinity increases as the solution concentration increases. An increase in solution concentration results in more chain entanglements and greater viscosity. The increased chain entanglements will resist the forces encouraging alignment and should therefore result in a further decrease in crystallinity. It has been proposed that crystallinity is affected by voltage in an 'inverted U' relationship whereby crystallinity increases with increased voltage up to a point, beyond which any further increases in voltage leads to a decrease in crystallinity [141]. It may be the case that the voltage for the 1.5% solution is above the optimum value and the increase in acceleration of the jet leading to reduced flight time and therefore reduced crystallinity, may outweigh the orientation effect. When the concentration is increased the chain entanglements resisting the electric field forces will be greater and therefore less acceleration will take place, this will increase the flight time and allow more time for crystallisation.

Table 26: Comparison of the % crystallinity of PHB samples obtained using different carbon sources and electrospun from different solution concentrations

PHB	Crystallinity (%)			
	Non-Electrospun	**Electrospun from 1.5% solution**	**Electrospun from 2% solution**	**Electrospun from 2.5% solution**
O-PHB	54.2	45.8	52.2	53.4
R-PHB	52.2	41.9	42.1	47.4
G-PHB	53.5	50.2	51.1	52.6

Ordinarily a high crystallinity is a desirable property as it is attributed with high stiffness, however if the crystallinity is too high it can result in the polymer being too brittle [227]. This has been found to be the case with PHB, whereby it is too brittle to be used in application [228]. The results of the present study show that an effect of the electrospinning process is to reduce the crystallinity by up to 10%. This could markedly improve the materials properties for application and is an interesting area for future research.

4. CONCLUSIONS

PVA was electrospun at different solution concentrations 8 wt% and 10 wt% under a variable applied voltage ranging from 10-25 kV. It was observed that average fibre diameters were increased under all operating parameters when the solution concentration was increased. However, the effect voltage had on fibre diameter was statistically insignificant. Thermal analysis showed that the crystallinity was substantially reduced by the electrospinning process from 26.6 % in the as-received powder to 14.1% when electrospun at 10 kV. Increasing the voltage resulted in increasing the crystallinity; however despite this increase even at 25 kV the crystallinity value was still lower than PVA powder. Increasing the solution concentration also increased the crystallinity at all applied voltages.

Chitosan could not be electrospun on its own either in a dilute 2% acetic acid solution or a more concentrated 90% acetic acid solution under all tested operating parameters despite previous reports showing that chitosan can be electrospun from concentrated acetic acid solutions. This may be due to the higher M_w of chitosan used in the present study, which differed from the previous successful report. Chitosan could be electrospun when PVA was added to the solution in ratios of 90:10 and 80:20 PVA:chitosan. However, the formation of fibres was inhibited above this ratio. The presence of both chitosan and PVA in the produce scaffolds was confirmed by FTIR analysis. The blend ratio and solution concentration had a great influence on the morphology of fibres. As solution concentrations increased, the morphology changed from thin bead-on-a-string morphologies to uniform fibres the diameter of which also increased with increased concentration.

A chitosan-hydroxybenzotriazole-PVA-water system was successfully prepared and nanofibres produced without using acetic acid or an alternative toxic solvent when hyroxybenzotriazole was added to chitosan in a 1:1 ratio. Fibres produced from this

system were comparable to fibres produced from the chitosan-PVA-acetic acid system. A ratio of 80:20 PVA:chitosan was still the maximum ratio that lead to fibre formation. Without the presence of PVA, fibres could not be formed.

PHB was successfully produced by bacterial synthesis from R. *eutropha* using 20 g/l of olive oil, rapeseed oil and glucose as carbon sources. The use of olive oil and rapeseed oil produced a much greater yield of PHB at 36 % w/w as compared to the more traditional glucose which only produced 12 % w/w. Material analysis showed that the choice of carbon substrate used in the fermentation process did not have an effect on the thermal and chemical properties of the produced material and no significant differences were exhibited in molecular properties. In this respect, olive oil and rapeseed oil can be considered viable replacements for the use of more traditional sugar substrates such as glucose.

Olive oil was selected as a more premium oil source as due to its high cost this substrate would not be suitable for scaling up the process to industrial process. However, the results of this study show that rapeseed oil, selected for being a low cost alternative to olive oil produced a comparable yield to the more expensive oil. Rapeseed oil is therefore a viable option for use as a substrate on an industrial scale due to the low material costs and high PHB yield. Rapeseed oil is also extensively used as cooking oil; research [161, 218] has been carried out looking into the use of waste oils in the production of PHB, which could reduce the cost of PHB production by this method even further.

Nanofibres were successfully produced using the electrospinning process from the PHB produced from all three carbon sources from 1.5, 2 and 2.5 % w/v chloroform solutions at an applied voltage of 7 kV, needle tip distance of 12.5 cm and flow rate

of 1 ml/min. The average diameter of the produced fibres was found to be similar between the three carbon sources which was expected given the use of identical operating parameters and the materials similar properties and M_w. The fibre diameters were large by electrospinning standards with an average value of around 1 µm for uniform fibres from a 2% solution. These large diameters are in keeping with the previous literature, but the addition of the salt BTEAC reduced diameters to ~660 nm.

Comparisons between the FTIR spectra of the PHB samples both before and after electrospinning showed that the peak placements were identical and the ester carbonyl band at 1720 – 140 cm^{-1}, which is a prominent marker in the identification of PHB, was present in all tested samples from each carbon source both before and after electrospinning. Peak intensities were seen to be higher in non-electrospun PHB samples as compared to the electrospun samples. This can be an indication of a lower crystallinity in the electrospun samples. % crystallinity calculations derived from the DSC traces confirmed this, showing that electrospinning had the effect of reducing the crystallinity compared to the as-produced material. The crystallinity of non-electrospun PHB was found to be ~54% while the electrospun PHB had crystallinity as low as ~46 % or as high as ~53 % depending on solution concentration. This shows that it is possible to control the degree of crystallinity within PHB fibres which may be highly advantageous for use in biomedical applications. High crystallinity is associated with brittleness but also lower degradation rates. The ability to control the crystallinity may lead to finding an appropriate balance between the strength required and degradation rate for specific applications.

5. FUTURE WORK

In order to better understand the effect the applied voltage is having on the morphology of electrospun fibres it would be beneficial to raise the voltage in smaller increments in order to see the effects this parameter is having on the resultant fibres. More experimental work should be carried out on the solution properties of the electrospun solutions in order to quantify factors such as viscosity, surface tension and conductivity in order to better explain the effects on fibre morphologies.

Electrospinning above 25 kV was not possible with the equipment used in the present work. In this study it was shown that crystallinity increased when applied voltage was increased. As crystallinity has been shown to exhibit an 'inverted U' relationship with the applied voltage it was concluded that the electrospinning parameters in this study were below the optimum voltage. It would be interesting to increase the voltage above 25 kV and see at what point crystallinity began to decrease in order to determine the optimum parameters.

The mechanical properties of the produced scaffold, such as the tensile strength should be studied and compared under different operating parameters. This would require the production of aligned fibres which would require modification of the electrospinning equipment to include a rotating collector.

In the present work electrospinning of PHB was carried out with fixed parameters across all solution concentrations from each of the three carbon sources. This was to enable fair comparisons between samples; however these parameters were not optimum for all of the samples. It would be beneficial to alter the operating parameters while electrospinning PHB to determine the optimum parameters to achieve the smallest fibre diameters with uniform morphologies. This would also give a better understanding on how to tailor the crystallinity.

Many polymer blends consist of a natural polymer blended with a synthetic polymer; however the superior properties of natural polymers make the prospect of making a natural polymer blend more appealing. It would be interesting to create a blend of chitosan and PHB in order to produce electrospun fibres from two natural polymers both with individual, desirable properties in one tissue engineering scaffold. A barrier to this is that chitosan does not dissolve in chloroform, the solvent used for PHB. However Ma et al. [229] have shown that treating chitosan with triethylamine, acetone and then cinnamoyl chloride can produce a chitosan derivative that can be dissolved in chloroform. Zong et al. [230] have also produced hexanoyl chitosan which is soluble in chloroform and may be suitable for blending with PHB.

6. References

1. Nerem, R., M. Sambanis, A., *Tissue Engineering: From biology to biological substitutes.* Tissue Engineering, 1995. **1**(1): p. 3-13.
2. NHS. *organ donation nhs*. 2013 [cited 2013 08/03/2013]; Available from: http://www.organdonation.nhs.uk/.
3. Tullius, S.G. and N.L. Tilney, *Both Alloantigen-dependent and Independent Factors Influence Chronic Allograft Rejection.* Transplantation, 1995. **59**(3): p. 313-318.
4. Brahatheeswaran, D., Yoshida, Y., Maekawa, T & Kumar, D. S., *Polymeric Scaffolds in Tissue Engineering Application: A Review.* International Journal of Polymer Science, 2011. **2011**.
5. Robert Lanza, R.L., Joseph P. Vacanti, *Principles of Tissue Engineering*. 1995: Elsevier Academic press.
6. *Nanotechnology at NASA*. 16/03/2013]; Available from: http://www.ipt.arc.nasa.gov/nanotechnology.html.
7. Nusnii. *Polymer Nanofibers - an Overview of Applications and Current Research into Processing Techniques*. 2005 [cited 2013; Available from: http://www.azonano.com/article.aspx?ArticleID=1280#_Current_Research_into_Methods%20for%20P.
8. Ramakrishna, S., Fuhihara, K., Teo, W., Lim, T. & Ma, Z, *An Introduction to Electrospinning and Nanofibres*. 2005, Singapore: World Scientific Publishing Co. Ltd.
9. Ramakrishna, S., Fujihara, K., Teo, W., Ma, Z. & Ramaseshan, R. , *Electrospun nanofibres: solving global issues.* Materials Today, 2006. **9**: p. 40-50.
10. Huang, Z., Zhang, Y. Z., Kotaki, M. & Ramakrishna, S, *A review on polymer nanofibres by electrospinning and their applications in nanocomposites.* Composites Science and Technology, 2003. **63**: p. 2223-2253.
11. Bajakova, J.C., J. Lukas, D. Lacarin, M., *Drawing - The Production of Individual Nanofibers by Experimental Method*, in *Nanocon* 2011: Czech Republic. p. 21-23.

12. Ondarcuhu, T.J., C., *Drawing a single nanofibre over hundreds of microns.* Europhysics Letters, 1998. **42**(2): p. 215-220.

13. Barnes, C.P., Sell, S. A., Boland, E. D., Simpson, D. G. & Bowlin, G. L., *Nanofiber technology: Designing the next generation of tissue engineering scaffolds.* Advanced Drug Delivery Reviews, 2007. **59**: p. 1413-1433.

14. Zhang, S., *Fabrication of novel biomaterials through molecular self-assembly.* Nature Biotechnology, 2003. **21**: p. 1171-1178.

15. Huczko, A., *Template-based synthesis of nanomaterials.* Applied Physics A, 2000. **70**: p. 365-376.

16. Laudenslager, M., J. Sigmund, W, M., *Developments in electrohydrodynamic forming: Fabricating nanomaterials from charged liquids via electrospinning and electrospraying* American Ceramic Society Bulletin, 2011. **90**: p. 22-27.

17. Filatov, Y.B., A. Kirichenko, V., *Electrospinning of Micro-And Nanofibers: Fundamentals and Applications in Separation and Filtration Processes* 2007, New York, USA: Begell House Inc.

18. Taylor, G., *Disintegration of Water Drops in an Electric Field.* Proceedings of the Royal Society A: Mathematical, Physical and Engineering Sciences, 1964. **280**: p. 383-397.

19. Doshi, J.a.D.H.R., *Electrospinning process and applications of electrospun fibers.* Journal of Electrostatics, 1995. **35**: p. 151-160.

20. Reneker, D., H. Chun, I, *Nanometre diameter fibres of polymer, produced by electrospinning.* Nanotechnology, 1996. **7**: p. 216-223.

21. Bhattarai, S.R., et al., *Novel biodegradable electrospun membrane: scaffold for tissue engineering.* Biomaterials, 2004. **25**(13): p. 2595-2602.

22. Park, W.H., et al., *Effect of chitosan on morphology and conformation of electrospun silk fibroin nanofibers.* Polymer, 2004. **45**(21): p. 7151-7157.

23. Cuiru, Y., et al. *Comparisons of fibers properties between vertical and horizontal type electrospinning systems*. in *Electrical Insulation and Dielectric Phenomena, 2009. CEIDP '09. IEEE Conference on*. 2009.

24. Barnes, C.P., Sell, S. A., Boland, E. D., Simpson, D. G. & Bowlin, G. L., *Nanofibre technology: Designing the next generation of tissue engineering scaffolds.* Advanced Drug Delivery Reviews, 2007. **59**: p. 1413-1433.

25. He, J.-H., Y. Wu, and W.-W. Zuo, *Critical length of straight jet in electrospinning.* Polymer, 2005. **46**(26): p. 12637-12640.

26. Yarin, A.L., S. Koombhongse, and D.H. Reneker, *Taylor cone and jetting from liquid droplets in electrospinning of nanofibers.* Journal of Applied Physics, 2001. **90**: p. 4836-4846.

27. Yarin, A.L., S. Koombhongse, and D.H. Reneker, *Bending instability in electrospinning of nanofibers.* Journal of Applied Physics, 2001. **89**(5): p. 3018-3026.

28. Reneker, D., H. Yarin, A. L., *Electrospinning jets and polymer nanofibers.* Polymer, 2008. **49**: p. 2387-2425.

29. Shin, Y.M., Hohman, M. M., Brenner, M. P. & Rutledge, G. C., *Electrospinning: A whipping fluid jet generates submicron polymer fibers.* Applied Physics Letters, 2001. **78**: p. 1149-1151.

30. Shenoy, S.L., et al., *Role of chain entanglements on fiber formation during electrospinning of polymer solutions: good solvent, non-specific polymer–polymer interaction limit.* Polymer, 2005. **46**(10): p. 3372-3384.

31. Deitzel, J.M., J. Kleinmeyer, D. Harris, and Tan, N. C. B. , *The effect of processing variables on the morphology of electrospun nanofibers and textiles.* Polymer, 2001. **42**: p. 261-272.

32. Eda, G.S., S, *Bead-to-fiber transition in electrospun polystyrene.* Journal of Applied Polymer Science, 2007. **106**(1): p. 475-487.

33. Fong, H.C., I. Reneker, D,H., *Beaded nanofibers formed during electrospinning.* Polymer, 1999. **40**(16): p. 4585-4592.

34. Lee, K., H. Kim, H, Y. Bang, H, J. Jung, Y, H. Lee, S, G., *The change of bead morphology formed on electrospun polystyrene fibers.* Polymer, 2003. **44**(14): p. 4029-4034.

35. Mit-Uppatham, C.N., M & Supaphol,P, *Effects of solution concentration, emitting electrode polarity, solvent type, and salt addition on electrospun polyamide-6 fibers: A preliminary report.* Macromolecular Symposia, 2004(216): p. 293-299.

36. Boland, E.D., et al., *Electrospinning polydioxanone for biomedical applications.* Acta Biomaterialia, 2005. **1**(1): p. 115-123.

37. Yang, Q.L., Z. Hong, Y. Zhao, Y. Qiu, S. Wang, C. Wei, Y., *Influence of solvents on the formation of ultrathin uniform poly(vinyl pyrrolidone) nanofibers with electrospinning.* Journal of Polymer Science, Part B: Polymer Physics, 2004. **42**(20): p. 3721-3726.

38. Cross, M.M., *Viscosity, molecular weight and chain entanglement.* Polymer, 1970. **11**(5): p. 238-244.

39. Koski, A.Y., K. Shivkumar, S., *Effect of molecular weight on fibrous PVA produced by electrospinning.* Material Letters, 2004. **58**(3-4): p. 493-497.

40. Kwaambwa, H.M., et al., *Viscosity, molecular weight and concentration relationships at 298 K of low molecular weight cis-polyisoprene in a good solvent.* Colloids and Surfaces A: Physicochemical and Engineering Aspects, 2007. **294**(1–3): p. 14-19.

41. Theron, S.A., E. Zussman, and A.L. Yarin, *Experimental investigation of the governing parameters in the electrospinning of polymer solutions.* Polymer, 2004. **45**(6): p. 2017-2030.

42. Huang, C.C., S. Lai, C. Reneker D H. Qui, H. Ye, Y. Hou, H., *Electrospun polymer nanofires with small diameters.* Nanotechnology, 2006. **17**: p. 1558-1563.

43. Angammana, C.J. and S.H. Jayaram, *Analysis of the Effects of Solution Conductivity on Electrospinning Process and Fiber Morphology.* Industry Applications, IEEE Transactions on, 2011. **47**(3): p. 1109-1117.

44. Zhang, C., X. Yuan, L. Wu, Y. Han, and J. Sheng *Study on morphology of electrospun poly(vinyl alcohol) mats.* European Polymer Journal, 2005. **41**: p. 423-432.

45. Zhao, S., Wu, X., Wang, L. and Huang, Y., *Electrospinning of ethyl–cyanoethyl cellulose/tetrahydrofuran solutions.* Journal of Applied Polymer Science, 2004. **91**: p. 242-246.

46. Buchko, C.J., Chen, L. C, Shen, Y. and Martin, D. C., *Processing and microstructural characterization of porous biocompatible protein polymer thin films.* Polymer, 1999. **40**: p. 7397-7407.

47. Megelski, S., Stephens, J.S., Chase, D.B. and Rabolt, J.F., *Micro- and nanostructured surface morphology on electrospun polymer fibers.* Macromolecules, 2002. **35**: p. 8456-8466.

48. Lee, J.S., Choi, K. H., Ghim, H. D., Kim, S. S., Chun, D. H., Kim, H. Y. & Lyoo, W. S, *Role of molecular weight of atactic poly(vinyl alcohol) (PVA) in the structure and properties of PVA nanofabric prepared by electrospinning.* Journal of Applied Polymer Science, 2004. **93**: p. 1638-1646.

49. Tong, H.W.W., M., *An Investigation into the Influence of Electrospinning Parameters on the Diameter and Alignment of Poly(hydroxybutyrate-co-hydroxyvalerate) Fibers.* Journal of Applied Polymer Science, 2011. **120**: p. 1694-1706.

50. Pawlowski, K.J., Belvin, H. L., Raney, D. L., Su, J., Harrison, J. S. and Siochi, E. J., *Electrospinning of a micro-air vehicle wing skin.* Polymer, 2003. **44**: p. 1309-1314.

51. Jenkins, M.J. and K.L. Harrison, *The effect of crystalline morphology on the degradation of polycaprolactone in a solution of phosphate buffer and lipase.* Polymers for Advanced Technologies, 2008. **19**(12): p. 1901-1906.

52. Rosato, D.V., N.R. Schott, and M.G. Rosato, *Plastics Institute of America Plastics Engineering, Manufacturing & Data Handbook*. 2001: Springer.

53. Ero-Phillips, O., . Jenkins, M,. Stamboulis, A., *Tailoring Crystallinity of Electrospun Plla Fibres by Control of Electrospinning Parameters.* Polymers, 2012. **4**(3): p. 1331-1348.

54. Homayoni, H., S.A.H. Ravandi, and M. Valizadeh, *Electrospinning of chitosan nanofibers: Processing optimization.* Carbohydrate polymers, 2009. **77**(3): p. 656-661.

55. Chowdhury, M., . Stylios, G., *Effect of experimental parameters on the morphology of electrospun Nylon 6 fibres* International Journal of Basic & Applied Sciences, 2010. **10**(6): p. 116-131.

56. Rutledge, G.C., Li, Y., Fridrikh, S., Warner, S. B., Kalayci, V. E. and Patra, P., *Electrostatic Spinning and Properties of Ultrafine Fibers,.* National Textile Centre, 2000: p. 1-10.

57. Frenot, A.C., I, S, *Polymer nanofibers assembled by electrospinning.* Current Opinion in Colloids and Interface Science, 2003. **8**: p. 64-75.

58. Demir, M.M., YilGor, I., Yilgor, E. & Erman, B, *Electrospinning of polyurethane fibers.* Polymer, 2002. **43**: p. 3303.

59. Alfrey, T., . Bartovics, A,. and Mark, H., *The Effect of Temperature and Solvent Type on the Intrinsic Viscosity of High-Polymer Solutions.* Rubber Chemistry and Technology, 1942. **15**(4): p. 820-825.

60. Casper, C., L, Stephens, J, S,. Tassi, N, G,. Chase, D, B,. and Rabolt, J, F., *Controlling surface morphology of electrospun polystyrene fibers: Effect of humidity and molecular weight in the electrospinning process.* Macromolecules, 2004. **37**(2): p. 573-578.

61. Luo, C.J., M. Nangrejo, and M. Edirisinghe, *A novel method of selecting solvents for polymer electrospinning.* Polymer, 2010. **51**(7): p. 1654-1662.

62. Zhou, Y., Yang, D., Chen, X., Xu, Q., Lu, F. & Nie, J, *Electrospun Water-Soluble Carboxyethyl Chitosan/Poly(vinyl alcohol) Nanofibrous Membrane as Potential Wound Dressing for Skin Regeneration.* Biomacromolecules, 2008. **9**: p. 349–354.

63. Chen, H., et al., *Biocompatible polymer materials: Role of protein–surface interactions.* Progress in Polymer Science, 2008. **33**(11): p. 1059-1087.

64. Moore, C.J., *Synthetic polymers in the marine environment: A rapidly increasing, long-term threat.* Environmental Research, 2008. **108**(2): p. 131-139.

65. Monteiro, S., et al., *Natural-fiber polymer-matrix composites: Cheaper, tougher, and environmentally friendly.* JOM, 2009. **61**(1): p. 17-22.

66. Xia, W., et al., *Tissue engineering of cartilage with the use of chitosan-gelatin complex scaffolds.* Journal of Biomedical Materials Research Part B: Applied Biomaterials, 2004. **71B**(2): p. 373-380.

67. Chandy, T.S.C.P., *Chitosan-- as a biomaterial.* Biomater Artif Cells Artif Organs, 1990. **18**(1): p. 1-24.

68. Ravi Kumar, M.N.V., *A review of chitin and chitosan applications.* Reactive and Functional Polymers, 2000. **46**(1): p. 1-27.

69. Fabritius, H., C. Sachs, C. Raabe, D., Nikolov, S., Friak, M., and Neugebauer, J., *Chitin in the Exoskeletons of Arthropoda: From Ancient Design to Novel Materials Science.* Topics in Geobiology 2011. **34**: p. 35-60.

70. Pillai, C.K.S., W. Paul, and C.P. Sharma, *Chitin and chitosan polymers: Chemistry, solubility and fiber formation.* Progress in Polymer Science, 2009. **34**(7): p. 641-678.

71. Dumitriu, S., *Polymeric Biomaterials* 2001: CRC Press. 1168.

72. Sashiwa, H. and S.-i. Aiba, *Chemically modified chitin and chitosan as biomaterials.* Progress in Polymer Science, 2004. **29**(9): p. 887-908.

73. Tsai, G.J. and W.H. Su, *Antibacterial activity of shrimp chitosan against Escherichia coli.* J Food Prot, 1999. **62**(3): p. 239-43.

74. Shahidi, F., J. Arachchi, K, V., and Y. Jeon, *Food applications of chitin and chitosans.* Trends in Food Science and Technology, 1999. **10**: p. 37-51.

75. Tayel, A.A., et al., *Inhibition of microbial pathogens by fungal chitosan.* International Journal of Biological Macromolecules, 2010. **47**(1): p. 10-14.

76. Kong, M., et al., *Antimicrobial properties of chitosan and mode of action: A state of the art review.* International Journal of Food Microbiology, 2010. **144**(1): p. 51-63.

77. Muzzarelli, R., et al., *Biological activity of chitosan: ultrastructural study.* Biomaterials, 1988. **9**(3): p. 247-252.

78. Malette, W.G.Q., H. J, *Method of achieving hemostasis inhibiting fibroplasia, and promoting tissue regeneration in a tissue wound*, U.S.P.a.T. Office, Editor. 1985: USA.

79. Yarema, K., J., *Carbohydrate Engineering*. 2005: CRC Press. 944.

80. Ohkawa, K., Cha, D., Kim, H., Nishida, A. & Yamamoto, H, *Electrospnning of chitosan.* Macromolecular rapid communications, 2004. **25**: p. 1600-1605.

81. Zhang, Y.Z., Su, B., Ramakrishna, S. & Lim, C. T., *Chitosan Nanofibers from an Easily Electrospinnable UHMWPEO-Doped Chitosan Solution System.* Biomacromolecules, 2008. **9**: p. 136-141.

82. Bhattarai, N., et al., *Electrospun chitosan-based nanofibers and their cellular compatibility.* Biomaterials, 2005. **26**(31): p. 6176-6184.

83. Li, L.H., Y. , *Chitosan bicomponent nanofibers and nanoporous fibers.* Carbohydrate research, 2006. **341**: p. 374-381.

84. Min, B.-M., et al., *Chitin and chitosan nanofibers: electrospinning of chitin and deacetylation of chitin nanofibers.* Polymer, 2004. **45**(21): p. 7137-7142.

85. Hasegawa, M., et al., *Dissolving states of cellulose and chitosan in trifluoroacetic acid.* Journal of Applied Polymer Science, 1992. **45**(10): p. 1857-1863.

86. Vrieze, S., et al., *Electrospinning of chitosan nanofibrous structures: feasibility study.* Journal of Materials Science, 2007. **42**(19): p. 8029-8034.

87. Geng, X., Kwon, O. & Jang, J, *Electrospinning of chitosan dissolved in concentrated acetic acid solution.* Biomaterials, 2005. **26**: p. 5427–5432.

88. Ryan, A.J., *Polymer science: Designer polymer blends.* Nat Mater, 2002. **1**(1): p. 8-10.

89. Rakkapao, N., et al., *Miscibility of chitosan/poly(ethylene oxide) blends and effect of doping alkali and alkali earth metal ions on chitosan/PEO interaction.* Polymer, 2011. **52**(12): p. 2618-2627.

90. Naveen Kumar, H.M.P., et al., *Compatibility studies of chitosan/PVA blend in 2% aqueous acetic acid solution at 30 °C.* Carbohydrate polymers, 2010. **82**(2): p. 251-255.

91. Salomé Machado, A.A., V.C.A. Martins, and A.M.G. Plepis, *Thermal and Rheological Behavior of Collagen. Chitosan blends.* Journal of Thermal Analysis and Calorimetry, 2002. **67**(2): p. 491-498.

92. Duan, B., Dong, C., Yuan, X., and Yao, K,, *Electrospinning of chitosan solutions in acetic acid with poly(ethylene oxide).* Journal of Biomaterials Science Polymer Edition, 2004. **15**(6): p. 797-811.

93. Desai, K., Kit, K., Li, J. and Zivanovic, S., *Morphological and Surface Properties of Electrospun Chitosan Nanofibers.* Biomacromolecules, 2008. **9**: p. 1000-1006.

94. Ignatova, M., Manolova, N., Markova, N. and Rashkov, I., *Electrospun Non-Woven Nanofibrous Hybrid Mats Based on Chitosan and PLA for Wound-Dressing Applications.* Macromolecular Bioscience, 2009. **9**: p. 102-111.

95. Chen, Z.G., et al., *Electrospun collagen–chitosan nanofiber: A biomimetic extracellular matrix for endothelial cell and smooth muscle cell.* Acta Biomaterialia, 2010. **6**(2): p. 372-382.

96. Zhang, Y., et al., *Electrospun biomimetic nanocomposite nanofibers of hydroxyapatite/chitosan for bone tissue engineering.* Biomaterials, 2008. **29**(32): p. 4314-4322.

97. Ito, Y., et al., *A composite of hydroxyapatite with electrospun biodegradable nanofibers as a tissue engineering material.* Journal of Bioscience and Bioengineering, 2005. **100**(1): p. 43-49.

98. Lin, T., Fang, J., Wang, H., Cheng, T. & Wang, X, *Using chitosan as a thickener for electrospinning dilute PVA solutions to improve fibre uniformity.* Nanotechnology,, 2006. **17**: p. 3718-3723.

99. Jia, Y., Gong, J., Gu, X., Kim, H., Dong, J. & Shen, X., *Fabrication and characterization of poly (vinyl alcohol)/chitosan blend nanofibers produced by electrospinning method.* Carbohydrate polymers, 2007. **67**: p. 403–409.

100. Sangsanoh, P. and P. Supaphol, *Stability Improvement of Electrospun Chitosan Nanofibrous Membranes in Neutral or Weak Basic Aqueous Solutions.* Biomacromolecules, 2006. **7**(10): p. 2710-2714.

101. Sangsanoh, P., et al., *In vitro biocompatibility of electrospun and solvent-cast chitosan substrata towards Schwann, osteoblast, keratinocyte and fibroblast cells.* European Polymer Journal, 2010. **46**(3): p. 428-440.

102. Haider, S. and S.-Y. Park, *Preparation of the electrospun chitosan nanofibers and their applications to the adsorption of Cu(II) and Pb(II) ions from an aqueous solution.* Journal of Membrane Science, 2009. **328**(1–2): p. 90-96.

103. Huang, X.-J., D. Ge, and Z.-K. Xu, *Preparation and characterization of stable chitosan nanofibrous membrane for lipase immobilization.* European Polymer Journal, 2007. **43**(9): p. 3710-3718.

104. Zhang, Y., et al., *Preparation of electrospun chitosan/poly(vinyl alcohol) membranes.* Colloid and Polymer Science, 2007. **285**(8): p. 855-863.

105. Kriegel, C., et al., *Electrospinning of chitosan–poly(ethylene oxide) blend nanofibers in the presence of micellar surfactant solutions.* Polymer, 2009. **50**(1): p. 189-200.

106. Desai, K., et al., *Nanofibrous chitosan non-wovens for filtration applications.* Polymer, 2009. **50**(15): p. 3661-3669.

107. Jung, K.-H., et al., *Preparation and antibacterial activity of PET/chitosan nanofibrous mats using an electrospinning technique.* Journal of Applied Polymer Science, 2007. **105**(5): p. 2816-2823.

108. Yang, X., X. Chen, and H. Wang, *Acceleration of Osteogenic Differentiation of Preosteoblastic Cells by Chitosan Containing Nanofibrous Scaffolds.* Biomacromolecules, 2009. **10**(10): p. 2772-2778.

109. Zhang, H., et al., *Studies on electrospun nylon-6/chitosan complex nanofiber interactions.* Electrochimica Acta, 2009. **54**(24): p. 5739-5745.

110. Duan, B., et al., *A nanofibrous composite membrane of PLGA–chitosan/PVA prepared by electrospinning.* European Polymer Journal, 2006. **42**(9): p. 2013-2022.

111. Chen, J.-P., G.-Y. Chang, and J.-K. Chen, *Electrospun collagen/chitosan nanofibrous membrane as wound dressing.* Colloids and Surfaces A: Physicochemical and Engineering Aspects, 2008. **313–314**(0): p. 183-188.

112. Zhou, Y., et al., *Electrospun Water-Soluble Carboxyethyl Chitosan/Poly(vinyl alcohol) Nanofibrous Membrane as Potential Wound Dressing for Skin Regeneration.* Biomacromolecules, 2007. **9**(1): p. 349-354.

113. Neamnark, A., R. Rujiravanit, and P. Supaphol, *Electrospinning of hexanoyl chitosan.* Carbohydrate polymers, 2006. **66**(3): p. 298-305.

114. Feng, Z.-Q., et al., *The effect of nanofibrous galactosylated chitosan scaffolds on the formation of rat primary hepatocyte aggregates and the maintenance of liver function.* Biomaterials, 2009. **30**(14): p. 2753-2763.

115. Ignatova, M., et al., *Electrospun nano-fibre mats with antibacterial properties from quaternised chitosan and poly(vinyl alcohol).* Carbohydrate research, 2006. **341**(12): p. 2098-2107.

116. Duan, K., et al., *One-step synthesis of amino-reserved chitosan-graft-polycaprolactone as a promising substance of biomaterial.* Carbohydrate polymers, 2010. **80**(2): p. 498-503.

117. Charernsriwilaiwat, N., et al., *Preparation and characterization of chitosan-hydroxybenzotriazole/polyvinyl alcohol blend nanofibers by the electrospinning technique.* Carbohydrate polymers, 2010. **81**(3): p. 675-680.

118. Shen, K., et al., *Preparation of chitosan bicomponent nanofibers filled with hydroxyapatite nanoparticles via electrospinning.* Journal of Applied Polymer Science, 2010. **115**(5): p. 2683-2690.

119. Yang, D., et al., *Fabrication and characterization of chitosan/PVA with hydroxyapatite biocomposite nanoscaffolds.* Journal of Applied Polymer Science, 2008. **110**(6): p. 3328-3335.

120. An, J., et al., *Preparation and antibacterial activity of electrospun chitosan/poly(ethylene oxide) membranes containing silver nanoparticles.* Colloid and Polymer Science, 2009. **287**(12): p. 1425-1434.

121. Zhuang, X., et al., *Electrospun chitosan/gelatin nanofibers containing silver nanoparticles.* Carbohydrate polymers, 2010. **82**(2): p. 524-527.

122. Ramaraj, B., *Crosslinked poly(vinyl alcohol) and starch composite films. II. Physicomechanical, thermal properties and swelling studies.* Journal of Applied Polymer Science, 2007. **103**(2): p. 909-916.

123. Tubbs, R.K., *Sequence distribution of partially hydrolyzed poly(vinyl acetate).* Journal of Polymer Science Part A-1: Polymer Chemistry, 1966. **4**(3): p. 623-629.

124. Schildknecht, C.E., *Polyvinyl alcohol, properties and applications, C. A. Finch, Wiley, New York, 1973. 622 pp. $37.50.* Journal of Polymer Science: Polymer Letters Edition, 1974. **12**(2): p. 105-106.

125. Hassan, C. and N. Peppas, *Structure and Applications of Poly(vinyl alcohol) Hydrogels Produced by Conventional Crosslinking or by Freezing/Thawing Methods*, in *Biopolymers · PVA Hydrogels, Anionic Polymerisation Nanocomposites*. 2000, Springer Berlin Heidelberg. p. 37-65.

126. Verlinden, R., A,. Hill, D, J,. Kenward, M, A,. WIlliams, C, D,. and Radecka, I., *Bacterial synthesis of biodegradable polyhydroxyalkanoates.* Journal of Applied Microbiology, 2007. **102**: p. 1437-1449.

127. Rehm, B., H,. Steinbuchel, A., *Biochemical and genetic analysis of PHA synthasis and other proteins required for PHA synthesis.* International Journal of Biological Macromolecules, 1999. **25**: p. 3-19.

128. Lemoigne, M., *Produit de déshydratation et de polymérisation de l'acide β-oxybutyrique.* Bulletin de la Societe de Chimie Biologique, 1926. **8**: p. 770-782.

129. Byrom, D., *Polymer synthesis by micro-organisms: technology and economics.* Trends in Biotechnology, 1987. **5**: p. 246-250.

130. Salehizadeh, H.a.V.L., M, C., *Production of polyhydroxyalkanoates by mixed culture: recent trends and biotechnological importance.* Biotechnology Advances, 2004. **22**(3): p. 261-279.

131. Holmes, P.A., *Applications of PHB - A Microbially Produced Biodegradable Thermoplastic.* Physics Technology, 1985. **16**: p. 32-36.

132. Rios, L.M., C. Moore, and P.R. Jones, *Persistent organic pollutants carried by synthetic polymers in the ocean environment.* Marine Pollution Bulletin, 2007. **54**(8): p. 1230-1237.

133. Lemos, P.C., L.S. Serafim, and M.A.M. Reis, *Synthesis of polyhydroxyalkanoates from different short-chain fatty acids by mixed cultures submitted to aerobic dynamic feeding.* Journal of Biotechnology, 2006. **122**(2): p. 226-238.

134. Yamane, T., *Yield of poly-D(-)-3-hydroxybutyrate from various carbon sources: A theoretical study.* Biotechnology and Bioengineering, 1993. **41**(1): p. 165-170.

135. Budde, C., et al., *Growth and polyhydroxybutyrate production by Ralstonia eutropha in emulsified plant oil medium.* Applied Microbiology and Biotechnology, 2011. **89**(5): p. 1611-1619.

136. Yamane, T., *Cultivation engineering of microbial bioplastics production.* FEMS Microbiology Letters, 1992. **103**(2–4): p. 257-264.

137. Abe, A., et al., *Biopolymers: Lignin, Proteins, Bioactive Nanocomposites*. 2010: Springer.

138. Brown, W., et al., *Organic Chemistry*. 2008: Cengage Learning.

139. Ikejima, T., N. Yoshie, and Y. Inoue, *Influence of tacticity and molecular weight of poly (vinyl alcohol) on crystallization and biodegradation of poly (3-hydroxybutyric acid)/poly (vinyl alcohol) blend films.* Polymer Degradation and Stability, 1999. **66**(2): p. 263-270.

140. *Chemistry in its element - polyhydroxybutyrate*. 2011 05/04/2014]; Available from: http://www.rsc.org/chemistryworld/podcast/CIIEcompounds/transcripts/polyhydroxybutyrate.asp.

141. Ero-Phillips, O., M. Jenkins, and A. Stamboulis, *Tailoring Crystallinity of Electrospun Plla Fibres by Control of Electrospinning Parameters.* Polymers, 2012. **4**(3): p. 1331-1348.

142. Kaplan, D., *Biopolymers from Renewable Resources*. 1998: Springer. 417.

143. Lee, K., D. Kaplan, and C. Chan, *Tissue Engineering I: Scaffold Systems for Tissue Engineering*. 2006: Springer.

144. Larsen, T.a.N., N, I, *Fluorometric determination of beta-hydroxybutyrate in milk and blood plasma*. Journal of Dairy Science, 2005. **88**(6): p. 2004-2009.

145. Wong, P.A.L., Cheung, M.K., Lo, W.-H., Chua, H. and Yu, P.H.F, *Investigation of the effects of the types of food waste utilized as carbon source on the molecular weight distributions and thermal properties of polyhydroxy-butyrate produced by two strains of microorganisms.* e-Polymers, 2004. **31**: p. 1-11.

146. Labuzek, S.a.R., I., *Biosynthesis of copolymers of PHB tercopolymer by Bacillus cereus UW85 strain.* Journal of Applied Microbiology, 2001. **90**: p. 353-357.

147. Katırcıog˘lu, H., Aslim, B., Yu¨ksekdað, Z.N., Mercan, N. and Beyatli, Y., *Production of poly-beta-hydroxybutyrate (PHB) and differentiation of putative Bacillus mutant strains by SDS-PAGE of total cell protein.* African Journal of Biotechnology, 2003. **2**: p. 147-149.

148. Bra¨mer, C.O., Vandamme, P., Silva, L.F.d., Gomez, J.G.C. and Steinbu¨chel, A., *Burkholderia sacchari sp. nov., a polyhydroxyalkanoate-accumulating bacterium isolated from soil of a sugar-cane plantation in Brazil. .* International Journal of Systematic and Evolutionary Microbiology, 2001. **51**: p. 1709-1713.

149. Keenan, T.M., et al., *Production and Characterization of Poly-ß-hydroxyalkanoate Copolymers from Burkholderiacepacia Utilizing Xylose and Levulinic Acid.* Biotechnology Progress, 2004. **20**(6): p. 1697-1704.

150. Qi, Q.a.R., B.H.A, *Polyhydroxybutyrate biosynthesis in Caulobacter crescentus: molecular characterization of the polyhydroxybutyrate synthase.* Microbiology, 2001. **147**: p. 3353-3358.

151. Mahishi, L.H., G. Tripathi, and S.K. Rawal, *Poly(3-hydroxybutyrate) (PHB) synthesis by recombinant Escherichia coli harbouring Streptomyces aureofaciens PHB biosynthesis genes: Effect of various carbon and nitrogen sources.* Microbiological Research, 2003. **158**(1): p. 19-27.

152. Quillaguamán, J., et al., *Poly(β-hydroxybutyrate) production by a moderate halophile, Halomonas boliviensis LC1 using starch hydrolysate as substrate.* Journal of Applied Microbiology, 2005. **99**(1): p. 151-157.

153. James, B.W., et al., *Poly-3-hydroxybutyrate in Legionella pneumophila, an energy source for survival in low-nutrient environments.* Applied and Environmental Microbiology, 1999. **65**(2): p. 822-827.

154. Wendlandt, K.D., et al., *Possibilities for controlling a PHB accumulation process using various analytical methods.* Journal of Biotechnology, 2005. **117**(1): p. 119-129.

155. Akar, A., et al., *Accumulation of polyhydroxyalkanoates by Microlunatus phosphovorus under various growth conditions.* Journal of Industrial Microbiology and Biotechnology, 2006. **33**(3): p. 215-220.

156. Kichise, T., et al., *Biosynthesis of polyhydroxyalkanoates (PHA) by recombinant Ralstonia eutropha and effects of PHA synthase activity on in vivo PHA biosynthesis.* International Journal of Biological Macromolecules, 1999. **25**(1–3): p. 69-77.

157. Mercan, N.a.B., Y., *Production of poly-betahydroxybutyrate (PHB) by Rhizobium meliloti, R. viciae and Bradyrhizobium japonicum with different carbon and nitrogen sources, and inexpensive substrates.* Zuckerindustrie, 2005. **130**: p. 410-415.

158. Mukhopadhyay, M., A. Patra, and A.K. Paul, *Production of poly(3-hydroxybutyrate) and poly(3-hydroxybutyrate-co-3-hydroxyvalerate) by Rhodopseudomonas palustris SP5212.* World Journal of Microbiology and Biotechnology, 2005. **21**(5): p. 765-769.

159. Jau, M.-H., et al., *Biosynthesis and mobilization of poly(3-hydroxybutyrate) [P(3HB)] by Spirulina platensis.* International Journal of Biological Macromolecules, 2005. **36**(3): p. 144-151.

160. Phoeby, A.L.W., et al., *Investigation of the effects of the types of food waste utilized as carbon source on the molecular weight distributions and thermal properties of polyhydroxybutyrate produced by two strains of microorganisms*, in *e-Polymers*. 2004. p. 324.

161. Verlinden, R., et al., *Production of polyhydroxyalkanoates from waste frying oil by Cupriavidus necator.* AMB Express, 2011. **1**(1): p. 1-8.

162. Hankermeyer, C.R., . Tjeerdema, R. S., *Polyhydroxybutyrate: plastic made and degraded by microorganisms.* Reviews of Environmental Contamination and Toxicology, 1999. **159**: p. 1-24.

163. Ghosh, A. *Biodegradable Plastics Production and Applications*. 2011 [cited 2013 09/06]; Available from: http://www.biotecharticles.com/

164. Rebrov, A.V.D., V. A. ; Nekrasov, Yu. P. ; Bonartseva, G. A. ; Stamm, M. ; Antipov, E.M., *Structural phenomena during elastic deformation of highly oriented poly(hydroxybutyrate).* Polymer Science, 2002. **44**: p. 32-35.

165. Kil'deeva, N.R., Vikhoreva, G. A, Gal'braĭkh, L. S, Mironov, A. V, Bonartseva, G. A, Perminov, P. A, Romashova, A. N, *Preparation of biodegradable porous films for use as wound coverings.* Prikladnaia Biokhimiia I Mikrobiologiia, 2006. **42**(6): p. 716-720.

166. Yan, Q., Sun, Y., Ruan, L.F., Chen, J. and Yu, P.H.F., *Biosynthesis of short-chain-length-polyhydroxyalkanoates during the dual-nutrient-limited zone by Ralstonia eutropha.* World Journal of Microbiology and Biotechnology, 2005. **21**: p. 17-21.

167. Xu, J., Guo, B., Zhang, Z., Wu, Q., Zhou, Q., Chen, J., Chen, G., & Li, G., *A mathematical model for regulating monomer composition of the microbially synthesized polyhydroxyalkanoate copolymers.* Biotechnology and Bioengineering, 2005. **90**(7): p. 821-829.

168. Farreh, W. *What is PHA*. 2011 [cited 2013 29/05]; Available from: http://naturalplastics.blogspot.co.uk/2011/05/what-is-pha.html.

169. Sombatmankhong, K., Suwantong, O., Waleetorcheepsawat, S., & Supaphol, P., *Electrospun Fiber Mats of Poly(3-Hydroxybutyrate), Poly(3-Hydroxybutyrate-co-3-Hydroxyvalerate), and Their Blends.* Journal of Polymer Science: Part B: Polymer Physics, 2006: p. 2923-2933.

170. Ma, P.X. and R. Zhang, *Synthetic nano-scale fibrous extracellular matrix.* Journal of Biomedical Materials Research, 1999. **46**(1): p. 60-72.

171. Suwantong, O., et al., *In vitro biocompatibility of electrospun poly(3-hydroxybutyrate) and poly(3-hydroxybutyrate-co-3-hydroxyvalerate) fiber mats.* International Journal of Biological Macromolecules, 2007. **40**(3): p. 217-223.

172. Choi, J.S., et al., *Effect of organosoluble salts on the nanofibrous structure of electrospun poly(3-hydroxybutyrate-co-3-hydroxyvalerate).* International Journal of Biological Macromolecules, 2004. **34**(4): p. 249-256.

173. Choi, J.-i. and S.Y. Lee, *Process analysis and economic evaluation for Poly(3-hydroxybutyrate) production by fermentation.* Bioprocess Engineering, 1997. **17**(6): p. 335-342.

174. Kahar, P., et al., *High yield production of polyhydroxyalkanoates from soybean oil by Ralstonia eutropha and its recombinant strain.* Polymer Degradation and Stability, 2004. **83**(1): p. 79-86.

175. Chodak, I., *Chapter 22 - Polyhydroxyalkanoates: Origin, Properties and Applications*, in *Monomers, Polymers and Composites from Renewable Resources*, B. Mohamed Naceur and G. Alessandro, Editors. 2008, Elsevier: Amsterdam. p. 451-477.

176. Billmeyer, F.W., *Textbook of Polymer Science*. 1984: John Wiley & Sons, Inc.

177. Tsuge, T., *Metabolic improvements and use of inexpensive carbon sources in microbial production of polyhydroxyalkanoates.* Journal of Bioscience and Bioengineering, 2002. **94**(6): p. 579-584.

178. Sichina, W.J. *DSC as Problem Solving Tool: Measurement of Percent Crystallinity of Thermoplastics*. 2000 29/10/2014]; Available from: http://www.perkinelmer.com/Content/applicationnotes/app_thermalcrystallinitythermoplastics.pdf

179. Probst, O., Moore, E. M., Resasco, D. E., and Grady, B. P., *Nucleation of polyvinyl alcohol crystallization by single-walled carbon nanotubes.* Polymer, 2004. **45**: p. 4437-4443.

180. Barham, P.J., et al., *Crystallization and morphology of a bacterial thermoplastic: poly-3-hydroxybutyrate.* Journal of Materials Science, 1984. **19**(9): p. 2781-2794.

181. Prapancham, B. *Gel Permeation Chromatography*. 28/04/2013]; Available from: http://biomed.tamu.edu/mte/files/gpc.pdf.

182. Bagheriasl, S., *Development and Characterisation of Polyhydroxybutyrate from Selected Bacterial Species*. 2012, University of Birmingham.

183. Buchko, C.J., et al., *Processing and microstructural characterization of porous biocompatible protein polymer thin films.* Polymer, 1999. **40**(26): p. 7397-7407.

184. Kwon, I.K., Kidoaki, S., Matsuda. T, *Electrospun nano- to microfiber fabrics made of biodegradable copolyesters: structural characteristics, mechanical properties and cell adhesion potential.* Biomaterials, 2005. **26**(18): p. 3929-3939.

185. Qiang, L., et al. *Preparation and Properties of Poly (vinyl alcohol) Nanofibers by Electrospinning*. in *Solid Dielectrics, 2007. ICSD '07. IEEE International Conference on*. 2007.

186. Sener, A.G., A.S. Altay, and F. Altay. *Effect of voltage on morphology of electrospun nanofibers*. in *Electrical and Electronics Engineering (ELECO), 2011 7th International Conference on*. 2011.

187. Thompson, C.J., et al., *Effects of parameters on nanofiber diameter determined from electrospinning model.* Polymer, 2007. **48**(23): p. 6913-6922.

188. Wilkes, C.E., et al., *PVC Handbook*. 2005: Hanser.

189. Lee, J., et al., *Properties of nano-ZnO/poly(vinyl alcohol)/poly(ethylene oxide) composite thin films.* Current Applied Physics, 2008. **8**(1): p. 42-47.

190. Tubbs, R.K., *Melting point and heat of fusion of poly(vinyl alcohol).* Journal of Polymer Science Part A: General Papers, 1965. **3**(12): p. 4181-4189.

191. Young, R.J. and P.A. Lovell, *Introduction to Polymers, Third Edition*. 2011: Taylor & Francis.

192. Casper, C.L., et al., *Controlling Surface Morphology of Electrospun Polystyrene Fibers: Effect of Humidity and Molecular Weight in the Electrospinning Process.* Macromolecules, 2003. **37**(2): p. 573-578.

193. Inai, R., Kotaki, M., Ramakrishna, S., *Structure and properties of electrospun PLLA single naofibres.* Nanotechnology, 2005. **16**(2): p. 208-213.

194. Bhattaraia, N., Edmondsona, D., Veiseha, O., Matsenb, A. F. & Zhanga, M., *Electrospun chitosan-based nanofibers and their cellular compatibility.* Biomaterials, 2005. **26**: p. 6176-6184.

195. Park, W.H., Jeonga, L., Yoob, D. I. & Hudson, S, *Effect of chitosan on morphology and conformation of electrospun silk fibroin nanofibers.* Polymer, 2004. **45**: p. 7151–7157.

196. Zhao, M.L., Sui, G., Deng, X. L., Lu, J. G., Ryu, S. K. & Yang, X. P, *PLLA/HA electrospin hybrid nanofiber scaffolds: Morphology, in vitro degradation and cell culture potential.* Aicam 2005, 2006. **11-12**: p. 243-246.

197. Zhong, X., Kim, K., Fang, D., Ran, S., Hsiao, B. S. & Chu, B, *Structure and process relationship of electrospun bioabsorbable nanofiber membranes.* Polymer, 2002. **43**(16): p. 4403-4412.

198. Zhao, S., Wu, X., Wang, L. & Huang, Y, *Electrospinning of ethyl-cyanoethylcellulose/tetrahydrofuran solutions.* Journal of Applied Polymer Science, 2004. **91**: p. 242-246.

199. Ahmad, A.L.O., B .S., *Properties-performance of thin-film composites membrane: Study on trimesoyl chloride content and polymerization time.* Journal of Membrane Science, 2005. **255**: p. 67-77.

200. El-Hefian, E.A., Nadef, M. M., & Yahaya, A. H., *The Preparation and Characterization of Chitosan / Poly (Vinyl Alcohol) Blended Films.* E-Journal of Chemistry, 2010. **7**(4): p. 1212-1219.

201. Mansur, H.S., et al., *FTIR spectroscopy characterization of poly (vinyl alcohol) hydrogel with different hydrolysis degree and chemically crosslinked with glutaraldehyde.* Materials Science and Engineering: C, 2008. **28**(4): p. 539-548.

202. Sahoo, D., Sahoo, S., Das, J., Dangar, T.K., and Na- yak, P. L. , *Antibacterial Activity of Chitosan Crosslinked with Aldehydes and Blended with Cloisite 30B.* NanoTrends, 2011. **10**: p. 1-9.

203. Suédina M.L. Silva, C.R.C.B., Marcus V.L. Fook, Claudia M.O. Raposo, Laura H. Carvalho and Eduardo L. Canedo, *Application of Infrared Spectroscopy to Analysis of Chitosan/Clay Nanocomposites, Infrared Spectroscopy - Materials Science, Engineering and Technology, Prof.Theophanides Theophile (Ed.)*. 2012: InTech. 510.

204. Pawlak, A. and M. Mucha, *Thermogravimetric and FTIR studies of chitosan blends.* Thermochimica Acta, 2003. **396**(1–2): p. 153-166.

205. Zeng, M., Z. Fang, and C. Xu, *Effect of compatibility on the structure of the microporous membrane prepared by selective dissolution of chitosan/synthetic polymer blend membrane.* Journal of Membrane Science, 2004. **230**(1–2): p. 175-181.

206. Sakurai, K., T. Maegawa, and T. Takahashi, *Glass transition temperature of chitosan and miscibility of chitosan/poly(N-vinyl pyrrolidone) blends.* Polymer, 2000. **41**(19): p. 7051-7056.

207. Dong, Y., et al., *Studies on glass transition temperature of chitosan with four techniques.* Journal of Applied Polymer Science, 2004. **93**(4): p. 1553-1558.

208. Parparita, E., Cheaburu, C. N. and Vasile. C., *Morphological, Thermal and Rheological Characterization of Polyvinyl Alcohol/Chitosan Blends.* Cellulose Chemistry and Technology, 2012. **46**(9-10): p. 571-581.

209. Hu, H., et al., *Glutaraldehyde–chitosan and poly (vinyl alcohol) blends, and fluorescence of their nano-silica composite films.* Carbohydrate polymers, 2013. **91**(1): p. 305-313.

210. Fangkangwanwong, J., Akashi, M., Kida, T., and Chirachanchai, S, *Chitosan-Hydroxybenzotriazole Aqueous Solution: A Novel Water-Based System for Chitosan Functionalization.* Macromolecular Rapid communications, 2006. **27**: p. 1039-1046.

211. Verlinden, R.A., *Bacterial synthesis of biodegradable polyhydroxyalkanoates.* Journal of Applied Mictrobiology, 2007. **102**(6): p. 1437-1449.

212. Randriamahefa, S., et al., *Fourier Transform Infrared Spectroscopy for Screening and Quantifying Production of PHAs by Pseudomonas Grown on Sodium Octanoate.* Biomacromolecules, 2003. **4**(4): p. 1092-1097.

213. Furukawa, T., et al., *Structure, Dispersibility, and Crystallinity of Poly(hydroxybutyrate)/Poly(l-lactic acid) Blends Studied by FT-IR Microspectroscopy and Differential Scanning Calorimetry.* Macromolecules, 2005. **38**(15): p. 6445-6454.

214. Huang, C.C., S. Lai, C. Reneker D H. Qui, H. Ye, Y. Hou, H. , *Electrospun polymer nanofibres with small diameters.* Nanotechnology,, 2006. **17**(6): p. 1558.

215. Kim, J.S.a.L., D. S, *Thermal properties of electrospun polyesters.* Polymer Journal, 2000. **32**: p. 616-618.

216. Zhou, H.G., T. B. and Joo, Y.L., *The thermal effects on electrospinning of polylactic acid melts.* Polymer, 2006. **47**: p. 7497-7505.

217. Wu, Q., Y. Wang, & G. Guo-Qiang, *Medical application of microbial biopolyesters polyhydroxyalkanoates.* Artificial cells blood substitute and immobilization biotechnology, 2009. **37**(1): p. 1-12.

218. Taniguchi, I.K., K. and Kimura Yoshiharu, *Microbial production of poly(hydroxyalkanoate)s from waste edible oils.* Green Chemistry, 2003. **5**: p. 545-548.

219. Hyakutake, M.S., Y. Tomizawa, S, Mizuno, K. and Tsuge, T, *Polyhydroxyalkanoate (PHA) Synthesis by Class IV PHA Synthases Employing Ralstonia eutropha PHB(-)4 as Host Strain.* Bioscience Biotechnology and Biochemistry, 2011. **75**(8): p. 1615-1617.

220. Merugu, R.G., S. and Reddy, S. M,, *Production of PHB (Polyhydroxybutyrate) by Rhodopseudomonas palustris KU003 under nitrogen limitation.* International Journal of Applied Biology and Pharmaceutical Technology 2010. **1**(2): p. 676-678.

221. Roa, J.P.P., P. S. Orefice, R. L. Lago, R. M., *Improvement of the Thermal Properties of Poly(3-hydroxybutyrate) (PHB) by Low Molecular Weight Polypropylene Glycol (LMWPPG) Addition.* Journal of Applied Polymer Science, 2012. **128**(5): p. 3019-3025.

222. Tokiwa, Y. and B. Calabia, *Biodegradability and Biodegradation of Polyesters.* Journal of Polymers and the Environment, 2007. **15**(4): p. 259-267.

223. Lomellini, P. and L. Lavagnini, *Molecular weight polydispersity effects on the melt viscoelasticity of styrene-acrylonitrile random copolymers.* Rheologica Acta, 1992. **31**(2): p. 175-182.

224. Gunaratne, L.M.W.K. and R.A. Shanks, *Melting and thermal history of poly(hydroxybutyrate-co-hydroxyvalerate) using step-scan DSC.* Thermochimica Acta, 2005. **430**(1–2): p. 183-190.

225. de Koning, G.J.M. and P.J. Lemstra, *Crystallization phenomena in bacterial poly[(R)-3-hydroxybutyrate]: 2. Embrittlement and rejuvenation.* Polymer, 1993. **34**(19): p. 4089-4094.

226. El-Hadi, A., et al., *Correlation between degree of crystallinity, morphology, glass temperature, mechanical properties and biodegradation of poly (3-hydroxyalkanoate) PHAs and their blends.* Polymer Testing, 2002. **21**(6): p. 665-674.

227. Kaufman, H.S. and J.J. Falcetta, *Introduction to polymer science and technology: an SPE textbook*. 1977: Wiley.

228. Savenkova, L., et al., *Mechanical properties and biodegradation characteristics of PHB-based films.* Process Biochemistry, 2000. **35**(6): p. 573-579.

229. Ma, G., et al., *Synthesize and properties of photosensitive organic solvent soluble acylated chitosan derivatives (2).* Carbohydrate polymers, 2011. **84**(1): p. 681-685.

230. Zong, Z., et al., *Characterization of chemical and solid state structures of acylated chitosans.* Polymer, 2000. **41**(3): p. 899-906.